MEMS

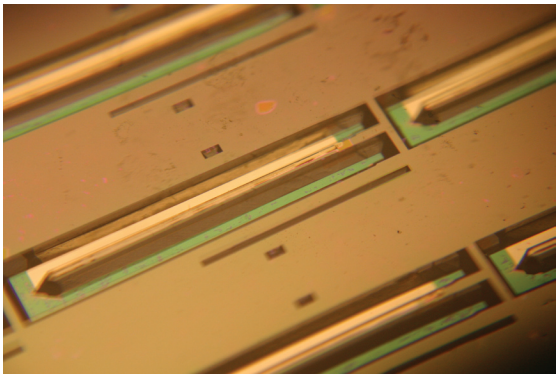

▲ Fabricated reformer-burner unit with palladium membranes (K. Deshpande, M.A. Schmidt, K.F. Jensen, p. 119).

for additional reading...

A Double-gated CNF Tip Array for Electron-impact Ionization and Field Ionization

L.-Y. Chen, L.F.V. Garcia, A.I. Akinwande
Sponsorship: DARPA

Carbon nanofibers have been investigated for a wide range of applications today. In particular, due to their remarkable conductivity, carbon nanofibers have generated a lot of interest for applications in vacuum microelectronic devices [1-2]. For example, the ionization sensor for gases is one of the most important applications since the conventional ionization sensors are bulky, require high-voltages, and consume high power. The purpose of this project is to fabricate carbon nanofiber field emission and field ionization arrays, which can be utilized in a micro-gas sensor. This device can help reduce the size of the sensor and operating voltages required for gas analysis.

In this project, the PECVD method is used to grow vertically oriented carbon nanofibers. The number of carbon nanofibers per site is controlled by the Ni catalyst dot size. It has been demonstrated that the diameter of the Ni catalysts disk must be 300 nm or less to ensure the growth of only a single carbon nanofiber [3]. The 250-nm Ni dots used in this work were defined by ebeam lithography. Figure 1 shows a close-up SEM picture of vertically aligned single carbon nanofiber array grown by PECVD. Later, these vertically-aligned single carbon nanofibers will be integrated into a double-gated field emission/ionization structure developed by L. Dvorson [4]. Figure 2 shows the schematic drawing of the final device.

Using the device shown in Figure 2, two approaches for ionizing gas molecules will be investigated for micro-gas sensors. One approach is electron impact ionization, which uses strong electric fields to emit electrons followed by collision between the energetic electrons and neutral gas molecules resulting in ionization. The second approach is field ionization, which is a gentler process in comparison to electron impact ionization. It results in molecular ionization and a simpler mass spectrum due to lower fragmentation of molecules.

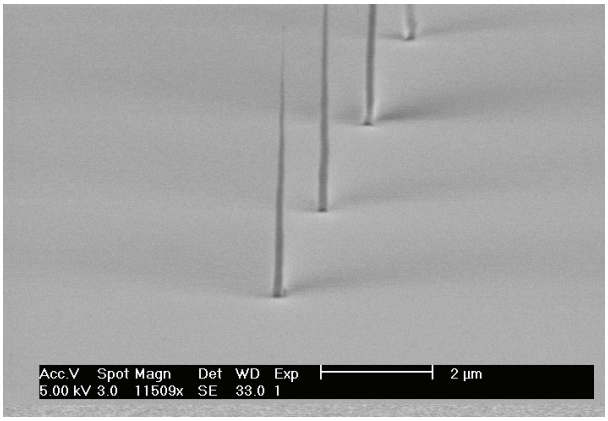

▲ Figure 1: A close-up SEM picture of vertically aligned single carbon nanofiber grown in an array patterned by PECVD.

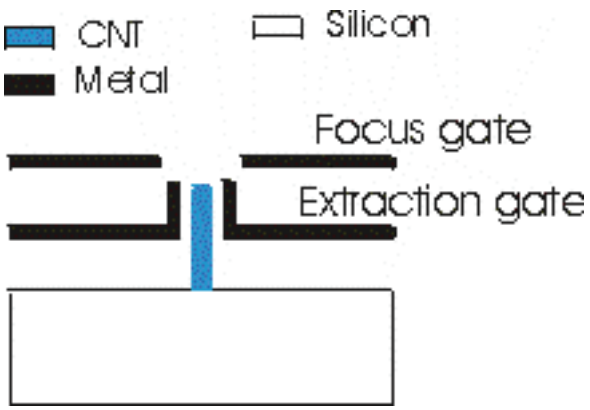

▲ Figure 2: The schematic drawing of the CNF field emission and field ionization device.

REFERENCES

[1] G. Pirio, P. Legagneus, D. Pribat, K.B.K. Teo, M. Chhowalla, G.A.J. Amaratunga, and W.I. Milne, "Fabrication and electrical characteristics of carbon nanotube field emission microcathodes with an integrated gate electrode," *Nanotechnology*, vol. 13, no. 1, pp. 1-4, Feb. 2002.

[2] W. Zhu, C. Bower, O. Zhou, G. Kochanski, and S. Jin, "Large current density from carbon nanotube field emitters," *App. Phys. Lett*, vol. 75, no. 6, pp. 873-875, Aug. 1999.

[3] K.B.K. Teo, S.-B. Lee, M. Chhowalla, V. Semet, V.T. Binh, O. Groening, M. Castignolles, A. Loiseau, G. Pirio, P. Legagneux, D. Pribat, D.G. Hasko, H. Ahmed, G.A.J. Amaratunga, and W.I. Milne, "Plasma-enhanced chemical vapour deposition carbon nanotubes/nanofiberes- how uniform do they grow?" *Nanotechnology*, vol. 14, no. 2pp. 204-211, Feb. 2003.

[4] L. Dvorson, I. Kymissis, and A.I. Akinwande, "Double-gated silicon field emitters," *J. of Vac. Sci. and Technol. B,* vol. 21, no. 1, pp. 486-494, Jan. 2003.

Hand-assembly of an Electrospray Thruster Electrode Using Microfabricated Clips

B. Gassend, L.F. Velasquez-Garcia, A.I. Akinwande, M. Martinez-Sanchez
Sponsorship: AFOSR, DARPA

This work [1] explores a method to precisely assemble two planar MEMS components. Our intended application is the assembly of the extractor electrode of an electrospray thruster, in which holes in the extractor must be aligned precisely with emitter needles or ridges (see [2] in this volume). In this method, the components can be accurately assembled by hand. Moreover, the assembly is made using a system of flexures, allowing considerable flexibility in the choice of materials and coatings for the components.

Figure 1 shows a diagram of our device. The extractor electrode (red) needs to be assembled in a recess on the base of the electrospray thruster (blue). To do this, the extractor is placed by hand in its recess. This step is easy as there are a few hundred micrometers of slack. The extractor is then rotated. As it rotates, features around its periphery force it to align its center to within 50 micrometers of its final position. As it continues the rotation, flexible fingers on the base part get flexed by the extractor, until the fingertips fall into notches in the sidewalls of the extractor.

Our devices, shown in Figure 2, were initially made out of Silicon using deep reactive-ion etching (DRIE). To show the flexibility of the method, we have also produced laser-cut polyimide extractors. The polyimide extractors have allowed us to achieve electrical insulation between the extractor and the rest of the device, which is vital for our intended application.

We have measured front-to-back alignment on all our silicon devices and found that they are within 9 micrometers RMS of their intended location. However, multiple assembly/disassembly cycles on a specific device show that the position is repeatable to within 1.5 micrometers of standard deviation. This measurement suggests that much of the misalignment we are observing occurs due to misalignments during the various photolithography and bonding steps.

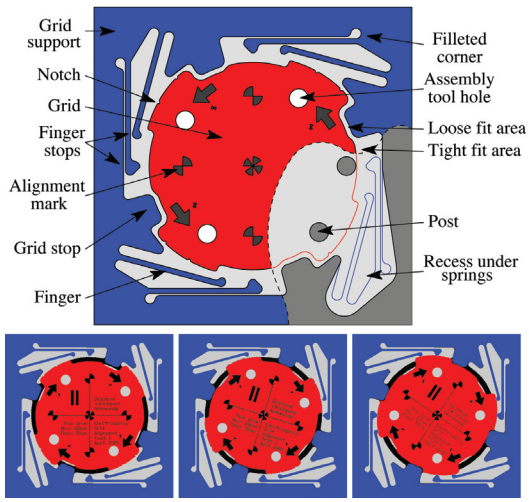

▲ Figure 1: Diagram of the device (top). Main assembly steps (bottom): first the extractor is placed in its recess, then it is brought into rough alignment, and finally the fingers lock into their notches.

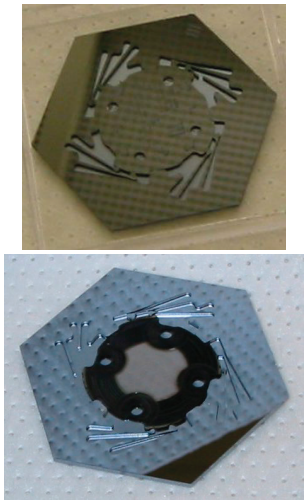

▲ Figure 2: Pictures of some assembled devices: a silicon extractor (top), an aluminum coated polyimide extractor (bottom).

REFERENCES

[1] B. Gassend, L.F. Velasquez-Garcia, A.I. Akinwande, and M. Martinez-Sanchez, "Mechanical assembly of electrospray thruster grid," in *Proc.29th Int'l. Electric Propulsion Conf.*, Princeton, NJ, Nov. 2005.

[2] B. Gassend, L.F. Velasquez-Garcia, A.I. Akinwande, and M. Martinez-Sanchez, "A fully microfabricated array of electrospray ridge emitters for space propulsion applications," Massachusetts Institute of Technology, Cambridge, MA, Microsystems Technology Laboratories Annual Research Report, 2006.

A Fully Microfabricated Planar Array of Electrospray Ridge Emitters for Space Propulsion Applications

B. Gassend, L.F. Velasquez-Garcia, A.I. Akinwande, M. Martinez-Sanchez
Sponsorship: AFOSR, DARPA

Electrospray thrusters work by extracting ions or charged droplets directly from a liquid surface using an electrostatic field and accelerating them in that field to produce thrust. This method could lead to more efficient and precise thrusters for space propulsion applications. The propellant liquid is generally placed at the tip of a needle to enhance the electrostatic field. The electrospray process limits the thrust from a single emitter needle. To get into the millinewton range will require an array with thousands of emitters. Batch microfabrication is well suited to making such an array.

We have designed and built a prototype thruster that consists of two silicon parts (Figure 1) made using deep reactive ion etching (DRIE) and SF6 plasma etching. The thruster base holds the electrospray emitters. Its surface is treated to control the areas where propellant can go. The extractor produces the electric field, which generates the electrospray. It is equipped with slits to allow the accelerated particles through. The two parts are positioned relative to each other using a kinematic mount, in which alumina balls rest in holes on the silicon dies (Figure 1). Alumina screws hold the assembly together.

In this design, we have replaced the needles that are typically used in electrospray thrusters by ridge emitters: vertical slabs with sharp tips spaced along their length (Figure 2). We have shown that our process for needles [1] can be extended to ridge shapes, and a modeling effort is underway to better control the shapes of the emitters.

Our thruster has been fired with the ionic liquid EMI-BF4. This experiment shows successful electrical insulation, even in the presence of the liquid. Challenges we now face are reducing the amount of emission that is intercepted by the extractor and determining where on the ridges the emission is coming from.

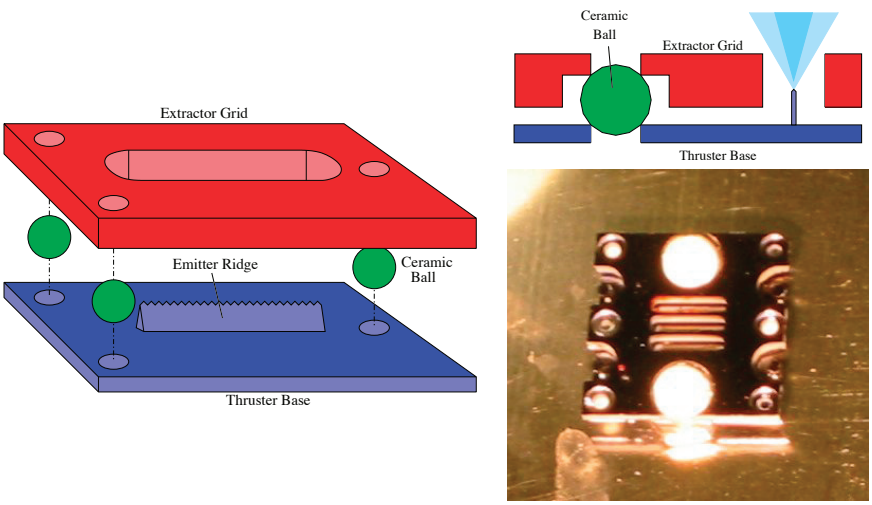

▲ Figure 1: Diagrams and picture of an electrospray thruster in which the extractor grid (red) is aligned to the base (blue) using ceramic balls (green). In the picture, the white alumina balls are visible in the top-left, bottom-left and center-right. Three slits in the center accommodate three ridge emitters.

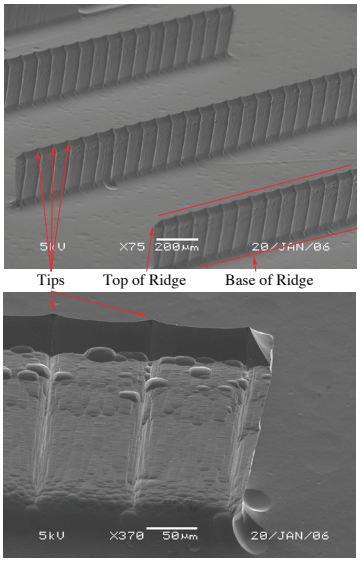

▲ Figure 2: Three parallel ridge emitters with tips spaced 100 micrometers apart (top). Close-up on one of the ridges (bottom).

REFERENCES

[1] L.F. Velasquez-Garcia, A. Akinwande, and M. Martinez-Sanchez, "Two-dimensional micro-fabricated colloid thruster arrays," in *Proc. 40th AIAA/ASME/SAE/ASEE Joint Propulsion Conference and Exhibit,* Fort Lauderdale, FL, July 11-14, 2004.

A Double-gated Silicon Tip, Electron-Impact Ionization Array

L.-Y. Chen, A.I. Akinwande
Sponsorship: CreatV Micro Tech, NIH, DARPA

A device with the ability to ionize gases is needed for a variety of applications, of which the mass spectrometer (MS) [1-2] is one of the most important. The ionization method in the majority of gas analyzers in MS is electron-impact ionization, which uses a beam of electrons that collides with gas molecules. Through this collision process, energy is transferred from the electrons to the gas molecules, which causes electrons on the gas molecules to be stripped off (i.e., ionization of the gas molecules).

Traditionally, thermionic emission, which consists of a filament that produces electrons when heated, is the most common way of generating electrons for MS using electron impact ionization. However, thermionic emission has several disadvantages: slow switch-on time, large power consumption, and lack of robustness. These disadvantages, however, are eliminated when field emission is used instead.

In this project, a double-gated silicon field emission device is used to generate the electron source for electron impact ionization. Figure 1 shows a SEM picture of a double-gated silicon field emission device used here. Using this device, we have demonstrated the linear relationship between the emission current (IE) and the ion current (II) at a fixed pressure (10-4 torr) as shown in Figure 2.

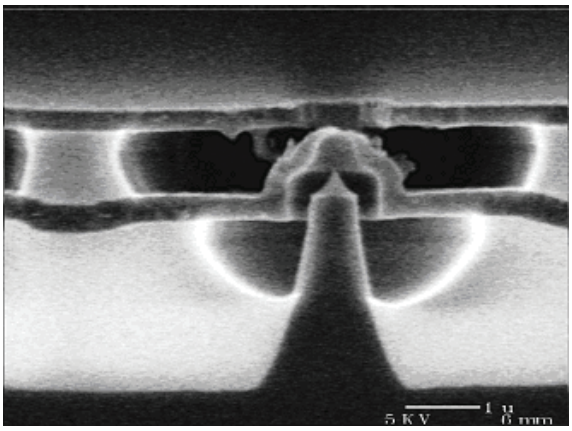

▲ Figure 1: The SEM picture of the cross section of the silicon field emission and field ionization array.

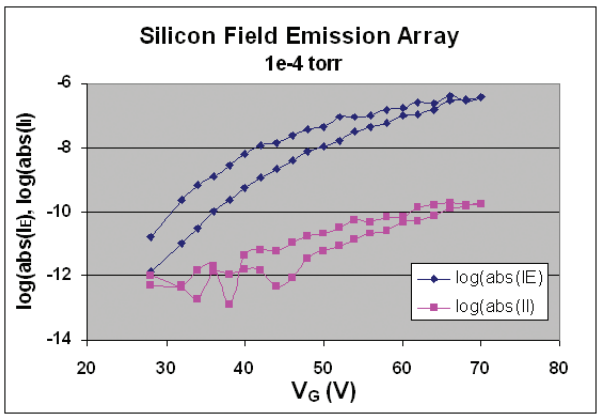

▲ Figure 2: Plot of emission current (I_E) and ion current (I_I) versus gate voltage (VG).

REFERENCES

[1] E. de Hoffmann and V. Stroobant, *Mass Spectrometry: Principles and Applications*, John Wiley & Sons, West Sussex, England, 2002.
[2] J.H. Gross, *Mass spectrometry: A textbook*, Springer-Verlag, Berlin, Germany, 2004.

A MEMS Electrometer for Gas Sensing

J. Lee, L.F. Velásquez-García, A. Seisha, A.I. Akinwande
Sponsorship: DARPA

The DARPA-funded micro gas analyzer program aims to develop portable, low-power, fast, and reliable gas analyzer technology for a wide range of applications. The system architecture of the gas analyzer contemplates a MEMS electrometer at the end of the system. The electrometer characterizes the ionized species that are filtered by the quadrupole. The sensitive element of the electrometer is a MEMS structure embedded in a feedback loop of a precise oscillator circuit. The electrometer has a comb drive that sets the electrometer to oscillate. Shifts in the oscillation frequency are related to changes in the capacitance of the electrometer due to ion interception. The resolution of the device is estimated at 100 e/√Hz in vacuum [1]. Figure 1 shows a fabricated MEMS electrometer. Figure 2 shows the experimental data of one of these MEMS electrometers, in air. The experimental resonant frequency is 6.2 kHz, and the conversion gain was estimated at 2×10^9 V/C (theoretical value is 7×10^9 V/C). Current research focuses on implement lock-in detection, which will remove the noise from the drive signal because the output has twice the frequency of the input signal.

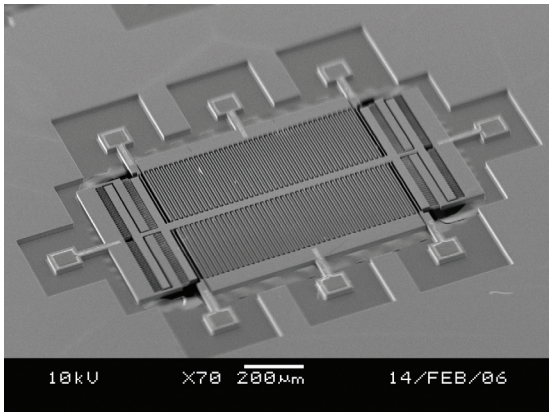

▲ Figure 1: A micro-fabricated MEMS electrometer. The comb drive (central part) sets the electrometer in oscillation. Changes in the variable capacitors (comb structures at both sides of the central comb drive) cause shifts in the oscillation frequency that are directly related to the ion current that impact the MEMS.

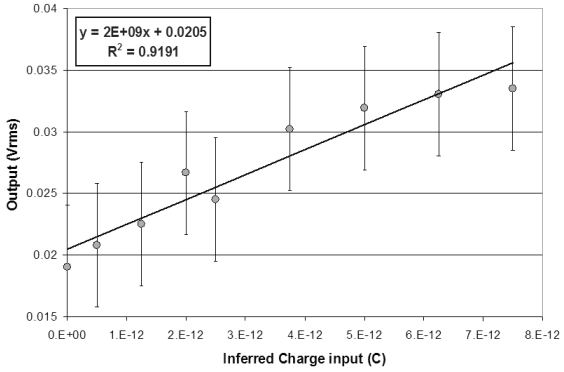

▲ Figure 2: Voltage versus charge characteristics for the MEMS quadrupole in air.

REFERENCES

[1] P. Riehl *et al.*,"Electrostatic charge and field sensors based on micro-mechanical resonators," *J. of Micromechanical Systems*, vol. 12, no. 5, p. 577, Oct. 2003.

A Single-Gated CNT Field-Ionizer Array with Open Architecture

L.F. Velasquez-Garcia, L.Y. Chen, A.I. Akinwande
Sponsorship: DARPA

The micro gas analyzer project aims to develop the technology for portable, real-time sensors intended for chemical warfare and civilian air purity control. The device is composed of four micro-fabricated subsystems: an ionizer, a mass filter based on a quadrupole array [1], an electrometer [2], and a positive displacement pump [3]. We are developing a single-gated fieldionizer array based on gated carbon nanotubes (CNTs). The devices achieve species ionization by tunneling of outer shell electrons due to the presence of high electric fields that the device sets. We use CNTs as field enhancers because of their small radii and high aspect ratio while the gate proximity ensures high fields at low voltage. State-of-the-art ionizers use electron-impact ionization (thermionic cathodes), incurring in excessive power consumption, low current, current density, ionization efficiency, and short lifetime. The field-ionizer arrays (Figure 1) are able to soft-ionize species, thus achieving molecule ionization. The reliability and lifespan of the field-ionizer arrays are larger than the corresponding values for electron-impact ionizer arrays because the CNTs are biased at the highest potential in the circuit, thus making it unlikely for ionized molecules to back-stream. Figure 2 shows two SEM pictures of a single-gated CNT array that implements a selective CNT-growth process. This process reduces the fabrication complexity of the device because it grows CNTs from an un-patterned catalyst (Ni). Current research efforts concentrate on improving the device and data acquisition, including benchmarking the performance of the ionizer in low-pressure oxidizing environments.

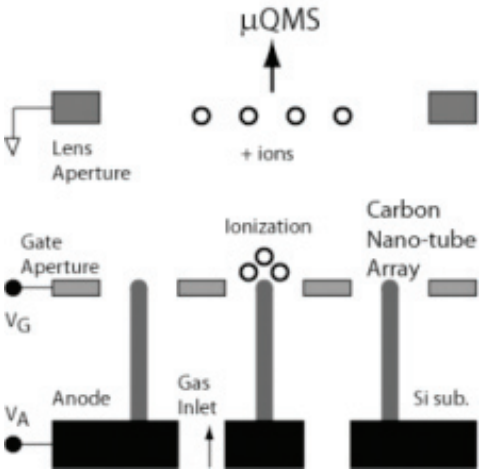

▲ Figure 1: Schematic of a field-ionizer array. The gas inlet provides neutral species to the field enhancers. If the molecules of the gas come close enough to the CNT tips, an electron from the outer shell of the molecule will tunnel to the CNT, thus ionizing the molecule.

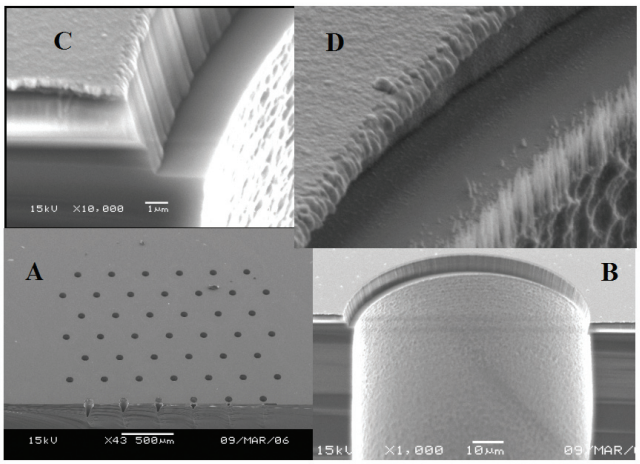

▲ Figure 2: A single-gated CNT field-ionizer array grown at MIT. (A) Field view of an array section; (B) cross section of a single ionizer well; (C) detail of the well foot intended to grow CNTs; (D) detail of the well foot when CNTs are grown. The ionizer well has a film of silicon dioxide 5-µm-thick below the gate that acts as electrical insulator between the gate and the CNTs. The gate can be made of either Ti, Au, or W. The CNT catalyst was 4-nm-thick Ni.

REFERENCES

[1] R.R.A. Syms, *et al.*, "Design of a micro-engineered electrostatic quadrupole lens," *IEEE Transactions on Electron Devices*, vol. 45, no. 11, p. 2304, Nov. 1998.

[2] P. Riehl *et al.* "Electrostatic charge and field sensors based on micro-mechanical resonators," *J. of Micromechanical Systems*, vol. 12, no. 5, p. 577, Oct. 2003.

[3] H.Q. Li, *et al.*, "A high-frequency, high-flow-rate piezoelectrically-driven MEMS micro-pump," in *Proc. IEEE Solid State Sensors and Actuators Workshop*, Hilton Head, SC, June 2000.

A MEMS Quadrupole that Uses a Meso-scaled DRIE-patterned Spring Assembly System

L.F. Velásquez-García, A.I. Akinwande
Sponsorship: DARPA

The DARPA-funded micro gas analyzer program aims to develop portable, low-power, fast, and reliable gas analyzer technology for a wide range of applications. One of the subsystems of the gas analyzer is a mass filter. An array of micro-fabricated quadrupole mass filters is being developed for this purpose. The quadrupoles will sort out the ions based on their specific charge. Both high sensitivity and high resolution are needed over a wide range of ion masses, from 20 to 200 atomic mass units. In order to achieve this performance, multiple micro-fabricated quadrupoles, each operating at a specific stability region and mass range, are operated in parallel. The proof-of-concept device is a single, linear quadrupole that has a micro-fabricated mounting head with meso-scaled DRIE-patterned springs. The mounting head allows micron-precision hand assembly of the quadrupole rods [1]–critical for good resolution and ion transmission. The micro-fabricated mounting head can implement quadrupoles with a wide range of aspect ratios for a given electrode diameter. There are currently two versions of the mounting head, able to interact with rods of diameters equal to 1588 and 559 micrometers. The choice of electrode diameter results from pondering the dimensional uncertainties and alignment capabilities with respect to the expected resolution and transmission goals. Figure 1 shows an assembled MEMS quadrupole, including some detail of the spring structure near the quadrupole transmission region. The quadrupoles that have been implemented so far span the aspect ratio range from 30 to 60. Figure 2 shows the experimental data of one of these quadrupoles on a FC-43 sample, where a mass resolution of 2 amu and a full mass range of 200 amu are demonstrated, while using a 1.2-MHz RF power supply to drive the quadrupole. Current research efforts concentrate on developing RF power supplies of higher frequency to obtain better performance from the same device.

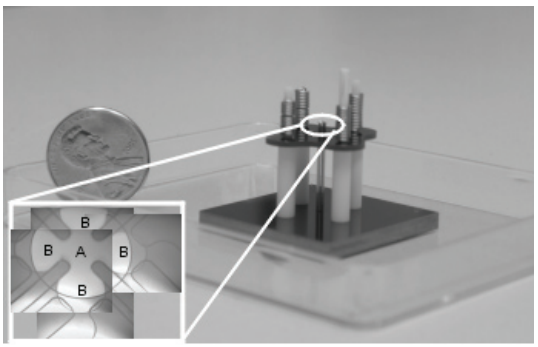

▲ Figure 1: A micro-fabricated quadrupole with electrode diameter equal to 559 micrometers, near a 1-cent coin for size reference. The micro-fabricated part of the device is the square base, which contains a system of meso-scaled DRIE-patterned springs. The structure of the quadrupole spring head near the transmission region is shown in a set of superimposed IR microscope pictures (lower left corner). The electrodes occupy the four cavities (A) that surround the axis of the quadrupole (B). The ion transmission occurs through the latter region.

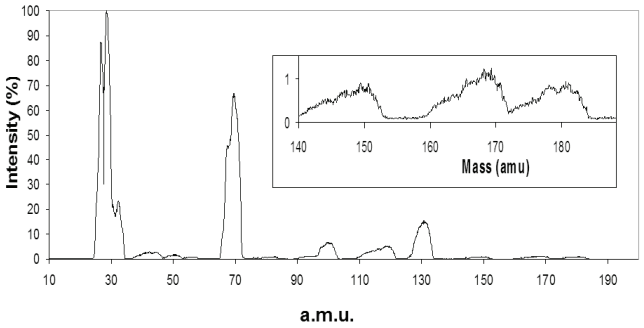

▲ Figure 2: Experimental characterization of a MEMS quadrupole, using the compound FC-43 to get peaks in the 1 – 200 amu mass range. The resolution is estimated at 2 amu, using an 1.2 MHz RF power supply On the upper right corner there is a zoom of the data near 200 amu.

REFERENCES

[1] L.F. Velásquez-García, A.I. Akinwande, and M. Martínez–Sánchez, "Precision hand assembly of MEMS subsystems using meso-scaled DRIE-patterned deflection spring structures: An assembly example of an out-of-plane substrate assembly," submitted to *The J. of MicroElectroMechanical Systems.*

Digital Holographic Imaging of Micro-structured and Biological Objects

J.A. Dominguez-Caballero, N. Loomis, J.H. Milgram, G. Barbastathis
Sponsorship: MIT Sea Grant

The need for understanding the trophodynamics of the ocean has led to the development of several instruments for monitoring plankton communities, critical indicators of the ocean's health and the base of the aquatic food chain. The three competing methods for plankton observation utilize direct, acoustic, and optical sampling techniques; however none of the current systems can provide the complete data set required for predictive modeling capabilities. The goal of this project is to develop a small, low-power, digital holographic imaging (DHI) system that allows for *in situ* monitoring of plankton and other aquatic communities. This system allows microbiologists to collect high-resolution, spatio-temporal data on species-specific population structures. In addition to biological studies, the DHI camera can be utilized in diverse areas such as medical analysis, quality control inspection, and MEMS device characterization.

DHI uses a digital sensor to record holograms, formed by the interference pattern between a reference wave and a field produced by scattered light from an illuminated object. The illumination source is coherent and typically provided by a laser. The recorded images are processed on a computer to reconstruct the original object field at a given axial location [1]. From the reconstructed images, information about the object such as morphology, topology, and 3D coordinates can be computed throughout a large sample volume. In addition, velocity and 3D trajectories are available under slightly modified methods.

Experiments have focused on biological applications, including marine and microbial organisms ranging from 5 to 2000 microns. In addition to the inline configuration (Figure 1), several setups have been implemented to explore smaller scales, including the use of spherical reference waves, 4f telescopes, and microscope objectives. Figure 1 shows our compact benchtop prototype DHI camera, currently being developed to be used as a sea-going instrument for deep-sea microbiology. Using a lens-free spherical configuration with a working distance of 50 mm, all lines on a 1951 USAF resolution target can be resolved, down to 2.2 microns in width. A 4f system was used to track the trajectories of 7 micron algae over several seconds. Small plankton, 50 to 500 microns long, have been imaged using all three setups with excellent clarity. Figure 2 shows a reconstruction from an inline configuration of an adult copepod. Future work includes incorporating the DHI camera into an underwater vehicle. Additional work will focus on tracking small particles under turbulent flow conditions.

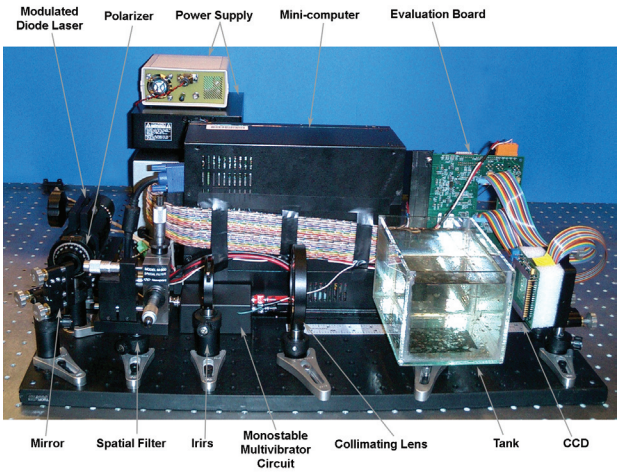

▲ Figure 1: The compact DHI camera developed for use in a deep-sea-going vehicle. An inline configuration is shown.

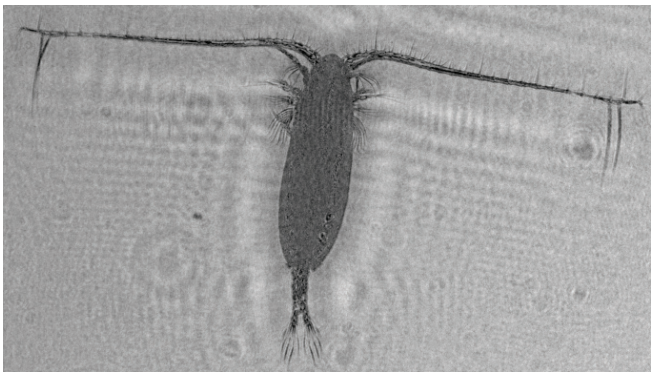

▲ Figure 2: Reconstruction of an adult copepod (*Calanus finmarchicus*) using the in-line setup with a modulated diode laser. The reconstruction distance is 101 mm.

REFERENCES

[1] J.H. Milgram and W. Li, "Computational reconstruction of images from holograms," *Appl. Opt.*, vol. 41, no. 5, pp. 853-864, Feb. 2002.

Aligning and Latching Nano-structured Membranes in 3D Micro-Structures

N.S. Shaar, G. Barbastathis, C. Livermore
Sponsorship: ISN

The 3D micro-electro-mechanical systems (MEMS) manufacturing is an emerging technology that promises to solve many of the problems in the microfabrication industry. In microelectronics, as the feature sizes of the components approach their physical limits, packing more transistors on a microprocessor or on a memory chip requires expanding the circuitry into the third dimension. In optical switches, the traditional 2D MEMS-based switches do not scale easily beyond 32 ports; to increase the number of ports, companies have been developing 3D micro-mirror arrays that can reflect light in multiple directions. The Nanostructured Origami™ 3D fabrication process is a two-step method for fabricating 3D MEMS; it involves patterning films on a surface and then folding the patterned films to create three-dimensional structures [1]. This method is advantageous because it uses state-of-the-art 2D patterning methods and it involves patterning all the parts of the structure in one step, eliminating problems of feature misalignment. However, in creating the 3D structures, two major challenges arise; the first is to accurately place the folded membranes in their desired positions and the second is to fix the membranes in those positions to maintain the final 3D configuration. Current positioning solutions involve the use of mechanical motion-limiters that prevent folded membranes from moving beyond a certain point [2]. We propose two methods for aligning and latching folded nano-patterned membranes in 3D microstructures. The first method uses photoresist pads to glue together two mating surfaces of the structure (Figure 1). What distinguishes this method from previous polymer gluing attempts is that we use dense gold patterns as a local heater to melt the photoresist pads. This allows us to control the membranes we latch and the time when we latch them. We use patterned gold wires to form the hinges that hold the membranes together. Thin dense gold patterns also serve as local heaters to melt the photoresist gluing pads. The surface tension in the molten pads aligns the surfaces and solidification of the photoresist latches them together. The second method uses mechanical alignment and latching features that allow edges-to-surface latching (Figure 2). One major advantage of this method is that the structural components and the alignment features are patterned in the same lithographic step, which lowers costs and minimizes misalignment errors. Another interesting aspect is the cascaded alignment; the alignment features are designed so that they function sequentially, starting from the features closest to the hinge. With proper design of those features, the alignment system can achieve accurate positioning using the features away from the hinge while tolerating a large initial positioning error range by virtue of the short radius sustaining the features closest to the hinge.

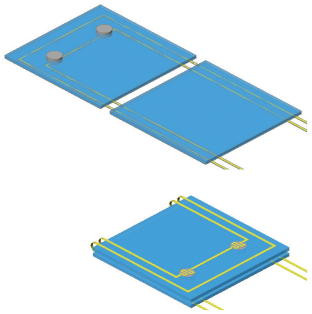

▲ Figure 1: Surface-to-surface alignment and latching of membranes by local heating of photoresist pads.

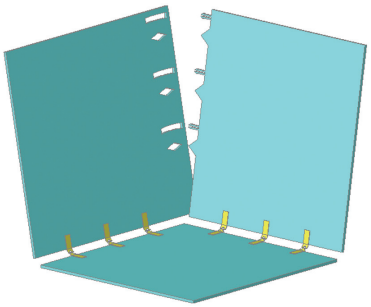

▲ Figure 2: Edge-to-surface alignment and latching of folded membranes using mechanical features.

REFERENCES

[1] H.J. In, W. Arora, T. Buchner, S.M. Jurga, H.I. Smith, and G. Barbasathis, "The Nanostructured Origami™ 3D fabrication and assembly process for nanomanufacturing," in *Proc. Fourth IEEE Conference on Nanotechnology*, Munich, Germany, Aug. 2004, pp. 358-360.

[2] Y.K. Hong, R.R.A. Syms, K.S.J. Pister, and L.X. Zhou, "Design, fabrication and test of self-assembled optical corner cube reflectors," *Journal of Micromechanics and Microengineering*, vol. 5, pp. 663-672, Jan. 2005.

A Microfabricated Platform for Investigating Multicellular Organization in 3-D Microenvironments

D.R. Albrecht, R.L. Sah, S.N. Bhatia
Sponsorship: Whitaker Foundation, NSF, NIH

Understanding how complex intrinsic and external cues are integrated to regulate cell behavior is crucial to the success of cell-based therapies in the treatment of human disease. Systematic and quantitative investigation of these microenvironment signals was first enabled by precise cell positioning using 2-D micropatterning tools [1]. However, cellular signaling is often altered in adherent tissue culture where structural cues are lacking (including tumor, stem, and differentiated cells), in contrast to 3-D culture systems that more closely resemble *in vivo* cell behavior [2]. Our goal was to develop new micropatterning tools capable of micron-scale cell patterning and organization within a 3-D hydrogel with tissue-like properties. We developed a technique for the rapid formation of reproducible, high-resolution, 3-D cellular structures within a photo-crosslinkable hydrogel using dielectrophoretic forces (Figure 1) [3]. We demonstrate parallel formation of ~20,000 cell clusters of precise size and shape within a 1 x 2 cm^2 slab of tissue (Figure 2a), with high cell viability and differentiated cell function maintained over 2 weeks in culture. By modulating cell-cell interactions in clusters of various size (independent of hydrogel geometry, chemistry, or volumetric seeding density; Figure 2b), we present the first evidence that 3-D microscale tissue organization regulates chondrocyte behavior (Figure 2c) [3]. This dielectrophoretic cell patterning (DCP) technology enables further investigation of the role of tissue architecture in many other multicellular processes from embryogenesis to regeneration to tumorigenesis.

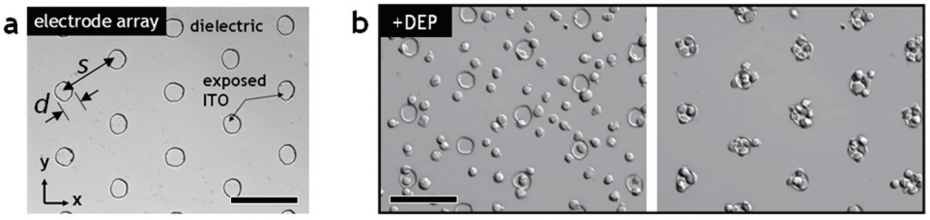

▲ Figure 1: Rapid, parallel dielectrophoretic cell patterning method. (**a**) Assembled DCP chamber viewed in inverted microscopy demonstrates the hexagonal electrode array. (**b**) Swiss 3T3 fibroblasts before and after electropatterning within a 15 wt% PEG-diacrylate prepolymer (viscosity: 3.3 cP) by +DEP toward high electric field at the electrodes, s = 100 μm apart, after 60 s exposure to 3.0 V_{rms} at 3.0 MHz.

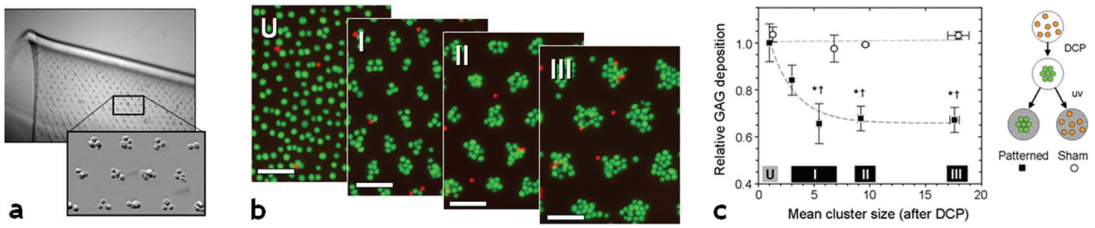

▲ Figure 2: Microscale organization alters cell function. (a) Thousands of micropatterned cell clusters are embedded within a thin hydrogel. (b) Cluster size (and cell-cell interaction) can be varied from single cells (U) to large clusters (III) within a single hydrogel slab. Cells have high viability (green), indicated by fluorescent staining. Scale bars, 100μm. (c) In articular chondrocytes, biosynthesis of a matrix molecule, GAG, is downregulated over 14 days in clusters of increasing size, independent of volumetric seeding density. "Sham" DCP hydrogels, in which cells were initially electropatterned but then randomized prior to hydrogel crosslinking, were indistinguishable from unpatterned controls. Data are mean ± s.e.m., n = 5 - 6. *, p<0.001 vs. "U"; †, p<0.001 vs. "Sham."

REFERENCES

[1] A. Khademhosseini, R. Langer, J. Borenstein, and J.P. Vacanti, "Microscale technologies for tissue engineering and biology," *PNAS*, vol. 103, pp. 2480-7, 2006.

[2] A. Abbott, "Cell culture: biology's new dimension," *Nature*, vol. 424, no. 6951, pp. 870-872, Aug. 2003.

[3] D.R. Albrecht, G.H. Underhill, T.B. Wassermann, R.L. Sah, and S.N. Bhatia, "Probing the role of multicellular organization in 3D microenvironments," *Nature Methods*, vol. 3, no. 5, pp. 369-75, May 2006.

Microfluidic Hepatocyte Bioreactor

D.T. Eddington, S.N. Bhatia

This project utilizes microfluidic systems to study how groups of liver cells acquire emergent tissue properties. Hepatocytes (the parenchymal cells of the liver) respond to many cues in their microenvironment: neighboring cells, growth factors, extracellular matrix, dissolved oxygen, and their interactions. One tissue property of interest is the compartmentalization of gene expression in multicellular domains along the liver sinusoid. This process, often described as "zonation," underlies much of liver physiology and regional susceptibility to toxins. We have previously shown oxygen gradients can be used to compartmentalize mixed populations of hepatocytes in a large-scale reactor [1]. Here, we present a microdevice that enables one to explore the crosstalk between two inputs (oxygen gradients and soluble growth factors) in a systematic fashion. The device consists of a two-layer PDMS microfluidic network with an on-chip dilution tree bound to a glass slide with an array of microreactors. Hepatocyte zonation is induced in each microreactor through local oxygen concentration, which is modulated through gas channels separated from the bioreactor by a 100-μm PDMS layer as shown in Figure 1. The local oxygen concentration in the microchannels is quantified in Figure 2. Primary rat hepatocytes are seeded into microreactors together with 3T3 fibroblasts, which act to stabilize the hepatocyte phenotype as described previously. This device will be useful to further explore liver tissue biology *in vitro* including the dynamics of zonation, mechanisms of oxygen sensing, and the role of growth factors in zonal response.

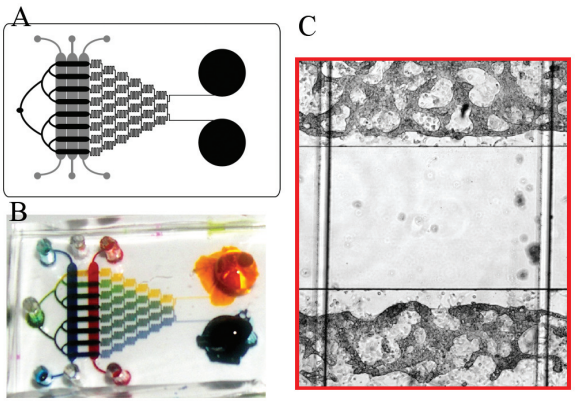

▲ Figure 1: A.) Schematic and B.)Picture of the microfluidic network. Two inlets (yellow and blue) feed a dilutiongradient generator to yield a titration, which feeds into 8 discreet bioreactors. Gas channels (dyed red and blue) run perpendicular to the bioreactors and each connected to a separate gas cylinder with a premixed oxygen concentration (21%, 10%, and 1 %). The gas channels are separated from the PDMS microchannels through a thin PDMS membrane. C.) Magnification of the red box in A showing two bioreactors and the gas channels. The arrows indicate how the gas and liquid flow in the channels.

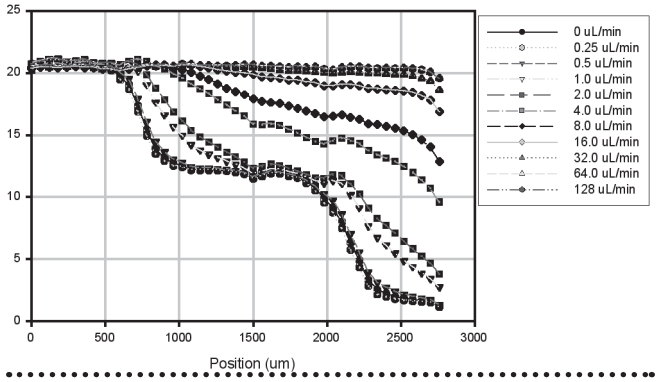

▲ Figure 2: Oxygen concentration along the length of the bioreactor as a function of distance and flow rate. This data was acquired through a rutheniummodified substrate which fluoresces under 450nm light and is quenched by oxygen. The data was calibrated and the intensities are directly related to the local oxygen concentration through the Stern-Vollmer logorithm.

REFERENCES

[1] J.W. Allen, and S.N. Bhatia, "Formation of steady-state oxygen gradients *in vitro* - Application to liver zonation" *Biotechnology and Bioengineering*, vol. 82, no.3, pp. 253-262, May 2003.

Micromechanical Control of Cell-Cell Interaction

E.E. Hui, S.N. Bhatia
Sponsorship: NIH NIDDK

Cellular behavior within tissues is driven by environmental cues that vary temporally and spatially with granularity on the order of individual cells. Local cell-cell interactions via secreted and contact-mediated signals play a critical role in these pathways. In order to study these dynamic small-scale processes, we have developed a micromechanical platform to control microscale cell organization so that cell patterns can be reconfigured dynamically. This tool has been employed to deconstruct the mechanisms by which liver-specific function is maintained in hepatocytes upon co-cultivation with stromal support cells. Specifically, we examine the relative roles of cell contact and short-range soluble signals, duration of contact, and the possibility of bi-directional signaling.

The device consists of two silicon parts that can be locked together either to allow cell-cell contact across the two parts or to separate the cells by a uniform gap of approximately 80 μm (Figs. 1 and 2). Switching between these two states is actuated simply by pushing the parts manually using tweezers; no micromanipulation machinery is necessary. Micron-scale precision is possible due to a 10:1 mechanical transmission ratio and microfabricated snap locks, both of which are monolithically incorporated into the silicon structure. The entire device is fabricated in a simple single-mask process using through-wafer deep reactive ion etching. To provide a surface compatible with cell culture, the surface is coated with a layer of polystyrene and plasma-treated, providing a standard tissue-culture surface.

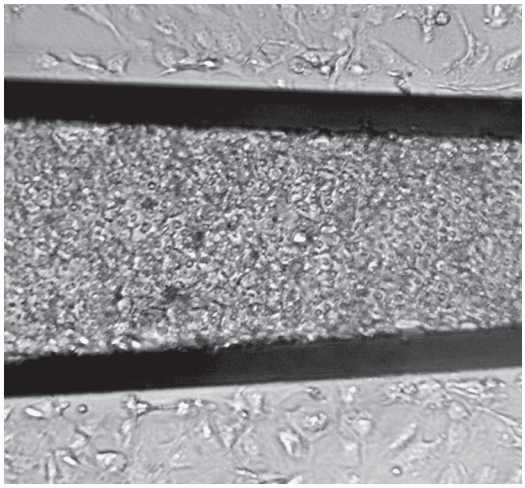

▲ Figure 1: Hepatocytes separated from stromal cells by 80-micron gaps, which prevent contact between the two cell types.

▲ Figure 2: Hepatocytes and stromal cells cultured with no separation. The system can be switched back and forth between the states shown in Figures 1 and 2.

Characterization and Modeling of Non-uniformities in DRIE

H.K. Taylor, H. Sun, A. Farahanchi, D.S. Boning
Sponsorship: Singapore-MIT Alliance

Our previous work on spatial non-uniformities in deep-reactive ion etch (DRIE) has provided a method by which an etching tool and associated "recipes" of operating parameters may be pre-characterized [1]. That work allowed the wafer-average pattern opening density (or "loading") to be related to wafer-scale etch rate variations. Such variations have been attributed to loading-dependent interactions of the flux densities of S_xF_y ions and F neutrals and to shifts in the gross flows of fluorine across the wafer [2]. Unlike some other approaches [3–5], our method captures asymmetries in the fluxes within the chamber. Our approach is now supplemented by an understanding of how uniformity depends on the localization of etched patterns within the wafer (Figure 1). A semi-physical model represents the diffusion of monatomic fluorine etchant parallel to the wafer's surface, giving a two-dimensional filter which translates a discretized map of pattern density into a prediction of how etch rate will vary within and between dies [6]. This die-level model is readily combined with the existing wafer-level model. To tune this combined model for a new recipe, a set of about five test wafers is etched, and fitting algorithms are run with etched-depth data. Collaborative experiments with Surface Technology Systems Ltd have demonstrated our approach in use with a prototype etch tool. Further experiments have compared the characteristics of different manufacturers' tools. We have also quantified a memory effect whereby the average pattern density of one etched wafer can affect the average rate and non-uniformity with which a subsequent wafer etches (Figure 2). In the future we aim to incorporate well-known feature size or aspect ratio effects into our model [7]. We envisage our approach being integrated into computer-aided design systems for MEMS and believe that it will be of particular use when one is keen to preserve a fast-average etch rate and is thus loath to win uniformity by reducing the chamber pressure.

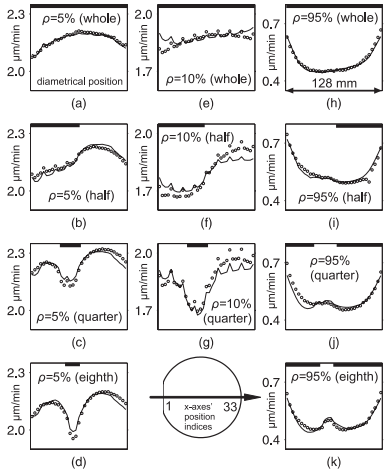

▲ Figure 1: Diametrical variation of etch rate for 11 wafers with differing average pattern density. Heavy bars indicate the portion of the diameter into which etched silicon was concentrated.

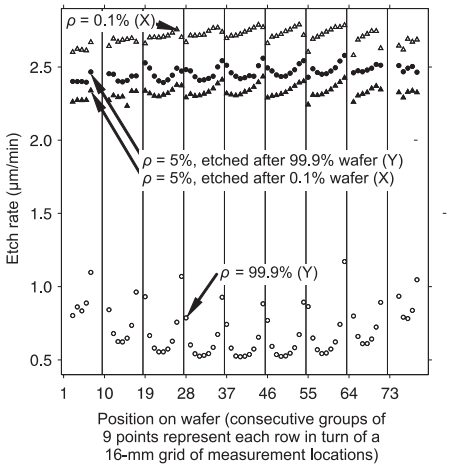

▲ Figure 2: The influence of the average pattern density (ρ) of one etched wafer upon the rate and uniformity with which the subsequent wafer etches. It is observed that a wafer's etch rate is slightly accelerated when the preceding wafer has a very high etched density; moreover, the shape of the nonuniformity is also echoed.

REFERENCES

[1] H. Sun *et al.*, "A two-level prediction model for deep reactive ion etch (DRIE)," in *Proc. MEMS '05*, Miami, FL, 2005, pp. 491–495.

[2] R.A. Gottscho, C.W. Jurgensen, and D.J. Vitkavage, "Microscopic uniformity in plasma etching," *J. Vac. Sci. Technol. B*, vol. 10, pp. 2133–2147, 1992.

[3] H.G. Stenger Jr. *et al.*, "Reaction kinetics and reactor modeling of the plasma etching of silicon," *AIChE J.*, vol. 33, pp. 1187–1196, 1987.

[4] S. Jensen *et al.*, "Uniformity-improving dummy structures for deep reactive ion etching (DRIE) processes," *Proc. SPIE*, vol. 5715, pp. 39–46, 2005.

[5] K. Janiak, and U. Niggebrügge, "Investigation of macroscopic uniformity during CH_4–OH_2 reactive ion etching of InP and its improvement by use of a guard ring," *J. Vac. Sci. Technol. B*, vol. 20, pp. 105–108, 2002.

[6] T.F. Hill, "Analysis of DRIE uniformity for microelectromechanical systems," Master's thesis, Massachusetts Institute of Technology, Cambridge, 2004.

[7] A.A. Ayón *et al.*, "Characterization of a time multiplexed inductively coupled plasma etcher," *J. Electrochem. Soc.*, vol. 146, pp. 339–349, 1999.

Understanding Uniformity and Manufacturability in MEMS Embossing

H.K. Taylor, D.S. Boning
Sponsorship: Singapore-MIT Alliance

The hot embossing of thermoplastic materials, such as polymethylmethacrylate (PMMA) or cyclo- olefin copolymer (COC), is a promising way to manufacture microfluidic channels and networks [1]. Hot embossing potentially offers lower per-area cost than the micromachining of quartz or silicon and easier scaling-up of production than soft lithography using polydimethylsiloxane [2]. In hot embossing, a microfabricated mold (typically of silicon or nickel) is pressed into a flat sample of polymeric material that has been softened by heating it above its glass-transition temperature. We are particularly interested in how the spatial distribution of mold features—their diameters, shapes, and areal densities—may influence the quality of embossed patterns. We are developing a simulation approach whose building-block is a simple model in which, for given embossing conditions, a feature-sized disk of viscous polymer is compressed at a rate inversely proportional to the square of the radius of the disk [3] (Figure 1). Such a model implies that the mold will sink into the substrate at a spatially uniform rate when the product of the areal density of mold features and the square of their average radius remains constant across the mold. We aim to construct a reliable model that is computationally efficient and that can predict the combination of embossing pressure and duration required by any mold design. We are investigating the measurement of birefringence of embossed samples [4] as a way of monitoring the embossing process (Figure 2). We are also pursuing a technique for the bonding of polymer surfaces that promises minimal deformation of pre-embossed features: the polymer surfaces are exposed to an oxygen plasma for ~1 minute and then pressed together [5].

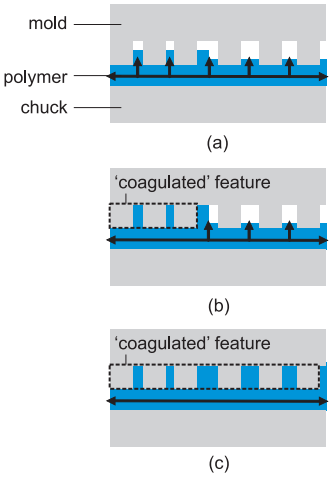

◀ Figure 1: Proposed model for the spatially non-uniform filling of embossing mold features with heated thermoplastic material (blue). Arrows indicate the displacement of material. Regions of the mold with higher areal densities of protruding features, e.g., on the left in this figure, are expected to be filled more quickly (a), and to "coagulate" into effectively larger features (b). Eventually all features would be filled and the polymeric substrate may continue to be compressed as one large disk (c).

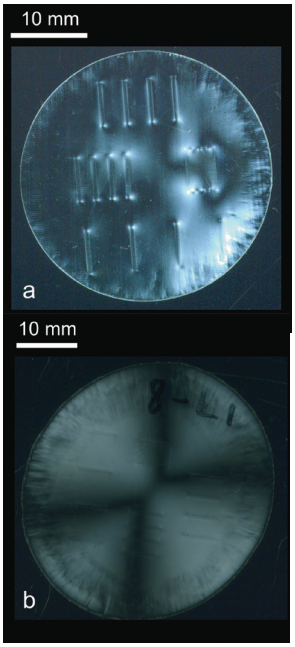

◀ Figure 2: Light transmitted by each of two embossed PMMA samples sandwiched between perpendicular polarizers. The two samples were embossed under ~1 MPa for equal lengths of time. At 110 °C (a), material within about 1 mm of the corners of embossed, 30 μm-deep rectangular channels exhibits substantially higher birefringence than the rest of the sample, implying concentrations of residual stress there. At 150 °C (b), feature-scale birefringence becomes less important than sample-scale birefringence. Samples fabricated by Wang Qi.

REFERENCES

[1] A. Pépin, P. Youinou, A. Lebib, and Y. Chen, "Nanoimprint lithography for the fabrication of DNA electrophoresis chips," *Microelectronic Eng.*, vol. 61–62, pp. 927–932, Jul. 2002.

[2] J.R. Anderson, D.T. Chiu, R.J. Jackman, O. Cherniavskaya, J.C. McDonald, H. Wu, S.H. Whitesides, and G.M. Whitesides, "Fabrication of topologically complex three-dimensional microfluidic systems in pdms by rapid prototyping," *Anal. Chem.*, vol. 72, no. 14, pp. 3158–3164, Jul. 2000.

[3] T. Hoffmann, "Viscoelastic properties of polymers," *Alternative Lithography,* Ed. C.M. Sotomayor Torres, NY: Kluwer, 2003.

[4] H.S. Lee, S.K. Lee, T.H. Kwon, and S.S. Lee, "Microlenses array fabrication by hot embossing process," *IEEE/LEOS Intl. Conf. on Optical MEMS*, 2002, pp. 73–74.

[5] J. Mizuno, S. Farrens, H. Ishida, V. Dragoi, H. Shinohara, T. Suzuki, M. Ishizuka, T. Glinsner, and S. Shoji, "Cyclo-olefin polymer direct bonding using low temperature plasma activation bonding," *Int'l. Conf. MEMS, Nano and Smart Systems*, 2005, pp. 1346–1349.

A MEMS Drug Delivery Device for the Prevention of Hemorrhagic Shock

H.L. Ho Duc, M.J. Cima
Sponsorship: ARO (Institute for Soldier Nanotechnology)

Hemorrhagic shock is the number one cause of preventable death on today's battlefield [1]. It is a hypotensive state of deficient organ perfusion caused by blood loss from wounds of the extremities or internal injuries. Hemorrhagic shock is normally treated by hemorrhage control, fluid replacement, and the injection of vasoconstrictors. Battlefield conditions, however, can prevent the timely administration of these measures. Hemostatic dressings developed for battlefield application are useful in controlling open wound hemorrhage but cannot stop internal bleeding or avert shock if too much blood has been lost [1]. Arginine vasopressin is a vasoconstrictor that causes peripheral and abdominal arteries to constrict, shunting blood to the vital organs in case of hemorrhage [2]. It improved survival by restoring blood pressure in pre-clinical experiments and clinical case studies of hemorrhagic shock when treatment was not immediately available [3-7]. This property makes it a perfect candidate for battlefield injection to keep wounded soldiers alive until they can be properly treated. Self-injection may not always be possible, however, due to the nature of these traumas.

We are currently developing an implantable drug delivery microelectromechanical system (MEMS) to deliver vasopressin to wounded soldiers on the battlefield. This device consists of a silicon substrate in which pyramidal wells are etched using common MEMS processing techniques. The wells are capped by metallic membranes and the chip is hermetically bonded to a Pyrex macroreservoir (Figure 1). The macroreservoir can be injected with 25 μL of a vasopressin solution to be released on demand. Applying an electric pulse through a metallic membrane melts it by resistive heating, exposing the macroreservoir to the environment. We also observed the formation of multiple thermal bubbles inside the macroreservoir, which enabled rapid delivery of the solution. We are redesigning the device to better control this mechanism. Future challenges include insuring long-term hermeticity and wireless activation of the device.

◀ Figure 1: Picture of the MEMS device showing the Pyrex macroreservoir (left) bonded to the silicon chip (right). The metallic layer on the silicon chip controls the opening of micro-wells allowing vasopressin out of the macroreservoir.

REFERENCES

[1] H. Alam, E. Koustova, and P. Rhee, "Combat casualty care research: from bench to the battlefield," *World J. of Surgery*, vol. 29, pp S7-S11, June 2005.

[2] K. Stadlbauer, V. Wenzel, A. Krismer, W. Voelckel, and K. Lindner, "Vasopressin during uncontrolled hemorrhagic shock: less bleeding below the diaphragm, more perfusion above," *Anesth. Analg.*, vol. 101, no. 3, pp. 830-832, Sept. 2005.

[3] W. Voelckel, C. Raedler, V. Wenzel, K. Lindner, A. Krismer, C. Schmittinger, H. Herff, K. Rheinberger, and A. Konigsrainer, "Arginine vasopressin, but not epinephrine, improves survival in uncontrolled hemorrhagic shock after liver trauma in pigs," *Crit. Care Med.*, vol. 31, pp. 1160-1165, April 2003.

[4] C. Raedler, W. Voelckel, V. Wenzel, A. Krismer, C. Schmittinger, H. Herff, V. Mayr, K. Stadlbauer, K. Lindner, and A. Koenigsrainer, "Treatment of uncontrolled hemorrhagic shock after liver trauma: fatal effects of fluid resuscitation versus improved outcome after vasopressin," *Anesth. Analg.*, vol. 98, pp. 1759-1766, June 2004.

[5] T. Haas, W. Voelckel, F. Wiedermann, V. Wenzel, and K. Lindner, "Successful resuscitation of a traumatic cardiac arrest victim in hemorrhagic shock with vasopressin: a case report and brief review of the literature," *J. of Trauma - Injury, Infection & Critical Care*, vol. 57, pp. 177-179, July 2004.

[6] A. Krismer, V. Wenzel, W. Voelckel, P. Innerhofer, K. Stadlbauer, T. Haas, M. Pavlic, H. Sparr, K. Lindner, and A. Koenigsrainer, "Employing vasopressin as an adjunct vasopressor in uncontrolled traumatic hemorrhagic shock - three cases and a brief analysis of the literature," *Der Anaesthesist*, vol. 54, pp. 220-224, 2005.

[7] R. Sharma and R. Setlur, "Vasopressin in hemorrhagic shock," *Anesth. Analg.*, vol. 101, pp. 833-834, Sept. 2005.

Application of Input Shaping® and HyperBit™ Control to Improve the Dynamic Performance of a Six-axis MEMS Nano-positioner

S. Chen, M.L. Culpepper, S. Jordan, J. Danieli, J. Wenger
Sponsorship: NSF

We have recently demonstrated how Input Shaping® and HyperBit™ control may be used to obtain fine-resolution motion and minimize vibration errors in all six axes of a six-axis, MEMS nano-positioner [1]. The dynamic problems in MEMS positioners, e.g., ringing/overshoot, that are conventionally addressed by damping must be resolved using control techniques since it is difficult to incorporate damping into micro-scale devices. Secondly, a positioner's range to resolution ratios has to be 1 million or larger and also its "on-chip" digital-to-analog converters would need to be minimized on the expensive silicon real estate. These issues will be resolved by the applying the Input Shaping and HyperBit control.

We first study the dynamic characterization of the nanopositioner, the microHexFlex [2], including the natural frequencies and their corresponding mode shapes. We then demonstrate the effect of Input Shaping and HyperBit on the nano-positioner's resolution and settling time. Using these techniques, it is possible to obtain ms settling times with sub-nanometer resolution. The practical implications of this work are that future small-scale precision devices will be able to use these techniques to provide low-cost, multi-axis positioning at high-speeds speed and with fine resolution.

The micro-HexFlex nanopositioner possess a 2.5-mm footprint and consists of two layers of single crystalline silicon with one layer of silicon dioxide in between. The stage of the micro-HexFlex is supported by axi-symmetric micro-scale flexures. Thermomechanical actuators are used to drive the Micro-HexFlex. In our tests, the thermomechanical actuators were driven via a voltage that was preconditioned using an Input-shaping controller. The controller [3] is an implementation of a feed-forward technique that acts to remove ringing and overshoot by modifying the input signal to the actuators so as to obtain the best possible performance from the positioner.

We also add HyperBit DAC technology, a recently developed technique [4] for extending the resolution of digital-to-analog converters (DACs), for instance using a 4-bit DAC to obtain 12-bit functionality. Since DAC update rate capabilities are significantly faster than the bandwidths of the devices being driven, this technique allows the idle time-domain capacity of "low-bit" DACs to emulate that of "high-bit" DACs. The improvement in resolution is therefore obtained with simpler DAC equipment/circuitry that is more easily fabricated and integrated with micro- and meso-scale devices. Experimental results indicate reduction in dynamic errors by two orders of magnitude when the positioner was given 100-Hz square wave commands.

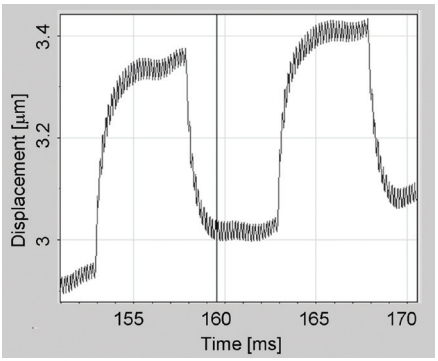

▲ Figure 1: Displacement response of microHexFlex to a 100-Hz square-wave without Input Shaping.

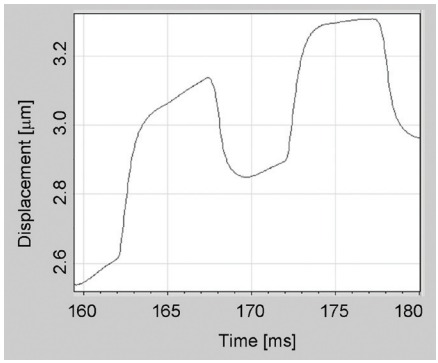

▲ Figure 2: Displacement response of microHexFlex to a 100-Hz square-wave with Input Shaping.

REFERENCES

[1] S. Chen, M.L. Culpepper, S. Jordan, J. Danieli, and J. Wenger, "Application of input shaping and hyperbit control to improve the dynamic performance of a xix-axis MEMS nano-positioner: Micro-HexFlex," *J. of MEMS*, April 2006, to be published.

[2] S. Chen and M.L. Culpepper, "Design of a six-axis micro-scale nano-positioner–Micro-HexFlex," *Prec. Eng.*, 2006, to be published.

[3] N.C. Singer and W.P. Seering, "Design and comparison of command shaping methods for controlling residual vibration," in *Proc. IEEE International Conference on Robotics Automation*, Scottsdale, AZ, May 1989, pp. 888-893.

[4] S. Jordan, U.S. Patent 6950050, 2005.

Multi-Axis Electromagnetic Moving-Coil Microactuator

D.S. Golda, M.L. Culpepper
Sponsorship: NSF

Electromagnetic (EM) micro-actuators are becoming increasingly important in micro-systems requiring moderate forces operating over a large range of motion. The applications that benefit from the performance advantages of EM micro-actuators include micro-scanning systems, micro-fluidic pumps, and positioning systems. Advantages of electromagnetic actuation over other classes of micro-actuators include low-voltage operation, moderate power density, large operating distances, linear response, multi-axis capability, and high bandwidth [1]. This work leverages the advantages of EM interactions to design a moving-coil micro-actuator that enables two-axes actuation with moderate forces (10+ mN) over large operating distances (10+ micrometers) at moderate mechanical frequencies (1+ kHz) using assembled permanent magnet field sources.

The two-axes electromagnetic actuator consists of moving coils suspended on compliant silicon flexure springs above an array of 3 rectangular permanent magnets, as shown in Figure 1. The phase of the stacked coils results in Lorentz forces that are independently controllable in-the-plane and out-of-the-plane. The coil-spring fabrication scheme includes electroplating of copper coils, followed by a deep reactive-ion etch (DRIE) to pattern and release the compliant springs. Millimeter-sized permanent magnets are then aligned to the spring layer using an alignment chip. Successfully fabricated micro-coil structures have been shown to sustain current densities over 1000 Amps per square millimeter.

A quasi-analytic electromagnetic force model for the device has been developed and experimentally validated against a centimeter-size bench-level prototype actuator. Figure 2 shows the predicted lateral-actuator force per coil-footprint versus current input for a typical actuator with 900-μm^2 coil cross section. The actuator will be implemented in a high-speed meso-scale nano-positioner with applications in nano-fabrication and scanning-probe microscopy. When equipped with this micro-actuator, the nano-positioner is expected to be able to position millimeter-sized samples in six axes of motion (x, y, z, tip, tilt, yaw) with repeatability better than 10 nanometers at frequencies greater than 1 kHz.

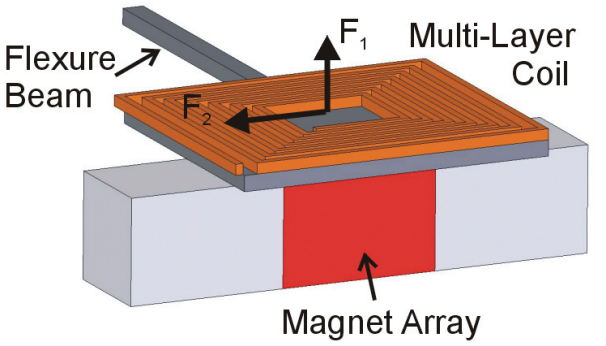

▲ Figure 1: Schematic representation of the electromagnetic moving-coil microactuator.

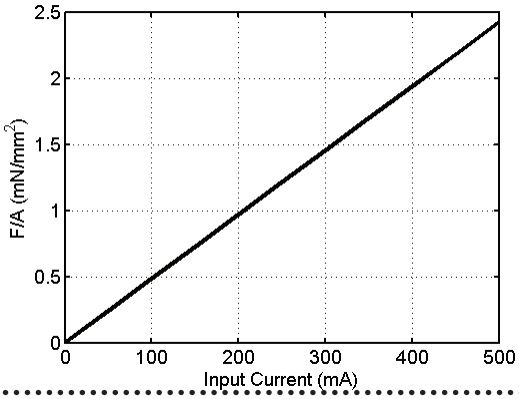

▲ Figure 2: Predicted force per coil area versus input current for a typical EM moving-coil microactuator.

REFERENCES

[1] O. Cugat, J. Delamare, and G. Reyne, "Magnetic micro-actuators and systems (MAGMAS)," *IEEE Transactions on Magnetics*, vol. 39, no. 5, pp. 3607-3612, 2003.

Multiwell Cell Culture Plate Format with Integrated Microfluidic Perfusion System

K. Domansky, S.W. Inman, J. Serdy, L.G. Griffith
Sponsorship: DuPont-MIT Alliance, Pfizer, Biotechnology Process Engineering Center

Recent reports indicate that it takes nearly $800 million dollars and 10-15 years of development to bring a drug to market. Nearly 90% of the lead candidates identified by current *in vitro* screens fail to become marketable drugs. One of the reasons for the high failure rate of drug candidates is the lack of adequate models. To address the problem, we have developed a new cell culture analog amenable to routine use in drug development. It is based on the standard multiwell cell culture plate format but it provides perfused three-dimensional cell culture capability.

The multiwell plate microbioreactor array [1, 2] consists of a fluidic and a pneumatic manifold with a diaphragm sandwiched in between them. The fluidic manifold contains an array of microbioreactor and reservoir pairs (Figure 1). Each microbioreactor/reservoir pair is fluidically isolated from all other microbioreactors on the plate. A key component of a microbioreactor is a scaffold for tissue morphogenesis (Figure 2). The scaffold is a thin wafer containing an array of channels in which cells self-assemble into 3D pieces of tissue. It is backed by a filter and a support scaffold. Tissue in the scaffold is perfused by cell culture medium. The medium is re-circulated between the reactor and reservoir by a diaphragm pump. The diaphragms of all pumps and rectifying valves are actuated in parallel via three pneumatic lines distributed by the pneumatic manifold. Fluidic capacitors control flow pulsatility.

The system provides a means to conduct high throughput assays for target validation and predictive toxicology in the drug discovery and development process. It can be also used for evaluation of long-term exposure to drugs or environmental agents and as a model to study viral hepatitis, cancer metastasis, and other diseases and pathological conditions.

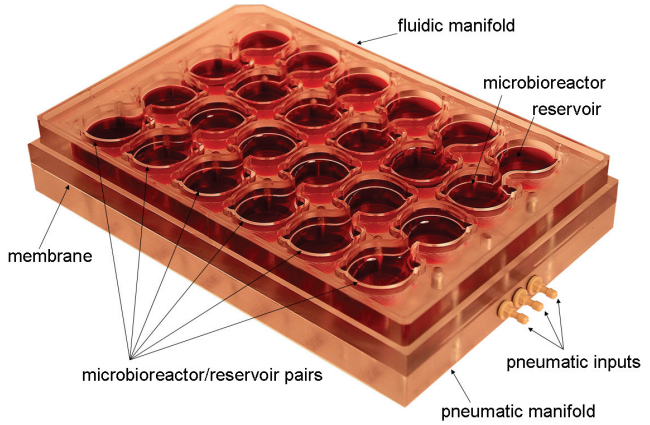

▲ Figure 1: Photograph of a 12-microbioreactor array occupying 24 wells. Cell culture medium is re-circulated between the reactor and reservoir wells. All reactor/reservoir pairs are fluidically isolated from each other.

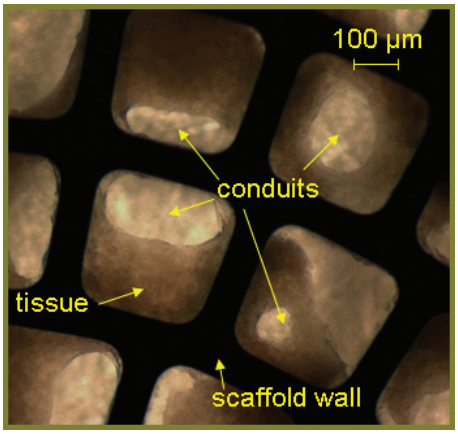

▲ Figure 2: Primary rat hepatocytes seeded in a silicon scaffold (day 7 after isolation). The channels were microfabricated by deep reactive ion etching. The size of each channel is 300 x 300 x 230 µm. Each channel can accommodate 500-1000 cells.

REFERENCES

[1] K. Domansky, W. Inman, J. Serdy, and L.G. Griffith, "Multiwell cell culture plate format with integrated microfluidic perfusion system," in *Proc. SPIE, Microfluidics, BioMEMS, and Medical Microsystems IV*, San Jose, CA, January 2006, vol. 6112, pp. 61120F:1–7.

[2] K. Domansky, W. Inman, J. Serdy, and L.G. Griffith, "3D Perfused liver microreactor array in the multiwell cell culture plate format," *Proceedings of the Ninth International Conference on Miniturized Systems for Chemistry and Life Sciences (µTAS)*, Boston, October 2005, pp. 853-855.

Characterization of Nanofilter Arrays for Biomolecule Separation

H. Bow, J. Fu, J. Han
Sponsorship: DuPont-MIT Alliance, NIH, Singapore-MIT Alliance

In the past decade, microfabricated devices have been developed that can separate, detect, and analyze various biomolecules [1]. In contrast to the sieving gels that are historically used in these studies, microfabricated devices are precisely designed and constructed. The deterministic structure of these devices facilitates experiment design and testing of theory. Periodic nanofilter arrays have been shown to separate DNA from 100 bp to 10 kbp [2]. These nanofilters consist of a regular sequence of free and constricted regions, with 50-100 nm being the characteristic dimension of the constricted region. In this context, the DNA is smaller than the constriction size, suggesting applicability of the Ogston sieving mechanism. Movement is characterized by the partitioning between the free and constricted regions due to steric constraints [3-4]. DNA has a persistence length of 50 nm (150 bp) and can be approximated as semi-rigid rods in this size range, facilitating theoretical analysis.

We investigated the effects on separation efficiency and resolution of changing various device and experiment parameters. These parameters include the strength of the electric field; depth of the deep region; depth of the thin and deep regions, while maintaining their ratio; silicon substrate bias; buffer strength; and period of the nanofilter array.

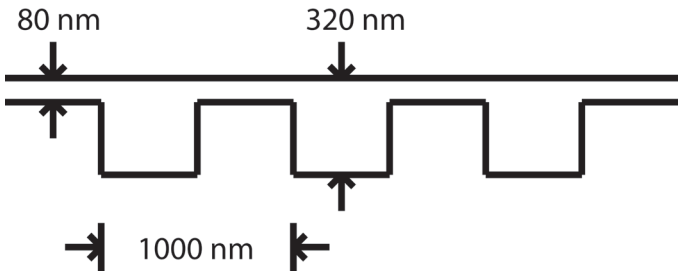

▲ Figure 1: Cross-section of basic device. The typical separation region length is 1 cm.

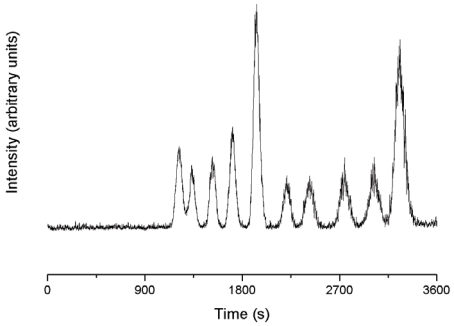

▲ Figure 2: Fluorescence intensity as a function of time. Separation of 100 bp to 1000 bp (100 bp interval) is achieved in less than 1 hr at 20 v/cm in an 80-nm thin-gap device.

REFERENCES

[1] C.F. Chou, R.H. Austin, O. Bakajin, J.O. Tegenfeldt, J.A. Castelino, S.S. Chan, E.C. Cox, H. Craighead, N. Darnton, T. Duke, J. Han, S. Turner, "Sorting biomolecules with microdevices," *Electrophoresis,* vol. 21, no. 1, pp. 81-90, Jan. 2000.

[2] J. Fu, P. Mao, and J. Han, " Nanofilter array chip for fast gel-free biomolecule separation," *App. Phys. Lett.*, vol. 87, no. 26, pp. 263902:1-3, Dec. 2005.

[3] A.G. Ogston, "The spaces in a uniform random suspension of fibres," *Transactions of the Faraday Society,* vol. 54, p. 1754, 1958.

[4] J.C. Giddings, E. Kucera, C.P. Russell, and M.N. Myers, " Statistical theory for the equilibrium distribution of rigid molecules in inert porous networks. Exclusion chromatography," *J. of Physical Chemistry,* vol. 72, no. 13, p. 4397, Dec. 1968

Patterned Periodic Potential-energy Landscape for Fast Continuous-flow Biomolecule Separation

J. Fu, J. Han
Sponsorship: NSF, Singapore-MIT Alliance, NIH NIBIB

Manipulation of charged biomolecules through confining environments has broad applications in life science. Recent progress in fabricating well-defined spatial constraints allows direct observation of novel molecular dynamic behavior in molecular-sized confining structures. Further, it shows exceptional promise for providing regular sieving media with superior separation performance. Here we demonstrate a continuous-flow, biomolecule-separation device that makes use of a patterned anisotropic sieving matrix consisting of a two-dimensional periodic array of nanofilters. The electrophoretic drift of biomolecules in the sieving medium involves a differential bidirectional motion through two-dimensional, periodically modulated, free-energy landscapes that results in a vectorial apparent electrophoretic mobility that directs molecules of different sizes to follow radically different paths. This method provides a novel basis for dispersing small fluid-borne biomolecules into distinct fractions. A fluorescently labeled dsDNA mixture (50-766 bp) used to characterize the device was separated in 1 minute with a resolution of about 10%. The patterned anisotropic sieve was also used for size-fractionation of SDS-protein complexes of size ranging from 11 to 200 kDa in 1 minute. By virtue of its gel-free and continuous-flow operation, this device suggests itself as a key component of an integrated microsystem that prepares and analyzes biomolecule samples.

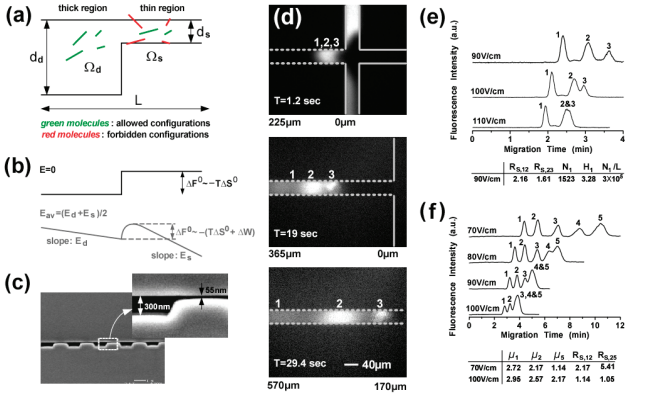

▲ Figure 1: (a) Partitioning of rigid, rod-like molecules in a slit-like nanofilter. (b) Free energy landscape of a nanofilter. (c) An SEM images of a periodic array of nanofilters with alternating thin and thick regions. (d-f) Separation of SDS-protein complexes (d & e) and dsDNA molecules (f) in a one-dimensional nanofilter array chip (d_s: 55 nm, d_d: 300 nm, L: 1 μm). Band assignment for SDS-protein complexes: (1) cholera toxin subunit B (MW: 11.4 kDa); (2) lectin phytohemaglutinin-L (MW: 120 kDa); (3) low-density human lipoprotein (MW: 179 kDa), for DNA: (1) 50 bp; (2) 150 bp; (3) 300 bp; (4) 500 bp; (5) 766 bp.

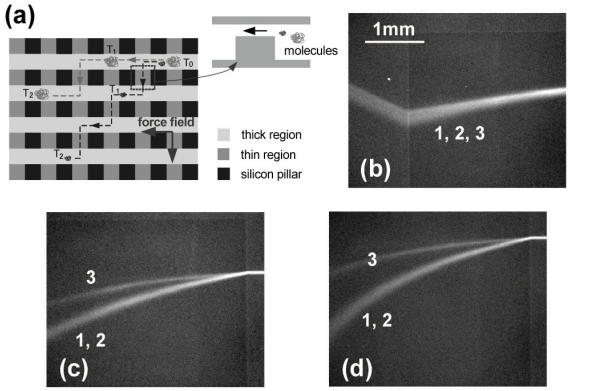

▲ Figure 2: (a) Bidirectional transport of biomolecules in the 2-D nanofilter arrays. (b) Fluorescence images of pulsefield separation of SDS complexes inside the 2-D nanofilter arrays. Different values of vertical and horizontal fields can be applied with different durations. Band assignments for SDS-protein are the same as in Figure 1.

REFERENCES

[1] J. Fu and J. Han, "Nanofilter array chip for fast gel-free biomolecule separation," *Appl. Phys. Lett.*, vol. 87, no. 26, pp. 263902-263904, Dec. 2005.

[2] J. Fu and J. Han, "A nanofilter array chip for fast gel-free biomolecule separation," in *Proc. Ninth Con. on Miniaturized Systems for Chemistry and Life Sciences* (*μTAS 2005*), Boston, Massachusetts, pp. 1531-1533, Oct. 2005.

Fabrication of Massively-parallel Vertical Nanofluidic Membranes for High-throughput Applications

P. Mao, J. Han
Sponsorship: KIST IMC, NSF

Nanofluidics has gained tremendous successes in the last few years because they provide unique capability in biomolecular manipulation and control. For nanofluidic applications, one critical issue is the availability of reliable, reproducible fabrication strategies for nanometer-sized structures. A simple technique, without nanolithography or special tools, has been developed to generate planar nanochannels with precise control of depths to the nanometer scale for many applications including separation [1] and preconcentration [2]. However, one big issue with these planar nanofluidic channels is the limited fluidic conductance that results in low throughput.

Here we describe a novel fabrication approach to generate massively-parallel vertical nanochannels with the well-controlled gap size down to 100 nm [3]. We use anisotropic wet etching (KOH) to make deep, vertical trenches on Si (110) substrate (Figure 1A). Alternatively, conventional deep reactive ion etching (DRIE) can be performed to produce very deep trenches, and then the sidewalls can be smoothed by a short KOH etching. Then the width of the trench channel is further decreased to a desired thickness even below 50 nm (Figure 1B), by growing thermal oxide. Also, backside etching of the Si wafer can yield thin membranes over a wide area (~ 6-inch wafer) with well-defined membrane thickness, if needed. Our method requires neither expensive nanolithography expertise nor other tools and allows the integration of a large number of narrow, vertical nanofluidic filters with fluidic conductance 10~100 times higher than planar nanochannels. Furthermore, we have demonstrated efficient, high-throughput separation of large DNA molecules in our vertical nanofilter array device based on the entropic trapping mechanism (Figure 2). We believe that these membrane devices could be a key to the high-throughput nanofluidic sample-preparation microsystems.

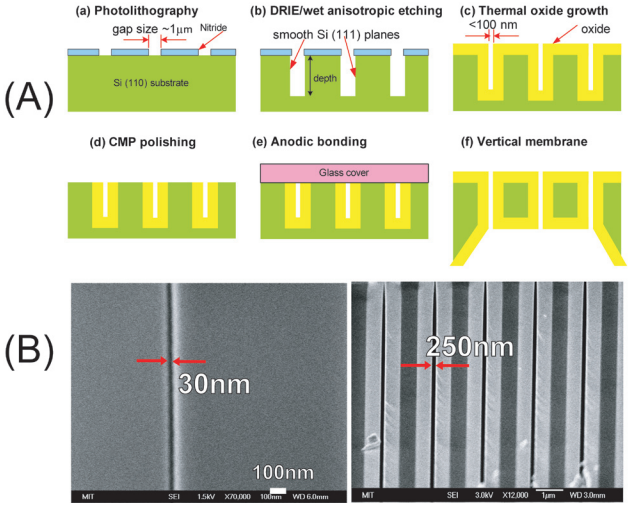

▲ Figure 1: (A) Schematic diagram of fabricating massively-parallel vertical nanofluidic membranes. (B) Cross-sectional SEM micrograph of vertical nanochannels with lateral gap sizes (widths) of 250 nm (left) and 30 nm (right).

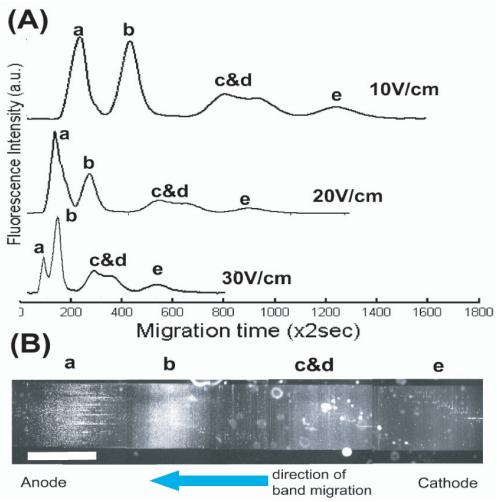

▲ Figure 2: (A) Separation of the mixture of λ-DNA and λ-DNA digested by Hind III in a lateral nanofilter array chip under different electrical fields. Peak assignment: (a) 48.5kbp,(b) 23kbp,(c) 9.4kbp,(d) 6.5kbp,and (e) 4.4kbp. (B) Direct observation of DNA bands separated at 10 V/cm. The scale bar is 1 mm.

REFERENCES

[1] J. Fu, P. Mao, and J. Han, "Nanofilter array chip for fast-gel-free biomolecule separation", *Appl. Phys. Lett.*, vol. 87, 263902, 2005

[2] Y. Wang, A. Stevens, and J. Han, "Million-fold preconcentration of proteins and peptides by nanofluidic filter", *Anal. Chem.*, vol. 77, pp. 4293-4299, 2005

[3] P. Mao and J. Han, "Fabrication and characterization of planar nanofluidic channels and massively-parallel nanofluidic membranes", in *Proc. of the MicroTAS 2005 Symposium*, Boston, USA, Oct. 2005

Continuous-flow pI-based Sorting of Proteins and Peptides in a Microfluidic Chip Using Diffusion Potential

Y.-A. Song, J. Han
Sponsorship: NSF CAREER Award, KIST-IMC, CSBi/Merck Fellowship

In this work, we have developed a simple microfluidic chip that can sort biomolecules based on their isoelectric point (pI) values in a simple buffer system. The new method differs from previous approaches such as transverse isoelectric focusing [1] or free-flow electrophoresis [2] in that this process involves no external power supply and no special ampholyte. Instead, we utilize the diffusion potential generated by the diffusion of different buffer ionic species *in situ* at the laminar flow junction. The use of diffusion potential in microfluidics was previously demonstrated with the mass transport of dye molecules between the two streams in [3]. However, they did not explicitly demonstrate a separation of two species. In our device, we establish a laminar flow junction between two buffers with different pH and concentrations. A potential gradient is developed across the liquid junction, generating a high-enough electric field to mobilize and to collect biomolecules at the boundary when their pI values fall between the two buffer pH values. The computational modeling shows a decreasing potential gradient from 17.1 V/cm to 6.9 V/cm along the 2-mm-long microchannel (20 μm deep, 100 μm wide), as the concentration gradient becomes shallower toward the end of the channel due to mixing (Figure 1). In our initial experiment, two pI-markers (Figure 2) as well as two proteins were successfully sorted in this device, with a flow rate of 5~10 μL/min. To characterize the accuracy of this pI-based sorting process, we tested sorting behavior of the device by changing the pH value of the sample buffer in 0.1 pH step. It was shown that a peptide can be sorted into a different output stream with a ~0.1pH unit resolution. We are currently working on the development of new buffer systems as well as on the hybrid approach with a superimposed external electric field to increase the sorting efficiency and resolution. Once fully developed, it can potentially be a pI-based sample fractionation tool for proteomic analysis of complex biomolecule samples.

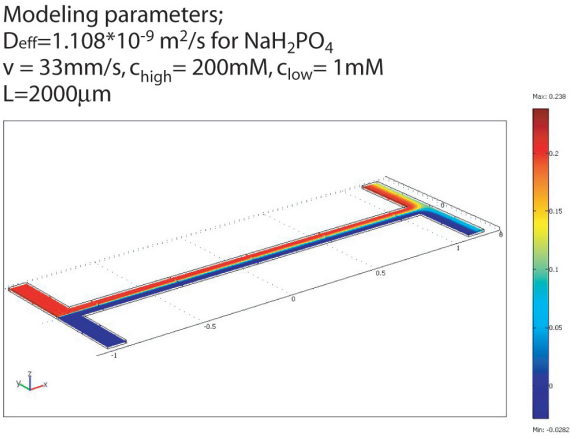

▲ Figure 1: A 3D steady-state concentration distribution in a 2-mm-long microfluidic channel with a concentration ratio of 200. Based on this concentration distribution, the diffusion potential as well as the potential gradient can be calculated.

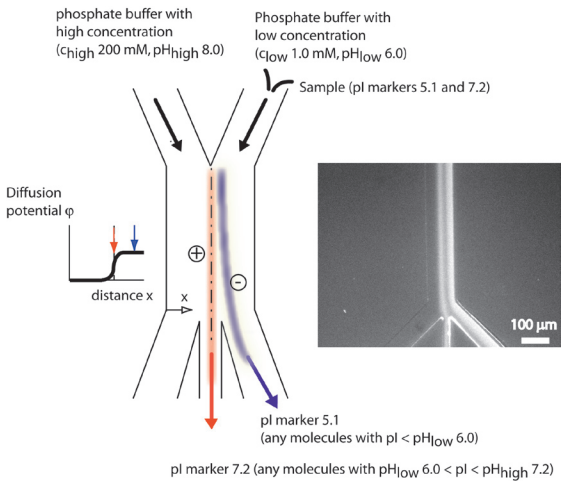

▲ Figure 2: Schematic view of the pI-based sorting process and separation of two pI markers with pI values of 5.1 and 7.2 using diffusion potential at a concentration difference of 200 and at a flow rate of 10 μl/min.

REFERENCES

[1] K. Macounova, C.R. Cabrera, and P. Yager, "Concentration and separation of proteins in microfluidic channels on the basis of transverse IEF" *Anal. Chem.*, vol. 73, pp. 1627–1633, 2001.

[2] C. Zhang and A. Manz, "High-speed free-flow electrophoresis on chip" *Anal. Chem.*, vol. 75, 2003, pp. 5759-5766.

[3] M. Munson, C. Cabrera, and P. Yager, "Passive electrophoresis in microchannels using liquid junction potentials" *Electrophoresis*, vol. 23, pp. 2642-2652, 2002.

Cell Stimulation, Lysis, and Separation in Microdevices

J. Albrecht, J. El-Ali, S. Gaudet, K.F. Jensen
Sponsorship: NIH

Quantitative data on the dynamics of cell signaling induced by different stimuli require large sets of self-consistent and dynamic measures of protein activities, concentrations, and states of modification. A typical process flow in these experiments starts with the addition of stimuli (cytokines or growth factors) to cells under controlled conditions of concentration, time, and temperature, followed at various intervals by cell lysis and the preparation of extracts. Microfluidic systems offer the potential to do this in a reproducible and automated fashion. Figure 1 shows quantification of the stimulation of a T-cell line with antibodies performed in a microfluidic device with integrated cell lysis. The device is capable of resolving the very fast kinetics of the cell pathways, with protein activation levels changing 4-fold in less than 15 seconds. The quantification of the lysate is currently performed off-chip using electrophoretic separation. To extract meaningful data from cellular preparations, many current biological assays require similar labor-intensive sample purification steps to be effective. Micro-electrophoretic separators have several important advantages over their conventional counterparts including shorter separation times, enhanced heat transfer, and the potential to be integrated into other devices on-chip. However, the high voltages required for these separations prohibit metal electrodes inside the microfluidic channel. A PDMS isoelectric focusing device with polyacrylamide gel walls has been developed to perform rapid separations by using electric fields orthogonal to fluid flow (Figure 2). This device has been shown to focus low molecular weight dyes, proteins, and organelles in seconds.

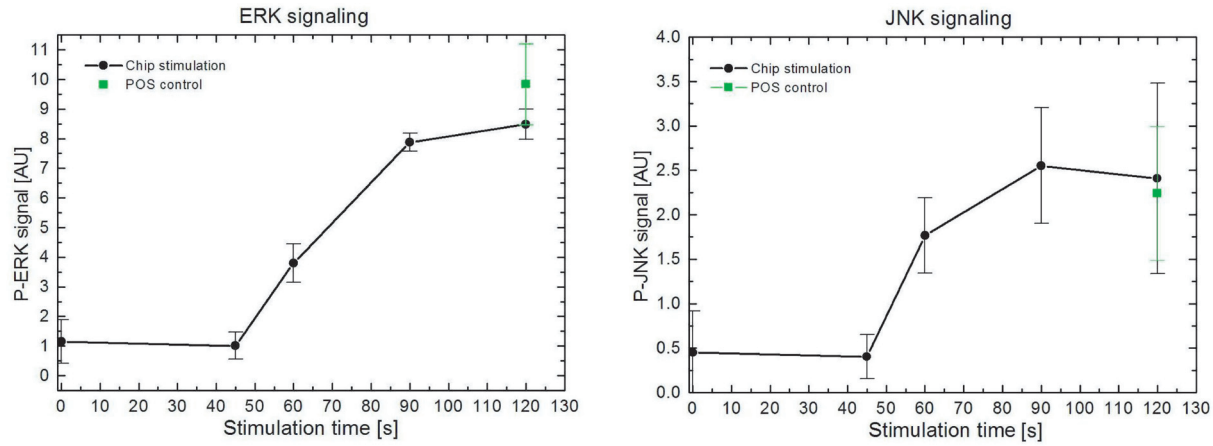

▲ Figure 1: ERK and JNK signaling in Jurkat E6-1 cells stimulated with α-CD3 for different times. Stimulation and cell lysis were performed with the microfluidic device (Chip stimulation) and with conventional methods (POS control). The error bars denote one standard deviation.

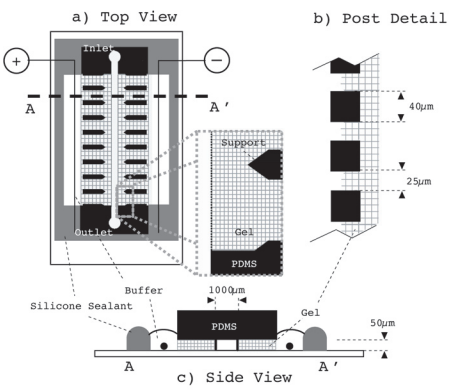

◀ Figure 2: Layout of transverse IEF device. Top view (a) shows the PDMS device with the sample channel bordered by left and right gel regions (cross-hatched areas) and anode and cathode, respectively. It is separated from the gel sections by 40 µm × 40 µm, 50 µm tall posts (b). The device presented has a single inlet and single outlet. Side view (c) shows the device in cross-section (not to scale).

Thermal Management in Devices for Portable Hydrogen Generation

B. Blackwell, M.A. Schmidt, K.F. Jensen
Sponsorship: ARO MURI

The development of portable-power systems employing hydrogen-driven solid oxide fuel cells continues to garner significant interest among applied science researchers. The technology can be applied in fields ranging from the automobile to personal electronics industries. This work focuses on developing microreaction technology that minimizes thermal losses during the conversion of fuels – such as light-end hydrocarbons, their alcohols, and ammonia – to hydrogen. Critical issues in realizing high-efficiency devices capable of operating at high temperatures have been addressed, specifically, thermal management, the integration of materials with different thermophysical properties, and the development of improved packaging and fabrication techniques.

A new fabrication scheme for a thermally insulated, high temperature, suspended-tube microreactor has been developed. The new design improves upon a monolithic design proposed by Arana *et al.*[1]. In the new modular design (Figure 1), a high-temperature reaction zone is connected to a low-temperature (~50°C) package via the brazing of pre-fabricated, thin-walled glass tubes. The design also replaces traditional deep reactive ion etching (DRIE) with wet potassium hydroxide (KOH) etching, an economical and time-saving alternative. A brazing formulation that effectively accommodates the difference in thermal expansion between the silicon reactor and the glass tubes has been developed.

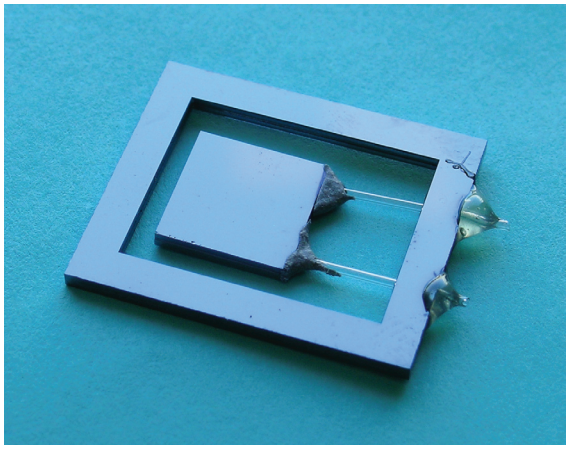

▲ Figure 1: Suspended-tube microreactor showing 2 pre-fabricated SiO_2 tubes, a microfabricated Si reaction chip, and a microfabricated Si frame. The modular design is assembled via a glass braze.

REFERENCES

[1] L.R. Arana, S.B. Schaevitz, A.J. Franz, Martin A. Schmidt, and K.F. Jensen, "A microfabricated suspended-tube chemical reactor for thermally-efficient fuel processing," *J. Microelectromechanical Systems*, vol. 12, pp. 600-612, 2003.

Autothermal Catalytic Micromembrane Devices for Portable High-Purity Hydrogen Generation

K. Deshpande, M.A. Schmidt, K.F. Jensen
Sponsorship: ARO MURI

The high efficiency and energy density of miniaturized fuel cells provide an attractive alternative to batteries in the portable power generation market for consumer and military electronic devices [1-3]. The best fuel cell efficiency is typically achieved with hydrogen, but safety and reliability issues remain with current storage options. Consequently, there is continued interest in reforming liquid fuels to hydrogen. The process typically involves high temperature reforming of fuel to hydrogen combined with a low temperature PEM fuel cell, which implies significant thermal loss. Owing to its high hydrogen content (66%) and ease of storage and handling, methanol is an attractive fuel. However, partial oxidation of methanol also generates some CO, which may poison the fuel cell catalyst.

Previously [4] we successfully demonstrated hydrogen purification using thin (~200 nm) Pd-Ag membranes using electrical heating. Further, integration of these devices with $LaNiCoO_3$ catalyst allowed methanol reforming at 475°C with 47% fuel conversion [5]. Since microreactors possess high surface area to volume ratio, minimizing heat loss is important. Hydrogen flux across the Pd membranes is an equilibrium controlled process. Thus to achieve thermal management, the unextracted hydrogen, generated CO, and unreacted methanol can be completely oxidized in a separate reactor.

In the current work, we explore the realization of autothermal hydrogen generation by fabricating silicon-based reactors using bulk micromachining techniques. The hydrogen generation unit comprises a 200-nm palladium-silver membrane coated with a reformer catalyst while the combustor is loaded with platinum catalyst. High thermal conductivity of silicon ensures autothermal operation. Upon thermal isolation using vacuum packaging [6], we characterize the performance of this integrated, autothermal hydrogen generation system in terms of energy efficiency and hydrogen production.

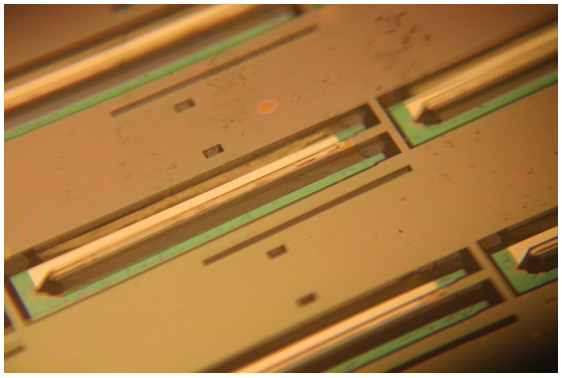

▲ Figure 1: Fabricated reformer-burner unit with palladium membranes.

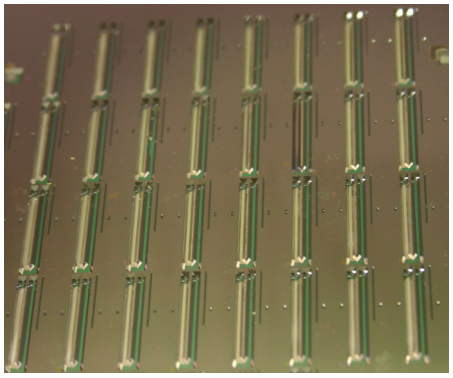

▲ Figure 2: Plan of silicon wafer with multiple reformer-burner units.

REFERENCES

[1] C.D. Baertsch, K.F. Jensen, J.L. Hertz, H.L. Tuller, S.T. Vengallatore, S.M. Spearing, and M.A. Schmidt, "Fabrication and structural characterization of self-supporting electrolyte membranes for a micro solid-oxide fuel cell," *J. Mater. Res.*, vol 19, no. 9, pp. 2604-2615, 2004.

[2] J.D. Morse, A.F. Jankowski, R.T. Graff, and J.P. Hayes, " Novel proton exchange membrane thin-film fuel cell for microscale energy conversion," *J. Vac. Sci. Technol. A.*, vol. 18, no. 4, pp. 2003-2005, 2000.

[3] J. Fleig, H.L. Tuller, and J. Maier, " Electrodes and electrolytes in micro-SOFCs: A discussion of geometrical constraints," *Solid State Ionics*, vol. 174, nos. 1-4, pp. 261-270, 2004.

[4] B.A. Wilhite, M.A. Schmidt, and K.F. Jensen, "Palladium-based micromembranes for hydrogen separation: Device performance and chemical stability, *Ind. Eng. Chem. Res.*, vol. 43, no. 22, pp. 7083-7091, 2004.

[5] B.A. Wilhite, S.J. Weiss, J. Ying, M.A. Schmidt, and K.F. Jensen "Demonstration of 23 wt % Ag-Pd micromembrane employing 8:1 $LaNi_{0.95}Co_{0.05}O_3$ /Al_2O_3 catalyst for high-purity hydrogen generation," *Adv. Mater.*, 2006, in press.

[6] L.R. Arana, S.B. Schaevitz, A.J. Franz, M.A. Schmidt and K.F. Jensen "A microfabricated suspended-tube chemical reactor for thermally efficient fuel processing," *J. Microelectromechanical Systems*, vol.12, no. 5, pp. 600-612, 2003.

Multiphase Transport Phenomena in Microfluidic Systems

A. Guenther, M.T. Kreutzer, K.F. Jensen
Sponsorship: Microchemical Systems Technology Center, ISN, Dutch Foundation for Applied Sciences (MTK)

Fluid interfaces provide unique opportunities for microfluidic and nanofluidic systems. Applications range from microscale heat exchangers and miniature fuel cells to microreactors for materials synthesis. Multiphase flow in such devices can be challenging, as the interfacial forces naturally favor axisymmetric geometries that are difficult to microfabricate. The advantages of surface tension dominated microfluidics include a much richer dynamic flow behavior and enhancement of heat and mass transfer by creating secondary flows. These advantages offer many uses beyond enabling gas-liquid and fluid-solid reactions [1].

In particular, we are interested in segmented flow of gas and liquid in hydrophilic channels. Figure 1 shows several key features of this flow for reaction purposes. The presence of bubbles reduces the amount of dispersion of liquid flowing through the channels, ensuring that reactants and products spend a uniform amount of time in the system. For nanoparticle synthesis in microfluidic networks, a uniform residence time distribution translates into narrowly distributed particle sizes [2-3]. Liquid segments are efficiently mixed by circulation motion and gas bubbles are separated from microchannel walls by only a thin film (thickness < 1 μm). Thin films reduce mass transfer resistance to components immobilized on the walls, such as catalysts [4] or analytical reagents and antibodies. We are also interested in the dynamics of multiphase flow through microchannels that are populated with a forest of micropillars (diameters: 50 μm – 100 μm). The observed flow patterns (Figure 2) connect to fundamental studies of flow in porous media and to catalysis. Gas-liquid and liquid-liquid flow patterns and their dynamics are determined in pulse-laser fluorescent micrographs and with microscale particle image velocimetry (PIV) measurements. Characteristics of such three-phase systems, such as persistent static fractions, axial dispersion and mixing, are compared with multiphase flow in macroscopic unstructured beds and porous media.

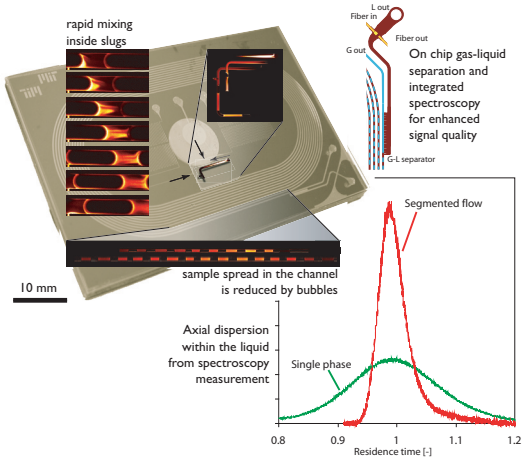

▲ Figure 1: Measurement of axial dispersion in single-phase (green curve) and segmented flow (red curve) through a 1.5 m long microchannel (300 μm wide, 300 μm deep) that is soft-lithographically patterned. To reduce background fluorescence in the integrated spectroscopy measurement, carbon black is dispersed in the PDMS, prior to molding.

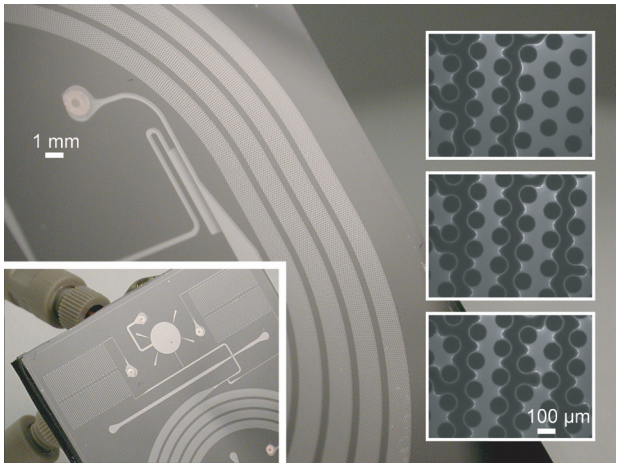

▲ Figure 2: Microchannel (width 1 mm, depth 300 μm) populated with 100 μm wide micropillars. The left inset shows the integrated gas-liquid feeding system. On the right side, fluorescent micrographs of instantaneous gas (dark) and liquid (bright) flow patterns between pillars are shown.

REFERENCES

[1] A. Guenther, S.A. Khan, F. Trachsel, M. Thalmann, and K.F. Jensen, "Transport and reaction in microscale segmented flow," *Lab on a Chip*, vol. 4, pp. 278-286, 2004.

[2] B.K.H. Yen, A. Guenther, M.A. Schmidt, K.F. Jensen, and M.G. Bawendi, "A microfabricated gas–liquid segmented flow reactor for high-temperature synthesis: The case of CdSe quantum dots," *Angewandte. Chemie – Int. Ed.*, vol. 44, pp. 5447-5451, 2005.

[3] A. Guenther, M. Jhunjhunwala, M. Thalmann, M.A. Schmidt, and K.F. Jensen, "Micromixing of miscible liquids in segmented gas liquid flow" *Langmuir*, vol. 21, pp. 1547-1555, 2005.

[4] M.T. Kreutzer, F. Kapteijn, J.A. Moulijn, and J.J. Heiszwolf, "Multiphase monolith reactors – chemical reaction engineering of segmented flow in microchannels," *Chem. Eng. Sci.*, vol. 60, pp. 5895-5916, 2005.

Microfluidic Synthesis and Surface Engineering of Colloidal Nanoparticles

S.A. Khan, K.F. Jensen
Sponsorship: Microchemical Systems Technology Center

Metal oxide colloidal particles such as silica (SiO_2) and titania (TiO_2) have many diverse applications ranging from catalysis, pigments and photonic band-gap materials to health care products. There has also been considerable research interest over the last decade in fabricating core-shell materials with tailored optical and surface properties. Core-shell particles such as titania-coated silica often exhibit improved physical and chemical properties over their single-component counterparts and hence are potentially useful over a broader range of applications. Newer methods of engineering such materials with controlled precision are required to overcome the difficulties with conventional production techniques, which are limited to multi-step batch processes. We have developed microfluidic routes for synthesis and surface-coating of colloidal silica and titania particles.

The chief advantages of a microfluidic platform are precise control over reactant addition and mixing and continuous operation. Microfluidic chemical reactors for the synthesis and overcoating of colloidal particles are shown in Figure 1a and Figure 1b, respectively [1-2]. Figure 2a is an SEM micrograph of silica particles synthesized in a microreactor (Figure 1a) operated in segmented gas-liquid flow mode. Figure 2b shows a silica nanoparticle coated with a thick shell of titania. We have also fabricated integrated devices combining synthesis and overcoating to enable continuous multi-step synthesis of core-shell particles.

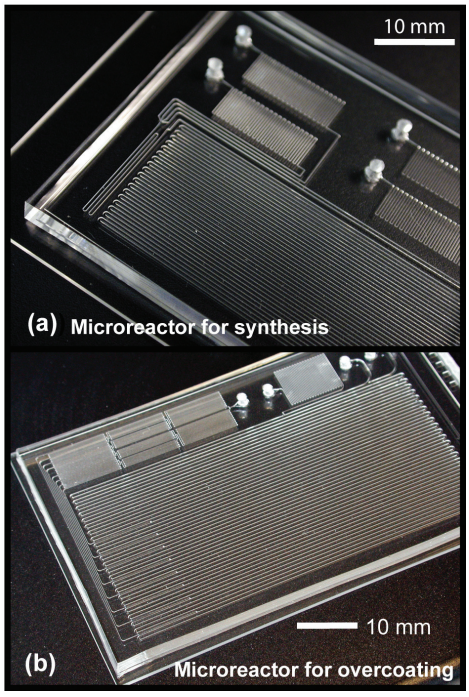

▲ Figure 1: Microfluidic reactor for (a) synthesis of colloidal silica, fabricated in PDMS, and (b) overcoating thick titania shells on silica particles.

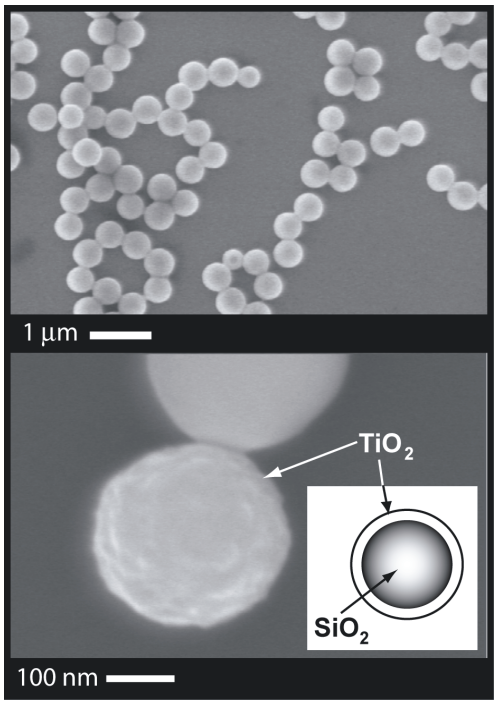

▲ Figure 2: (a) Silica synthesized in microreactor and (b) titania-coated silica.

REFERENCES:

[1] S.A. Khan, A. Günther, M.A. Schmidt, and K.F. Jensen, "Microfluidic synthesis of colloidal silica" *Langmuir*, vol. 20, no. 20, pp. 8604-8611, June 2004.

[2] S.A. Khan and K.F. Jensen, "Microfluidics surface-engineering of colloidal particles," in *Proc. µTAS 9*, Boston, MA, Oct. 2005, pp. 265-266.

Microreactor Enabled Multistep Chemical Synthesis

E.R. Murphy, H. Sahoo, J. Kralj, N. Zaborenko, K.F. Jensen
Sponsorship: Pacific Scientific

As a demonstration of how microsystems can enable quantitative study and improved production of chemistries that have been too hazardous to pursue via traditional means, the kinetics of direct sodium nitrotetrazolate (NaNT) synthesis were characterized and a microsystem for its commercial production has been constructed (Figure 1). A PDMS modular microreactor system capable of both multi-step synthesis and rapid scale-out was constructed. This system minimized the necessary volume of the unstable diazonium intermediate, enabling the study of NaNT, an energetic material used in the construction of fire suppression systems that was too dangerous to test with traditional techniques. In the direct synthesis of NaNT, 5-aminotetrazole (5-AT) reacts with nitrous acid to produce the diazonium intermediate that, in a second reaction, undergoes a Sandmeyer type reaction that displaces the diazonium group by the nitrite ion. The rapid mixing and safety advantages of microsystems were incorporated into a flexible architecture, presenting an improved ability to safely probe the conditions of the reaction. The modular design of this system also enabled the same set of modules to be rearranged as parallel reactor chains for small-scale production. A second generation microsystem was constructed from silicon micromixer modules (Figure 2); this micro-system is not only more robust than the PDMS design but also capable of accommodating higher flow rates (>2 mL/min) and higher temperatures. This system allows higher throughput and longer operational lifetimes and is currently being optimized for use as a full-scale production platform.

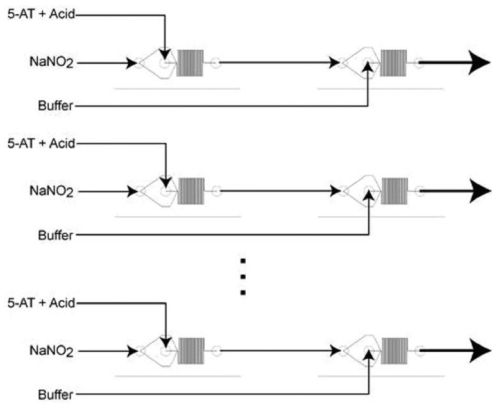

▲ Figure 1: Modular microsystem serial and parallel micromixer modules.

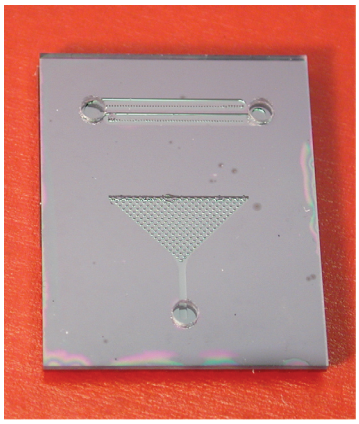

▲ Figure 2: Silicon micromixer module (top view).

REFERENCES

[1] A.F. Hegarty, "Kinetics and mechanisms of reactions involving diazonium and diazo groups," in *The Chemistry of Diazonium and Diazo Groups*, S. Patai, Ed. Chichester, New York: Wiley, 1978.

[2] J. Kralj, E.R. Murphy, K.F. Jensen,, M. Williams, and R. Renz, "Preparation of sodium nitrotetrazolate using microreactor technology," *41st AIAA/ASME/SAE/ASEE Joint Propulsion Conference and Exhibit*, Tucson, Arizona, July 10-13, 2005.

Integrated Microreactor System

H.R. Sahoo, E.R. Murphy, A. Guenther, N. Zaborenko, K.F. Jensen
Sponsorship: Deshpande Center for Technological Innovation

The realization of integrated microchemical systems will revolutionize chemical research by providing flexible tools for rapid screening of reaction pathways, catalysts, and materials synthesis procedures, as well as faster routes to new products and optimal operating conditions. Moreover, such microsystems for chemical production will require less space, use fewer resources, produce less waste, and offer safety advantages. The need for synthesizing sufficient quantities of chemicals for subsequent evaluation dictates that microchemical systems are operated as continuous systems. Such systems require fluid controls for adjusting reagent volumes and isolating defective units. The integration of sensors enables optimization of reaction conditions as well as the extraction of mechanistic and kinetic information.

We are developing integrated microchemical systems that have reactors, sensors, and detectors with optical fibers integrated on one platform. We are exploring new approaches for connecting modular microfluidic components into flexible fluidic networks. Real-time control of reaction parameters using online sensing of flowrate, temperature, and concentration allows for precise attainment of reaction conditions and optimization over a wide range of temperatures and flow-rates. The multiple microreactors on the system can be used together to give higher throughputs or they can be used independently to carry out different reactions at the same time. Figure 1 shows a schematic of an integrated microreactor platform along with an early stage microreactor "circuit board" [1].

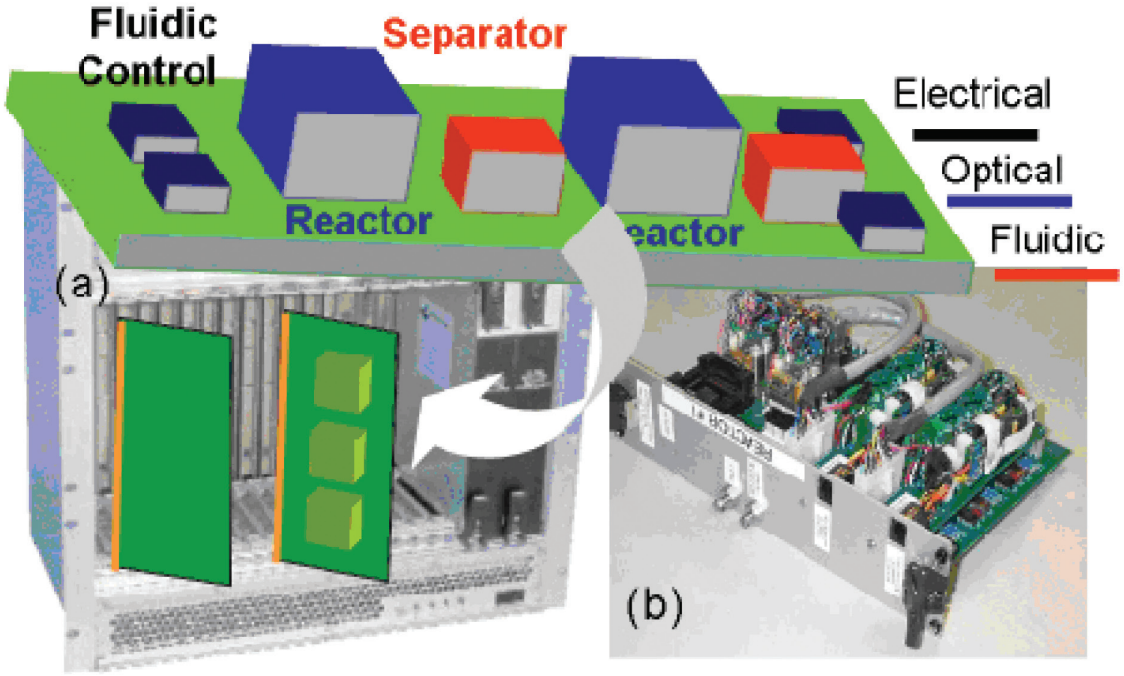

▲ Figure 1: Schematic of an integrated microreactor platform along with an early stage microreactor "circuit board" [1].

REFERENCES

[1] D.J. Quiram, "Characterization and Systems Integration of Microreactors," Ph.D. Thesis, Massachusetts Institute of Technology, Cambridge, 2002.

Crystallization in Microfluidic Systems

M. Sultana, K.F. Jensen
Sponsorship: Merck, Lucent Technologies

Microfluidic systems offer a unique toolset for discovering new crystal polymorphs and for studying the growth kinetics of crystal systems because of well-defined laminar flow profiles and online optical access for measurements. Traditionally, crystallization has been achieved in batch processes that suffer from non-uniform process conditions across the reactors and chaotic, poorly controlled mixing of the reactants, resulting in polydisperse crystal size distributions (CSD) and impure polymorphs. This reduces reproducibility and manufactures products with inhomogeneous properties. The short length scale in microfluidic devices allows for better control over the process parameters, such as the temperature and the contact mode of the reactants, creating uniform process conditions. Thus, these devices have the potential to produce crystals with a single morphology and a more uniform size distribution. In addition, microfluidic systems decrease waste, provide safety advantages, and require only minute amounts of reactants, which is most important when dealing with expensive materials such as pharmaceutical drugs.

Figure 1 shows a microfluidic device used for crystallization and Figure 2 shows optical images of different shapes and sizes of glycine crystals produced in reactor channels. A key issue for achieving continuous crystallization in microsystems is to eliminate heterogeneous crystallization – irregular and uncontrolled formation and growth of crystals at the channel surface, which ultimately clogs the reactor channel. We have developed a sheath flow microcrystallizer using microfabrication and hot embossing of poly(dimethylsiloxane) (PDMS) and cyclic olefin copolymer (COC) to prevent heterogeneous crystallization. We are currently working on integrating an online spectroscopy tool for *in situ* polymorph detection. Our ultimate goal is to develop an integrated microfluidic system for continuous crystallization with the ability to control polymorphism and online detection.

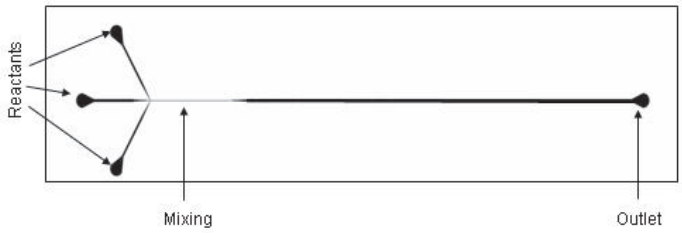

▲ Figure 1: Microfluidic reactor used for crystallization.

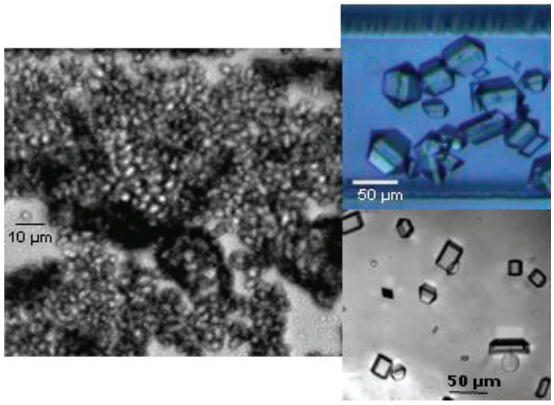

▲ Figure 2: Different sizes and shapes of glycine crystals produced in reactor channel.

Microreactors for Synthesis of Quantum Dots

B.K.H. Yen, A. Günther, M.A. Schmidt, M.G. Bawendi, K.F. Jensen
Sponsorship: Microchemical Systems Technology Center, NSF, ISN

We have fabricated a gas-liquid segmented flow reactor with multiple temperature zones for the synthesis of quantum dots (QDs). In contrast to single-phase flow reactors, the segmented flow approach enables rapid mixing and narrow residence-time distributions, factors which have a strong influence on the ultimate QD size distribution. The silicon-glass reactor accommodates a 1-m long reaction channel (hydraulic diameter ~400-μm) and two shallow side channels for collecting reaction aliquots (Figure 1). Two temperature zones are maintained, a heated reaction region (>260°C) and a cooled quenching region (<70°C). As a model system, monodisperse CdSe QDs with excellent optical properties were prepared using the reactor. Cadmium and selenium precursor solutions are delivered separately into the heated section. An inert gas stream is introduced further downstream to form a segmented gas-liquid flow, thereby rapidly mixing the precursors and initiating the reaction. The reaction is stopped when the fluids enter the cooled outlet region of the device. Under conditions for a typical synthesis, the gas and liquid segments are very uniform (Figure 2a-b), and the QDs produced in the reactor possess narrow spectral features, indicative of monodisperse samples. The narrow particle size distributions arise directly from the enhanced mixing and narrow residence-time distribution realized by the segmented flow approach. Furthermore, the QD size can be tuned without sacrificing monodispersity by varying the Cd and Se precursor flow rates. In Figure 2d, the Se/Cd molar ratio was varied while keeping the total liquid and gas flow rates constant. Decreasing Se/Cd results in a substantial red shift of the QD effective band-gap (first absorption feature and photoluminescence peak), corresponding to larger QD diameters.

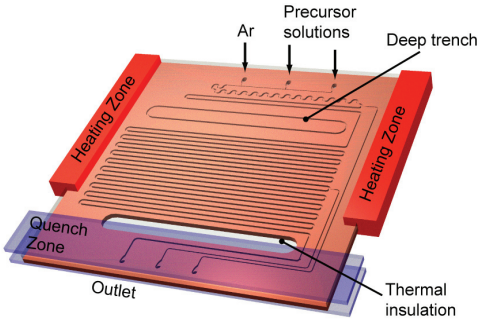

▲ Figure 1: Diagram of the reactor with heated reaction and cooled outlet regions. A through-etch section ensures that the two regions are thermally isolated. Channels etched in silicon (0.65-mm thick) were first passivated with an oxide layer (0.5-μm) and then sealed with an anodically bonded Pyrex wafer (0.76-mm thick).

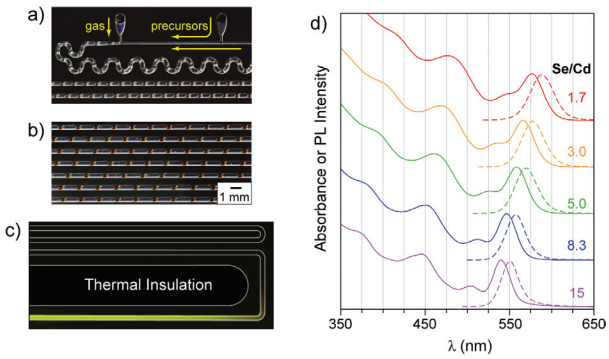

▲ Figure 2: Images of the a) heated inlet and b) main channel sections of device during synthesis. Red segments: CdSe QD reaction solution. Dark segments: Ar gas. c) Time-exposure image of the cooled outlet region under UV irradiation. At reaction temperature (260°C), the QD photoluminescence (PL) is completely quenched, but once the fluid reaches the cooled region (<70°C), yellow PL is observed. d) The QD absorbance (solid) and PL (dotted) spectra obtained by varying the precursor feed ratio. The Se/Cd molar ratio is indicated.

REFERENCES

[1] B.K.H. Yen, A. Günther, M.A. Schmidt, K.F. Jensen, and M.G. Bawendi, "A microfabricated gas-liquid segmented flow reactor for high temperature synthesis: The case of CdSe quantum dots," *Angew. Chem. Int. Ed.*, vol. 44, no. 34, pp. 5447-5451, Aug. 2005.

Polymer-based Microbioreactors for High Throughput Bioprocessing

Z. Zhang, G. Perozziello, Patrick Boyle, P. Boccazzi, A.J. Sinskey, K.F. Jensen
Sponsorship: DuPont-MIT Alliance

This project aims at developing high-throughput platforms for bioprocess developments. Based on the membrane-aerated microbioreactor [1], we have realized a microliter-volume, actively-mixed, and polymer-based microbioreactor by microfabrication and precision machining of PDMS and PMMA for batch [2] and continuous cultures [3] of microbial cells. Biological applications of microbioreactors, such as global gene expression of yeast cells [4], were demonstrated, and the parallel operation of multiple batch fermentations was realized by a multiplexed system [5].

As a very important operation for bioprocess developments, fed-batch process allows extensive control over environmental conditions in fermentations. Fed-batch fermentations in the microbioreactor were made possible by applying water evaporation through the PDMS membrane as a fluidic exit, and by combining passive feeding of water and active feeding of base, acid, and glucose solutions. Commercial microvalves were used to control pressure-driven liquid feeds to realize closed-loop pH control in the microbioreactor. For *Escherichia coli* fermentations, the pH value was successfully maintained within a certain range (Figure 1). Cells were physiologically healthier and remained active for longer periods of time (as shown by the dissolved oxygen curve), which in return yielded significantly higher biomass concentration at the end of experiments.

The microbioreactor was also integrated with the plug-*n*-pump microfluidic connectors [6], as well as incorporation of fabricated polymer micro-optical lenses and connectors for biological measurements to realize "cassettes" of microbioreactors (Figure 2). The fabrication process included precision machining and thermal bonding of PMMA devices. These integrations greatly simplified the setup and operation procedure and increased the signal-to-noise ratio for optical measurements for the cassettes, thus made the microbioreactors more compatible with high-throughput bioprocessing in multiplexed systems.

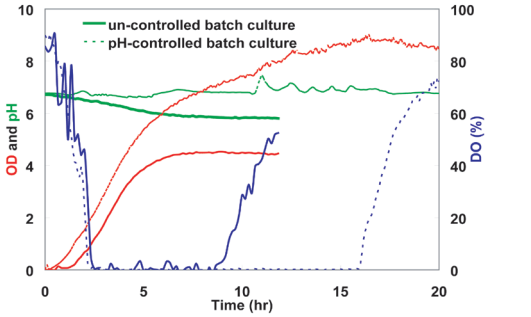

▲ Figure 1: Comparison of batch culture of E. coli FB21591 in rich LB media containing 8g/L glucose and 0.1 mol/L MES.

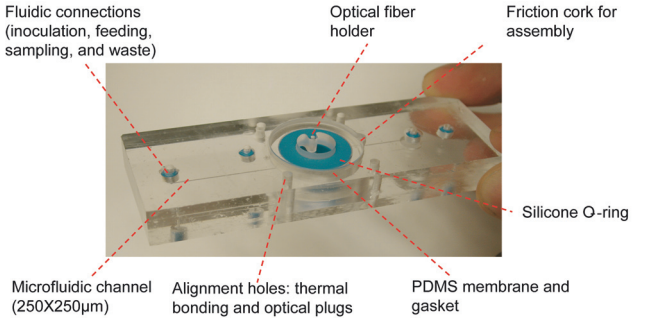

▲ Figure 2: Top view photograph of assembled and bonded microbioreactor "cassette."

REFERENCES:

[1] A. Zanzotto, N. Szita, P. Boccazzi, P. Lessard, A.J. Sinskey, and K.F. Jensen, "A membrane-aerated microbioreactor for high-throughput bioprocessing," *Biotechnology and Bioengineering*, vol. 85, pp. 376-381, 2004.

[2] Z. Zhang, N. Szita, P. Boccazzi, A.J. Sinskey, and K.F. Jensen, "A well-mixed, polymer-based microbioreactor with integrated optical Measurements," *Biotechnology and Bioengineering*, vol. 93, pp. 286-296, 2006.

[3] Z. Zhang, P. Boccazzi, H.-G. Choi, G. Perozziello, A.J. Sinskey, K.F. Jensen, "Microchemostat –microbial continuous culture in a polymer-based, instrumented microbioreactor." *Lab on a Chip*, to be published.

[4] P. Boccazzi, Z. Zhang, K. Kurosawa, N. Szita, S. Bhattacharya, K. Jensen, and A. Sinskey, "Differential gene expression analysis of *Saccharomyces Cerevisiae* Grown in Micro-scale Bioreactors Equipped with Internal Stirring, Sensors for *in-situ* and Real-time Measurements of growth kinetics." *Biotechnology Progress,* to be published.

[5] N. Szita, P. Boccazzi, Z. Zhang, P. Boyle, A.J. Sinskey, and K.F. Jensen, "Development of a multiplexed microbioreactor system for high-thoughput bioprocessing." *Lab on a Chip,* vol. 5, pp. 819-826, 2005.

[6] G. Perozziello, K.F. Jensen, J.E. Mc Cormack, F. Bundgaard, and O. Geschke, "Plug'n'pump fluidic interconnection," in *Proc. of μTAS*, 2004, pp. 575-577.

Micro-fluidic Bioreactors for Studying Cell-Matrix Interactions

S. Chung, P. Mack, V. Vickerman, J. Hsu, R. Kamm
Sponsorship: NIBIB, Draper Laboratories

Mechanical forces are important regulators of cell biology in health and disease. Cells in the vascular system are subjected to fluid shear stress, cyclic stretch, and differential pressure [1]. Numerous investigations have revealed the vast pathological and physical responses of endothelial cells to fluid shear stress by culturing the cells on the rigid surfaces of a flow chamber. This approach, however, fails to mimic the true environment of cells *in vivo* that grow on flexible, porous basement membranes with a defined microstructure [1-4]. In order to create an improved model for this *in vivo* condition, we developed a new microfluidic bioreactor system that enables us to study cell-matrix interactions on soft substrates made of gel under conditions of controlled shear stress and pressure difference. A gel cage consisting of three thin layers (Figure 1) is constructed from PDMS using a silicon master made by the deep RIE process. Flow chambers, also made of PDMS, are cured on an SU-8 patterned master. Separate channels are included that allow for filling this central chamber with a gel that mimics the extracellular matrix and also allows for independent control over the flows in the upper and lower channels. The assembled bioreactor is shown in Figure 2. To conduct experiments, we introduce a peptide solution into the gel cage, allow it to gel, and then seed cells on the gel surface exposed through the holes of gel cage. After cell adhesion, the flow chambers are sealed by the application of a vacuum to the top and bottom sides of the gel cage. Flows are then applied to each chamber with controlled pressures and flow rates. With this system, we will apply controlled shear stress and pressure on the cell layers. We plan to study the process of angiogenesis that entails the growth of vascular sprouts emanating from one endothelial surface and connecting with the other.

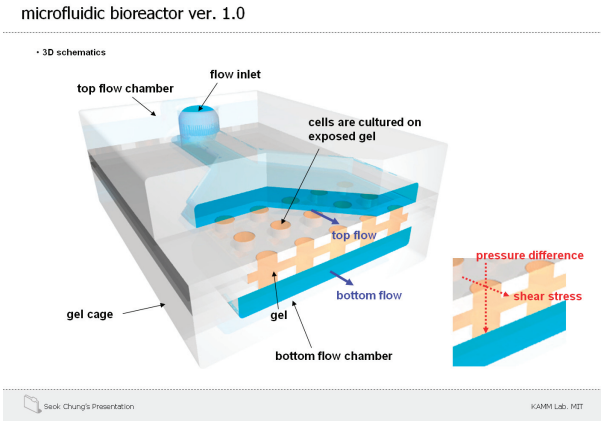

▲ Figure 1: Schematic drawing of microfluidic bioreactor. All layers are made of PDMS. Cells are cultured on exposed surfaces of gel in the holes of the gel cage; flows are induced in the channels above and below the gel cage.

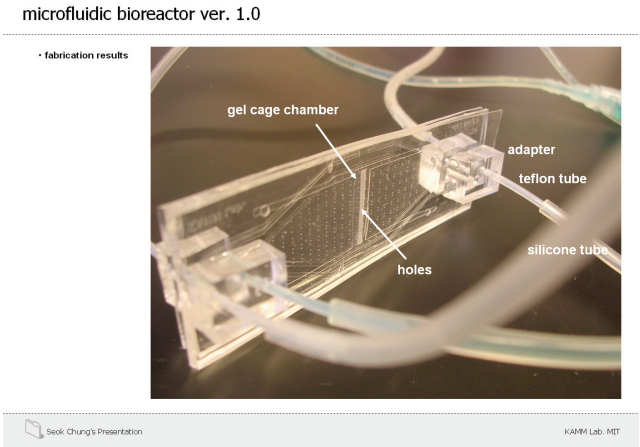

▲ Figure 2: Photograph of the fabricated and bonded bioreactor. The gel cage consists of 3 PDMS layers, bonded by oxygen plasma. Flow chambers above and below the gel cage are fixed by vacuum connected by silicon tubes.

REFERENCES

[1] L. You and C.R. Jacobs, "Cellular mechanotransduction," in *Nanoscale Technology in Biological Systems*, CRC Press, Fl, USA 2005.

[2] J.M. Tarbell, S. Weinbaum, and R.D. Kamm, "Cellular fluid mechanics and mechanotransduction," *Annals of Biomedical Eng.*, vol. 33, no. 12, pp. 1719-1723, 2005.

[3] C.G. Galbraith, R. Skalak, and S. Chien, "Shear stress induces spatial reorganization of the endothelial cell cytoskeleton," *Cell Motil. Cytoskeleton* 40, pp. 317-330, 1998.

[4] C.S.Chen, J.Tan, and J.Tien, "Mechanotransduction at cell-matrix and cell-cell contacts," *Ann. Rev. of Biomedical Eng.*, 6, pp. 275-302, 2004.

A Nanoscanning Platform for Biological Assays

S. Kim, S. Gouda, S.-G. Kim (P. So group)
Sponsorship: Intelligent Microsystems Center

An in-plane nanoscanning platform with switchable stiffness being developed at the Micro & Nano Systems Laboratory (MNSL) [1] can be an alternative to the existing atomic force microscope (AFM) system. The nanoscanning platform has a carbon nanotube (CNT) tip, which is known as one of the ideal candidates for AFM tips because of their superior mechanical and chemical properties. Raman Spectroscopy has gained a lot of interest as a tool for single molecule detection since it has easy and fast sample preparation and measurement compared to the existing technologies, such as X-ray crystallography and nuclear magnetic resonance. Among the several approaches attempted in order to enhance the weak Raman signals is tip enhanced raman spectroscopy (TERS). The enhancement of the electric field due to the plasmon resonance on the coated metal surface was predicted qualitatively [2]. The metal-coated CNT or CNT filled with Ag, Au, or Cu with a small diameter tip and high aspect ratio is ideal for TERS. The switchable stiffness AFM can work as a tool for imaging and placing the tip at the sub-nanometer proximity to a soft, molecular-scale biological sample, which would enhance the Raman signals.

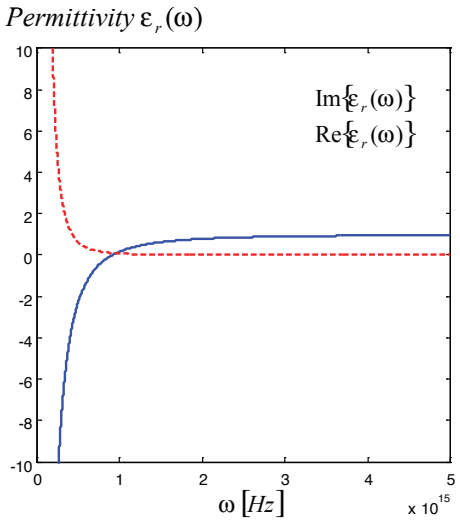

▲ Figure 1: Dependency of frequency on the permittivity of silver. The negative sign of the real part of permittivity contributes to the enhancement of the electric fields near the metal surface.

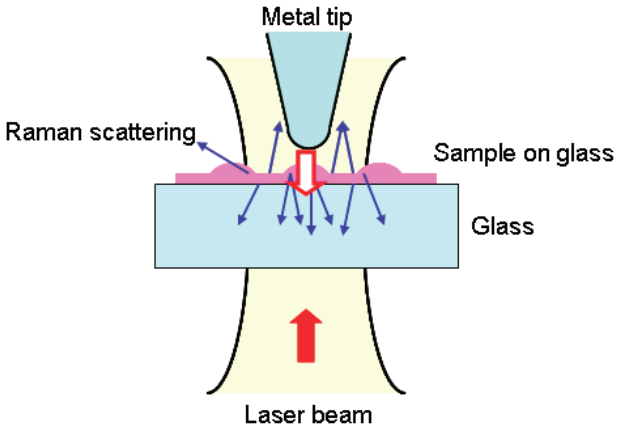

▲ Figure 2: Schematic of TERS showing the enhancement of electric fields near the metal tip or metal-coated CNT tip.

REFERENCES

[1] C. Mueller-Falcke, S.D. Gouda, S. Kim, and S. Kim, "A nano-scanning platform for bio-engineering: an in-plane probe with switchable stiffness," *Nanotechnology*, vol. 17, pp. 69-76, 2006.

[2] C.F. Bohren and D.R. Huffman, *Absorption and Scattering of Light by Small Particles*. New York: John Wiley & Sons, Inc., 1983.

A Large Strain, Arrayable Piezoelectric Microcellular Actuator

Z.J. Traina, S.-G. Kim
Sponsorship: Korean Institute of Metallurgy and Manufacturing (KIMM)

To provide a competitive actuating solution, micro-electromechanical-systems (MEMS)-based actuators need low operating power and form factors. Piezoelectrics provide substantially higher work-output/volume for a given voltage, when compared to other actuating solutions. A bow amplifier constructed of SU-8 beams and short length flexural pivots has been designed [1] and has demonstrated an amplification ratio of greater than 10:1. Current research focuses on increasing this amplification ratio and achieving the goal of 10% axial strain, while reducing parasitic out-of-plane bending inherent in the current fabrication process.

The overall goal of this project is to array one such actuator massively in series and in parallel in order to create a macro-scale, muscle-like actuator. Such a device would have widespread applications in mobile robotics, medicine, and aero/astronautics, where low power, high efficiency, and small form factors might be required.

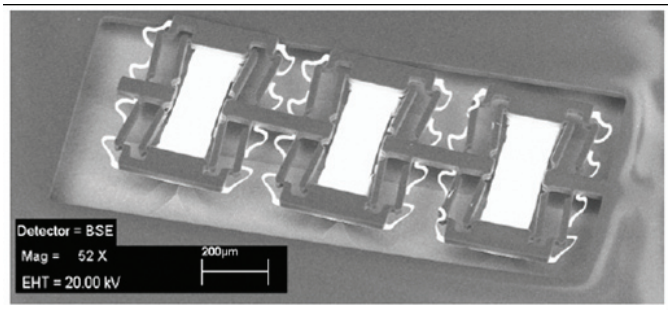

▲ Figure 1: SEM image of three-unit cell bow actuators developed by N. Conway and S.G Kim, fabricated in series. Peak static displacement measured via microvision was 1.18 µm at 10V, with peak blocking force 55 µN.

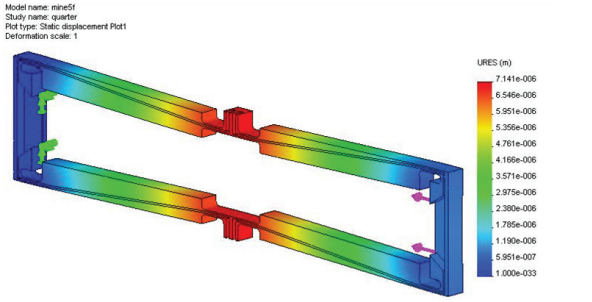

▲ Figure 2: Finite Element Analysis (FEA) of a second revision micro-cellular actuator, showing axial strain in excess of 10%, (up to 15 µm per cell), with an amplification ratio greater than 14:1. Predicted blocking force is on the order of 10 µN.

REFERENCES

[1] N. Conway and S.-G. Kim, "MEMS Amplification of Piezoelectric Strain for In Plane Actuation," Master's Thesis, Massachusetts Institute of Technology, Cambridge, 2003.

Self-powered Wireless Monitoring System Using MEMS Piezoelectric Micro Power Generator

R. Xia, C. Farm, W. Choi, S.-G. Kim
Sponsorship: NSF, Korean Institute of Machinery and Materials

A thin-film lead zirconate titanate $Pb(Zr,Ti)O_3$ (PZT), MEMS Piezoelectric Micro Power Generator has been integrated with a commercial wireless sensor, Telos, to simulate a self-powered RF temperature monitoring system (Figure 1). Such a system has many important applications, ranging from structure to rotary system monitoring. Telos consumes 2270 μJ for 221 ms per measurement. The PMPG and power management module are designed to satisfy such power requirements

The first prototype of PMPG provides an average 1 μW, with a natural frequency of 13.9 kHz (Figure 2). It has an energy density of 0.74 mW-h/cm^2, which compares favorably to lithium ion batteries [1]. The second generation PMPG is designed to provide 0.173 mW of power at 3 V with a natural frequency of 150 Hz and maximum strain of 0.12% [2]. We increased the effective mass of the PMPG by adding a Si substrate with thickness of 525 μm to the beam structure. The increase in the effective mass increases the energy store in the device and its power output. The beam length is also increased to achieve a low resonant frequency. The third generation PMPG will use a serpentine structure, which can achieve a low frequency with minimum volume.

Since PMPG offers limited power, a storage capacitor and a power management module are implemented to power the sensor node at discrete time intervals [3]. The PMPG is first connected to a rectifier that converts AC to DC voltage. Each cycle consists of a charging interval, in which PMPG charges the capacitor, and operation intervals, in which Telos uses the energy from capacitor. We developed a test bed, which mimics that of a liquid gas pipe used in the Alaska where the PMPG device will be used to generate power for temperature sensors. Scaling/dimension factors as well as cost and robustness are considered in the design.

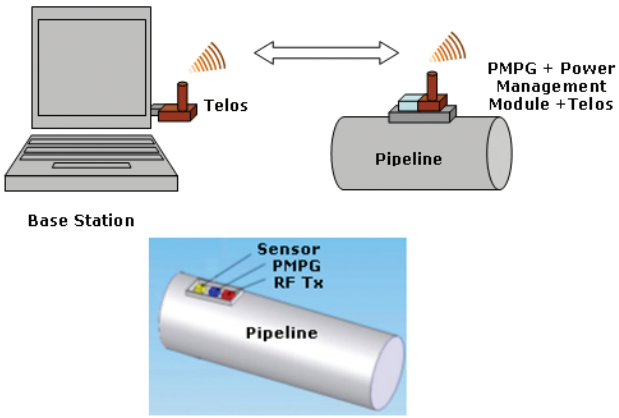

▲ Figure 1: Schematic of self-powered wireless monitoring system.

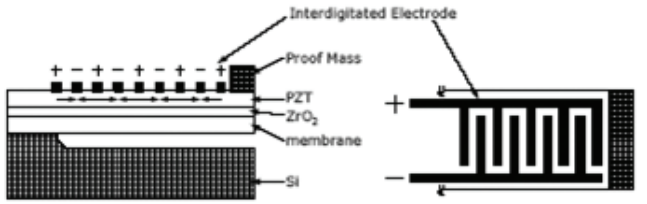

▲ Figure 2: First prototype for PMPG.

REFERENCES

[1] Y.R. Jeon, Sood, J.H. Jeong, S.G. Kim, "Piezoelectric micro power generator for energy harvesting," *Sensors and Actuators A: Physical,* 2005, in press.

[2] B.L. Wardle, N.E. DuToit, and S.G. Kim, "Design considerations for MEMS-scale piezoelectric variation energy harvesters," *Integrated Ferroelectric,* vol. 71, pp. 121-160, 2005.

[3] W.J. Choi, Y. Xia, J.A. Brewer, and S.G. Kim, "Energy harvesting MEMS device based on thin-film piezoelectric cantilevers," in *Proc. of INSS05,* San Diego, CA, June 27-28, 2005.

MEMS Pressure-sensor Arrays for Passive Underwater Navigation

V.I. Fernandez, S.M. Hou, F.S. Hover, J.H. Lang, M.S. Triantafyllou
Sponsorship: NOAA: MIT Sea Grant College Program

MEMS pressure sensors have had broad applications in fields such as mining, medicine, automobiles, and manufacturing. Another application to be explored is in underwater vehicular navigation. Objects within a flow generate pressure variations that characterize the objects' shape and size. Sensing these pressure variations allows the unique identification and location of obstacles for navigation (Figure 1). This concept is inspired by existing biological systems. Fish have such a sensory lateral line, which they use to monitor all aspects of their hydrodynamic environment, including obstacles [2,5].

We propose to develop low-power sensors that passively measure dynamic and static pressure fields with sufficient resolution to detect objects generating the disturbance. We will also develop processing schemes that use the information from the sensors to identify objects in the flow environment. These sensors and processing software emulate the capabilities of the lateral line in fish. While active acoustic means can be used for object detection, the process is power-intensive, and depends strongly on the acoustic environment. A simpler alternative is to use a passive system that can resolve the pressure signature of obstacles. The system consist of arrays of hundreds or thousands of piezoresistive pressure sensors fabricated on etched silicon and Pyrex wafers [1,3,4,6] with diameters around 1 mm; the sensors are arranged over a flat or curved surface in various configurations, such as a single line, a patch consisting of several parallel lines (Figure 2), or specialized forms to fit the hull shape of a vehicle or its fins. The sensors will be packaged close together at distances of a few millimeters apart in order to resolve pressure and flow features near the array spacing, which in turn can be used to identify the overall features of the flow.

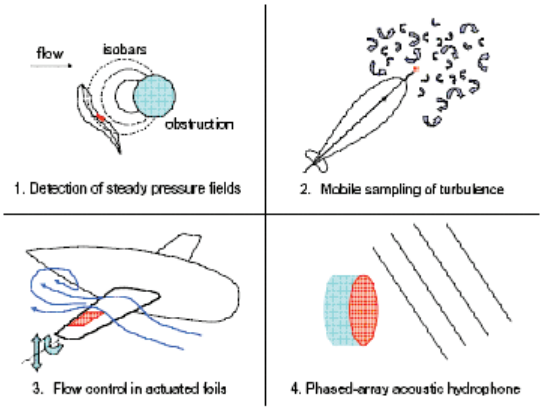

▲ Figure 1: Pressure-sensor array applications.

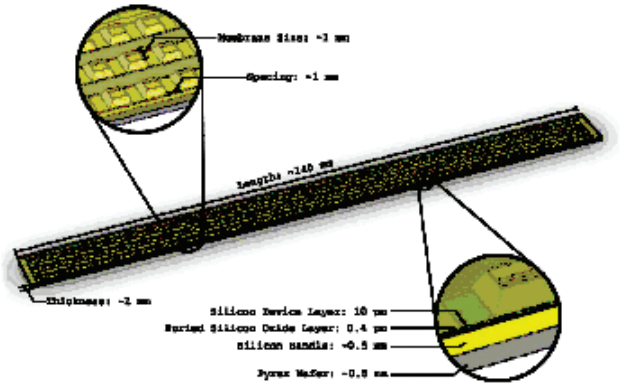

▲ Figure 2: Diagram of pressure-sensor array with basic structure depicted.

REFERENCES

[1] S.K. Clark and K.D. Wise, "Pressure sensitivity in anisotropically etched thin-diaphragm pressure sensors," *IEEE Transactions on Electron Devices*, vol. 26, no. 12, pp. 1887-1896, Dec. 1979.

[2] S. Dijkgraaf, "The functioning and significance of the lateral line organs," *Biological Review*, vol. 38, pp. 51-105, Apr. 1962.

[3] S.D. Senturia, *Microsystem Design*. Boston: Kluwer Academic Publishers, 2001.

[4] O.N. Tufte and D. Long, "Recent developments in semiconductor piezoresistive devices," *Solid-State Electronics*, vol. 6, pp. 323-338, 1963.

[5] S.M. van Netten, "Hydrodynamic detection by cupulae in a lateral line canal: Functional relations between physics and physiology," *Biological Cybernetics*, vol. 94, pp 67-85, 2006.

[6] M.-X. Zhou, Q.-A. Huang, M. Qin, and W. Zhou, "A novel capacitive pressure sensor based on sandwich structures," *Journal of Microelectromechanical Systems*, vol. 14, no. 6, pp. 1272-1282, Dec. 2005.

An Integrated Multiwatt Permanent Magnet Turbine Generator

B.C. Yen, M. Allen, F.F. Ehrich, A.H. Epstein, F. Herrault, L.C. Ho, S. Jacobson, J.H. Lang, H. Li, Z.S. Spakovszky, C. Teo, D. Veazie
Sponsorship: ARL Collaborative Technology Alliance

There is a need for compact, high-performance power sources that can outperform the energy density of modern batteries for use in portable electronics, autonomous sensors, robotics, and other applications. Previous research efforts on a micro-scale, axial-flux, permanent-magnet turbine generator [1-2] culminated in a spinning rotor test stand that delivered 8 W DC output power through a diode bridge rectifier with an overall generator system efficiency of 26.6%. In these experiments, the generator rotor was mounted via a steel shaft to an air-driven, ball-bearing supported spindle and spun to the desired operational speed.

Current research efforts aim to fully integrate the permanent-magnet (PM) generator design into the silicon micro-turbine engine fabrication process and create devices that can deliver 10 W DC output power when driven by compressed air. The integrated generator will couple energy from the compressed air to the rotor through microfabricated turbine blades attached to the backside of the rotor. One important challenge in this integration process is the structural integrity of the magnetic rotor spinning at a tip speed near 300 m/s, or equivalently 450 krpm.

Based on power requirements, a 300-μm thick circular NdFeB PM with an inner radius of 2.5 mm and an outer radius of 5 mm must be embedded into the silicon rotor on top of a 150 μm FeCoV back iron. FEA analysis shows that the maximum principle stress at 450 krpm in the silicon rotor, 900-μm thick and 12 mm in diameter, with bonded annular PM and back iron pieces, will be approximately 180 MPa through the entire structure. This stress is well below the tensile strength of silicon and FeCoV. However, because the PM is brittle and has a typical tensile strength around 83 MPa, it is unclear whether the material will fracture. Tests are currently underway to characterize the reference strength and Weibull modulus of the PM, and from these results, a working rotor design will be proposed.

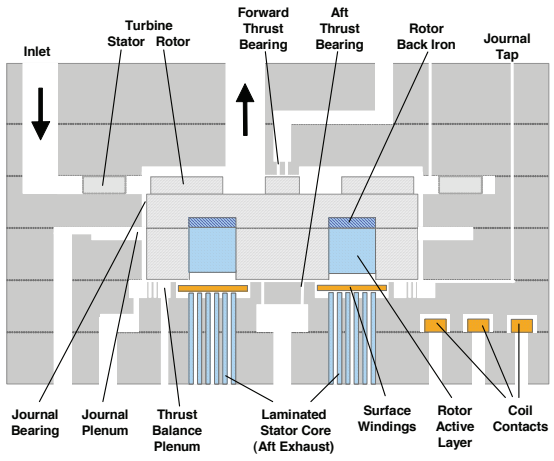

▲ Figure 1: Conceptual schematic of the fully integrated surface-wound permanent magnet turbine generator. The bottom two wafers constitute the stator and coil winding of the generator while wafers 3, 4, and 5 form the magnetic rotor. A center-fed journal-bearing design is shown in the schematic, but an axial-fed design is also possible.

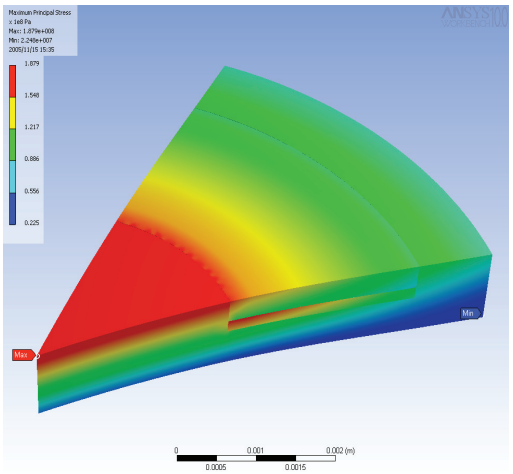

▲ Figure 2: An FEA simulation for the magnetic rotor structure spinning at 450 krpm. Because of the fully-bonded boundary conditions, most of the load is carried by the silicon hub. The maximum principal stresses in the silicon, PM, and back iron are 176.7 MPa, 188.0 MPa, and 184.5 Mpa, respectively.

REFERENCES

[1] D.P. Arnold, *et al.*, "High-speed characterization and mechanical modeling of micro-scale, axial-flux, permanent-magnet generators," in *Digest Tech. Papers Transducers '05 Conference*, Seoul, South Korea, June 10-14, 2005, pp. 284-287.

[2] S. Das, "Magnetic machines and power electronics for power MEMS applications," Ph.D. thesis, Massachusetts Institute of Technology, Cambridge, MA, 2005.

Micro-scale Singlet Oxygen Generator for MEMS-based COIL Lasers

T. Hill, B. Wilhite, L. Velasquez, H. Li, A.H. Epstein, K.F. Jensen, C. Livermore
Sponsorship: DARPA, MDA

Conventional chemical oxygen iodine lasers (COIL) offer several important advantages for materials processing, including short wavelength (1.3 μm) and high power. However, COIL lasers typically employ large hardware and use reactants relatively inefficiently. This project is creating an alternative approach called microCOIL. In microCOIL, most conventional components are replaced by a set of silicon MEMS devices that offer smaller hardware and improved performance. A complete microCOIL system includes micro-chemical reactors, micro-scale supersonic nozzles, and micro-pumps. System models incorporating all of these elements predict significant performance advantages in the microCOIL approach [1].

Initial work focuses on the design, microfabrication, and demonstration of a chip-scale singlet oxygen generator (SOG), a micro-chemical reactor that generates singlet delta oxygen gas to power the laser. Given the extensive experience with micro-chemical reactors over the last decade [2-4], it is not surprising that a micro-SOG would offer a significant performance gain over large-scale systems. The gain stems from basic physical scaling; surface-to-volume ratio increases as the size scale is reduced, which enables improved mixing and heat transfer. The SOG chip demonstrated in this project, shown in Figure 1, employs an array of micro-structured packed-bed reaction channels interspersed with micro-scale cooling channels for efficient heat removal. Production of singlet oxygen has been confirmed via spontaneous emission (as shown in Figure 2) and mass spectrometry techniques. The yield (or fraction of singlet oxygen produced) is estimated at 70%, making the micro-SOG competitive with macro-scale alternatives.

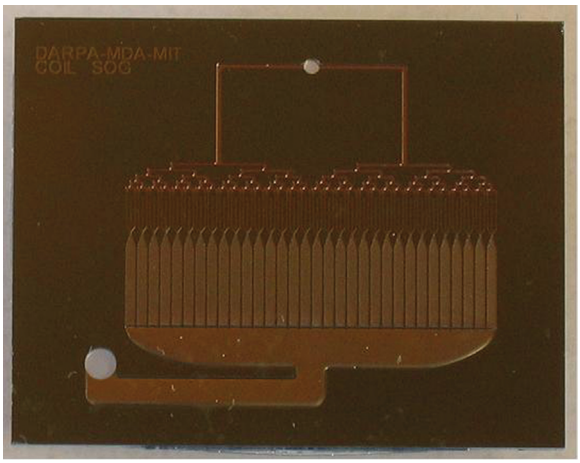

▲ Figure 1: Photograph of completed microSOG device.

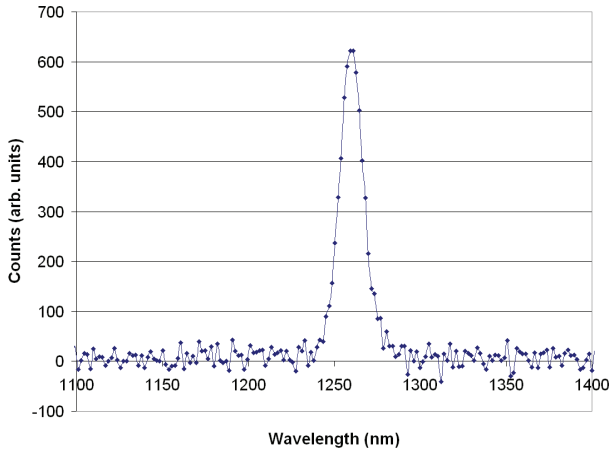

▲ Figure 2: The IR spectrum measured at the μSOG gas outlet. The peak at 1268 nm indicates the spontaneous decay of singlet oxygen into its triplet state.

REFERENCES:

[1] B.A. Wilhite, C. Livermore, Y. Gong, A.H. Epstein, and K.F. Jensen, "Design of a MEMS-based micro-chemical oxygen-iodine laser (mCOIL) system," *IEEE J. of Quantum Electronics*, vol. 40, pp. 1041-1055, 2004.

[2] N. de Mas, R.J. Jackman, M.A. Schmidt, and K.F. Jensen, "Microchemical systems for direct fluorination of aromatics," *Proc. Fifth Int'l. Conf. on Microreaction Tech.* (IMRET5) 2001.

[3] S.K. Ajmera, C. Delattre, M.A. Schmidt, and K.F. Jensen, "Microfabricated cross-flow chemical reactor for catalyst testing," *Sensors and Actuators B (Chemical)*, vol. B82, pp. 297-306, 2002.

[4] M.W. Losey, M.A. Schmidt, and K.F. Jensen, "Microfabricated multiphase packed-bed reactors: Characterization of mass transfer and reactions," *Ind. Eng. Chem. Res.*, vol. 40, pp. 2555-2562, 2001.

Label-free Microelectronic PCR Quantification

C.-S. Johnson Hou, N. Milovic, M. Godin, P. Russo, R. Chakrabarti, S.R. Manalis
Sponsorship: AFOSR, Hewlett Packard, MIT Sea Grant Program

The introduction of real-time monitoring of the polymerase chain reaction (PCR) represents a major breakthrough in specific nucleic acid quantification. This technique employs fluorescent intercalating agents or sequence-specific reporter probes to measure the concentration of amplified products after each PCR cycle. However, the need for optical components can limit the scalability and robustness of the measurement for miniaturization and field-uses. Moreover, the addition of external fluorescent reagents can induce inhibitory effects [1] and require extensive optimization [2].

We have developed a robust and simple method for direct label-free PCR product quantification using an integrated microelectronic sensor (Figure 1) [3]. The field-effect sensor can sequentially detect the intrinsic charge of multiple unprocessed PCR products and does not require sample processing or additional reagents in the PCR mixture. The sensor measures nucleic acid concentration in the PCR relevant range and specifically detects the PCR products over reagents such as Taq polymerase and nucleotide monomers. The sensor can monitor the product concentration at various stages of PCR and can generate a readout that resembles that of a real-time fluorescent measurement using an intercalating dye but without its potential inhibition artifacts (Figure 2). The device is mass-produced using standard semiconductor processes, can be reused for months, and integrates all sensing components directly on-chip. As such, our approach establishes a foundation for the direct integration of PCR-based *in vitro* biotechnologies with microelectronics.

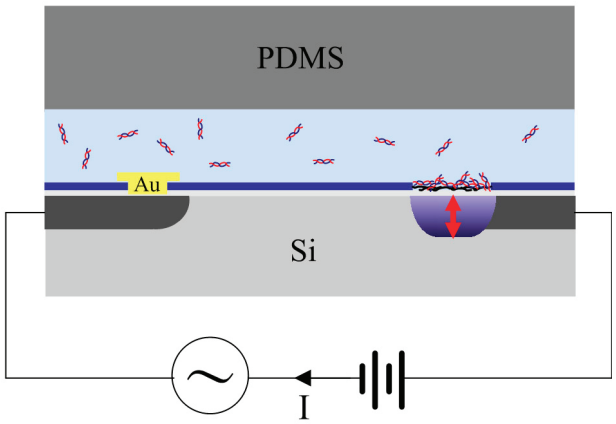

▲ Figure 1: Cross-sectional drawing demonstrating the basis of the device measurement. Binding of charged molecules such as DNA on the sensor's surface alters the distribution of positive mobile charge carrier in silicon, results in a modulation of the depletion depth (red arrow), hence changing the capacitance. This change in capacitance is monitored by measuring the AC current between the sensor and the gold electrode.

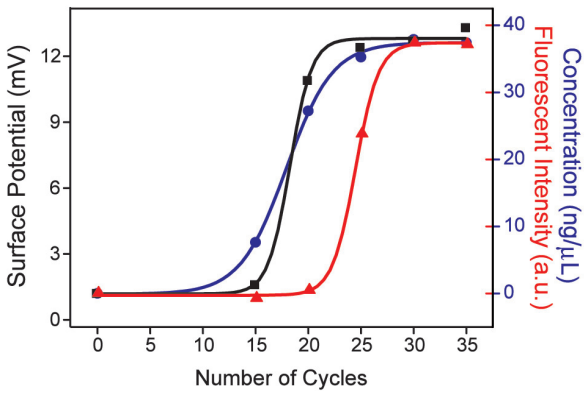

▲ Figure 2: Comparison between steady state response of electronic measurements (black), real-time monitoring of PCR using Sybr Green I intercalating dye (red), and concentration analysis of the products using DNA Labchip kits (blue). No fluorescent labels were used for electronic detection and concentration measurements. However the discrepancy with the Sybr Green I measurement is likely due to partial inhibition of the PCR reaction by the fluorescent reagent.

REFERENCES

[1] K. Nath, J.W. Sarosy, J. Hahn, and C.J. Di Como, "Effects of ethidium bromide and SYBR Green I on different polymerase chain reaction systems," *Journal of Biochemical and Biophysical Methods*, vol. 42, no. 1-2, pp. 15-29, Jan. 2000.

[2] M. Boeckh, M. Huang, J. Ferrenberg, T. Stevens-Ayers, L. Stensland, W.G. Nichols, and L.J Corey, "Optimization of quantitative detection of cytomegalovirus DNA in plasma by real-time PCR," *Journal of Clinical Microbiology*, vol. 42, no. 3, pp. 1142-1148, Mar. 2004.

[3] C.J. Hou, N. Milovic, M. Godin, P.R. Russo, R. Chakrabarti, and S.R. Manalis, "Label-free microelectronic PCR quantification," *Analytical Chemistry*, Mar. 2006, to be published.

Atomic Force Microscopy with Inherent Disturbance Suppression for Nanostructure Imaging

A. Sparks, S.R. Manalis
Sponsorship: AFOSR

Scanning probe imaging is often limited by disturbances, or mechanical noise, from the environment that couple into the microscope. We demonstrate on a modified commercial atomic force microscope that adding an interferometer as a secondary sensor to measure the separation between the base of the cantilever and the sample during conventional feedback scanning can result in real-time images with inherently suppressed out-of-plane disturbances (Figure 1) [1]. The modified microscope has the ability to resolve nanometer-scale features in situations where out-of-plane disturbances are comparable to or even several orders of magnitude greater than the scale of the topography. We present images of DNA in air from this microscope in tapping mode without vibration isolation, and show improved clarity using the interferometer as the imaging signal (Figure 2). The inherent disturbance suppression approach is applicable to all scanning probe imaging techniques.

We do not claim that image improvement will be comparable to these results on all SPMs and in all imaging environments. At present, this technique will be most effective in very noisy environments, such as a microfabrication facility, where Z disturbances overwhelm sample topography. However, there are two significant implications of this work: 1) vibration isolation, which is costly and consumes space, can be rendered unnecessary for noisy environments; and, 2) this technique can potentially outperform vibration isolation in any environment with further reduction of the interferometer noise floor.

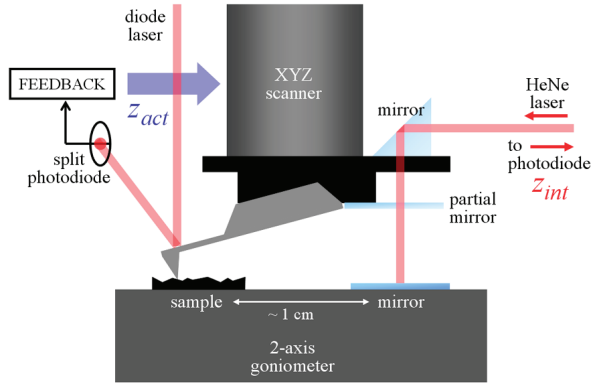

▲ Figure 1: Experimental schematic. Zact (actuator) is the signal that is used for conventional scanning probe microscopy and includes a superposition of topography and mechanical disturbances. However, Zint (interferometer) reveals only topography and suppresses the mechanical disturbances.

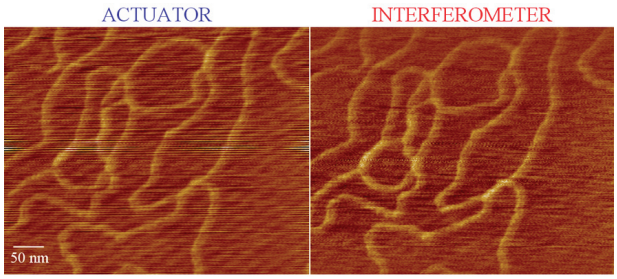

▲ Figure 2: Due to Z disturbance effects, the actuator image appears streaked, and diagonal background stripes are present which are likely due to a resonance of the microscope. The interferometer image does not exhibit streaking and shows suppressed background noise.

REFERENCES

[1] A.W. Sparks and S.R. Manalis, "Atomic force microscopy with inherent disturbance suppression for nanostructure imaging," *Nanotechnology*, vol. 17, pp. 1574, 2006.

Vacuum-Packaged Suspended Microchannel Resonant Mass Sensor for Biomolecular Detection

T.P. Burg, A.R. Mirza, N. Milovic, C.H. Tsau, G.A. Popescu, J.S. Foster, S.R. Manalis
Sponsorship: AFOSR, NIH

Microfabricated transducers enable the detection of biomolecules in microfluidic systems with nanoliter size sample volumes. Their integration with microfluidic sample preparation into lab-on-a-chip devices can greatly leverage experimental efforts in systems biology and pharmaceutical research by increasing analysis throughput while dramatically reducing reagent cost. Microdevices can also lead to robust and miniaturized detection systems with real-time monitoring capabilities for point-of-use applications.

We have recently fabricated, packaged, and tested a resonant mass sensor for the detection of biomolecules in a microfluidic format [1]. The transducer employs a suspended microchannel as the resonating element, thereby avoiding the problems of damping and viscous drag that normally degrade the sensitivity of resonant sensors in liquid (Figure 1). Our device differs from a vibrating tube densitometer in that the channel is very thin, which enables the detection of molecules that bind to the channel walls; this provides a path to specificity via molecular recognition by immobilized receptors. The fabrication is based on a sacrificial polysilicon process with low-stress LPCVD silicon nitride as the structural material, and the resonator is vacuum packaged on the wafer scale using glass frit bonding (Figure 2). Packaged resonators exhibit a sensitivity of 0.8 ppm/(ng•cm2) and a mechanical quality factor of up to 700. To the best of our knowledge, this quality factor is among the highest so far reported for resonant sensors with comparable surface mass sensitivity in liquid.

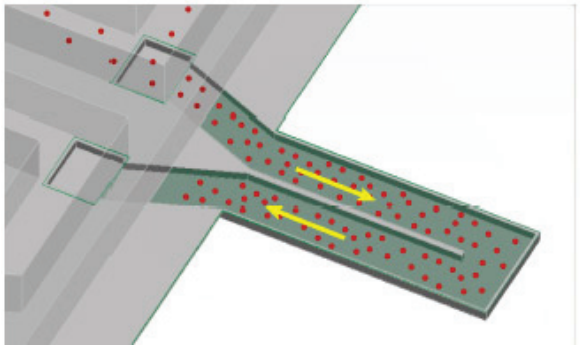

▲ Figure 1: Suspended microchannel resonator (SMR). In SMR detection, target molecules flow through a vibrating suspended microchannel and are captured by receptor molecules attached to the interior channel walls. What separates the SMR from existing resonant mass sensors is that the receptors, targets, and their aqueous environment are confined inside the resonator, while the resonator itself can oscillate at high Q in an external vacuum environment, thus yielding extraordinarily high sensitivity.

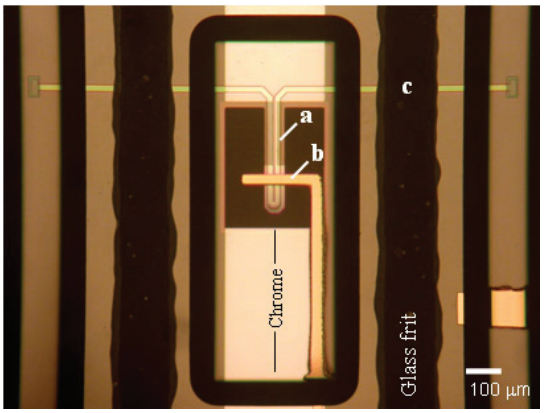

▲ Figure 2: Optical micrograph of a packaged cantilever resonator. The 300µm long beam contains a 1 x 20 µm microfluidic channel (a). An electrode on the glass surface above the cantilever enables electrostatic actuation (b). Glass frit conforms to the surface topography and does not collapse the thin channel in location (c) during bonding.

REFERENCES

[1] T.P. Burg, A.R. Mirza, N. Milovic, C.H. Tsau, G.A. Popescu, J.S. Foster, S.R. Manalis, "Vacuum-packaged suspended microchannel resonant mass sensor for biomolecular detection," *IEEE Journal of Microelectromechanical Systems,* to be published.

Microbial Growth in Parallel Integrated Bioreactor Arrays

H. Lee, R.J. Ram, P. Boccazzi, A. Sinskey
Sponsorship: DuPont-MIT Alliance

Bioprocesses with microbial cells play an important role in producing biopharmaceuticals such as human insulin and human growth hormone and other products such as amino acids and biopolymers. Because bioprocesses involve the complicated interaction between the genetics of the microorganisms and their chemical and environmental conditions, hundreds or thousands of microbial growth experiments are necessary to develop and optimize them. In addition, efforts to develop models for bioprocesses require numerous growth experiments to study phenotypes of microorganism.

We have designed and developed integrated arrays of microbioreactors that can provide the oxygen transfer and control capabilities of a stirred tank bioreactor in a high-throughput format. The devices comprise a novel peristaltic oxygenating mixer and microfluidic injectors (Figure 1), which are fabricated using a process that allows the combination of multiple scale (100 μm-1 cm) and multiple depth (100 μm-2 mm) structures in a single mold. The microbioreactors have a 100 μL working volume, a high oxygen-transfer rate ($k_La \approx 0.1s^{-1}$), and closed loop control over dissolved oxygen and pH (±0.1). Overall, the system supports eight simultaneous batch cultures in two parallel arrays with two dissolved oxygen thresholds, individual pH set points, and automated near real-time monitoring of optical density, dissolved oxygen concentration, and pH.

These capabilities allowed the demonstration of multiple *Escherichia coli* aerobic fermentations with growth to high cell densities (>12g-dcw/L, Figure 2), and individual bioreactor performance on par with bench scale stirred tank bioreactors. The successful integration of diverse microfluidic devices and optical sensors in a scalable architecture opens a new pathway for continued development of parallel bioreactor systems.

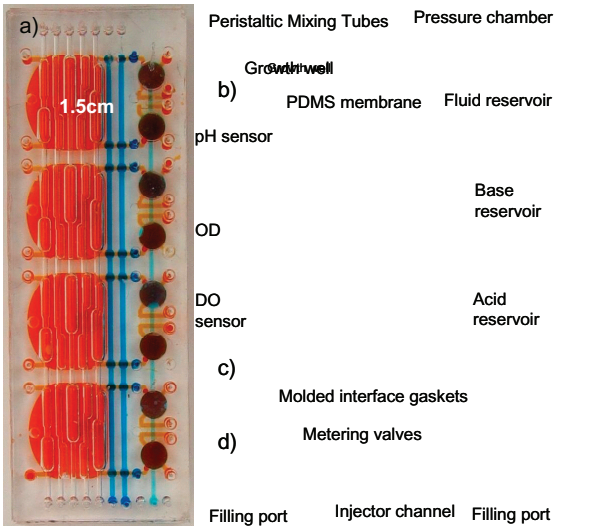

▲ Figure 1: Photograph and schematic of parallel integrated bioreactor array device. a) Photograph of four reactors integrated into a single module. b) Cross-section showing peristaltic oxygenating mixer tubes and fluid reservoir with pressure chamber. c) Top view of schematic showing optical sensors and layout of peristaltic oxygenating mixer and fluid injectors. d) Cross-section showing the fluid-injector membrane pinch valves.

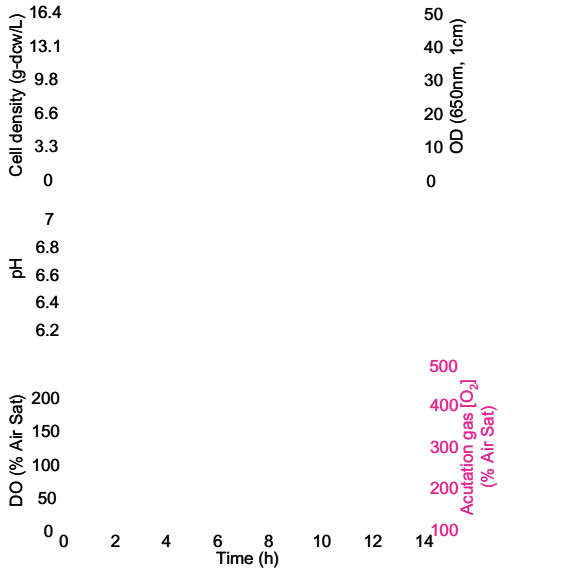

▲ Figure 2: Four *E. coli* fermentations on a defined medium performed in a single micro-bioreactor array module. The heavy black line indicates the mean of the cell density and pH replicates and the minimum of the dissolved oxygen replicates. The pH was controlled at 6.9 until the base reservoirs were depleted. Due to differences in the k_La, the oxygen concentration in three of the reactors did not remain near the set point. The oxygen concentration of the mixer actuation gas (bold magenta dashes) is shown by the orange dashed line and approximately follows the exponential growth of the cells.

Vacuum-Sealing Technologies for Micro-chemical Reactors

K. Cheung, K.F. Jensen, M.A. Schmidt
Sponsorship: ARO MURI

Current portable power sources may soon fail to meet the demand for increasingly larger power densities. To address this concern, our group has been developing MEMS power generation schemes that are focused around fuel cells and thermophotovoltaics. At the core of these systems is a suspended tube micro-reactor that has been designed to process chemical fuels [1]. Proper thermal management is critical for high reactor efficiency, but substantial heat loss is attributed to conduction through air. A straightforward solution is to eliminate the heat-loss pathways associated with air by means of a vacuum package. This work explores a glass-frit bonding method for vacuum sealing.

Optimization of pre-sintering and bonding parameters of the glass frit produced a repeatable and robust hermetic seal. Encounters with outgassing issues prompted an alternate two-step packaging process illustrated in Figure 1. New capping dies were fabricated, test devices were packaged, and the final seal-off was attempted with various materials [2]. Several experimental results appear in Figure 2. The glass frits are undesirable since they produce holes from material breakdown when heated in a vacuum. The gold-indium solder appears promising but holes formed due to internal outgassing. Extended heating to assist outgassing resulted in the delamination of the solder from the wetting metal. Recent work has been conducted to evaluate oxidized caps and lead-tin solder as solutions to these problems. Enhancements through the incorporation of non-evaporable getters will be assessed once a vacuum package is achieved.

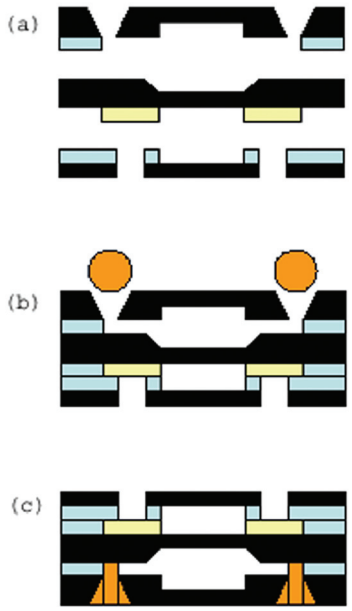

▲ Figure 1: Basic concept of the two-step approach. (a) Initial bond in box furnace (blue = frit, black = silicon, yellow = metallization); (b) place solder/frit (orange) into pump-out hole; and (c) final seal-off.

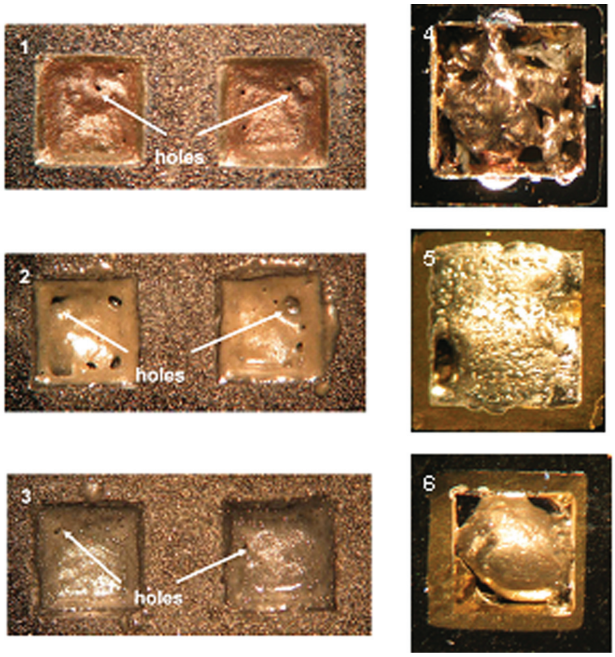

▲ Figure 2: Experimental results of final seal-off attempts with various materials and conditions (1) Diemat DM2700PF (2) Semcom B-10105 (3) Semcom B-10127 (4) 82Au/18In (5) 80Au/20In (6) 80Au/20In extended outgassing.

REFERENCES

[1] L.R. Arana, "High-temperature microfluidic systems for thermally-efficient fuel processing," Ph.D. thesis, Massachusetts Institute of Technology, Cambridge, 2003.

[2] K. Cheung, "Die-level glass frit vacuum packaging for a micro-fuel processor system," Master's thesis, Massachusetts Institute of Technology, Cambridge, 2005.

Direct Patterning of Organic Materials and Metals Using Micromachined Printheads

V. Leblanc, J. Chen, D.M. Schut, P. Mardilovich, V. Bulovic, M.A. Schmidt
Sponsorship: Hewlett-Packard

Organic optoelectronic devices are promising for many commercial applications if methods for fabricating them on large-area, low-cost substrates become available. Our project investigates the use of MEMS in the direct patterning of materials needed for such devices. By depositing the materials directly from the gas phase, without liquid phase coming in contact with the substrate, we aim to avoid the limitations of inkjet printing such materials.

In our first demonstration, we used an electrostatically actuated micromachined shutter integrated with an x-y-z manipulator to modulate the flux of evaporated organic semiconductors and metals and to generate patterns of the deposited materials. We printed arbitrary patterns of organic semiconductor Alq_3 (tris(8-hydroxyqunolinato) aluminum) and metal silver on glass substrates. We also printed pentacene/silver organic field effect transistor (OFET) and arrays of organic light emitting devices (OLED), as shown in Figure 1. This printing technique can pattern small-molecule organic light-emitting devices at high resolution (800 dpi).

The next stage of this project investigates the use of a microporous layer with integrated heaters for local evaporation of the materials. The microfabricated device is shown in Figure 2. The material to be printed is delivered to the porous region in liquid or gas phase and deposits inside the pores. An integrated heater then heats up the porous area and the material is re-evaporated from the pores onto the substrate. Compared to the first generation of printheads, the problems of crashing and stiction are avoided, since there is no moving part. Clogging is also limited since most of the material is removed during each printing cycle. Other advantages include the smaller quantity of organic material used, and the reduced substrate heating. Such a printhead would ultimately be integrated with an ink-jet printer for the delivery of liquid phase material into the porous region.

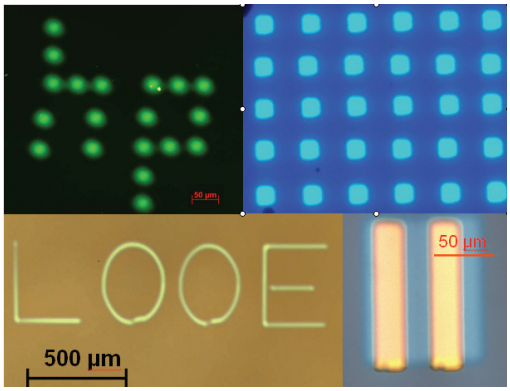

▲ Figure 1: Patterns obtained using our direct patterning method. Clockwise from top left: photoluminescence of Alq3 pixels, electroluminescence of OLED array with 30-micron pixels, and pictures of an OFET and a silver line pattern.

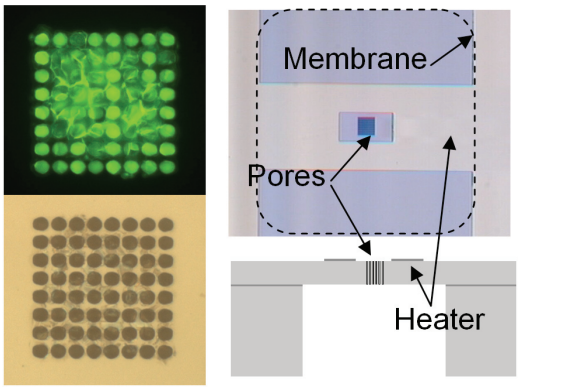

▲ Figure 2: Left: Pictures of the pores seen from the front of the device, top: fluorescent imaged after Alq3 was introduced from the back; bottom: optical microscope picture after the integrated heater re-evaporated the material. Right: Optical microscope image and schematic of device.

REFERENCES

[1] V. Leblanc, S.H. Kang, J. Chen, P.J. Benning, M.A. Baldo, V. Bulović, and M.A. Schmidt, "Micromachined printheads for the patterning of organic materials and metals," in *Proc. of Transducers 2005*, Seoul, Korea, June 2005, pp. 1429-1432.

[2] J. Chen, V. Leblanc, S.-H. Kang, M.A. Baldo, P.J. Benning, V. Bulović, and M.A. Schmidt, "Direct patterning of organics and metals using a micromachined printhead," in *Proc. MRS Spring 2005*, San Francisco, CA, Mar/Apr. 2005, pp. H1.8:1-7,

A Thermophotovoltaic (TPV) MEMS Power Generator

O.M. Nielsen, K.F. Jensen, M.A. Schmidt
Sponsorship: ARO MURI

For a number of years, batteries have not kept up with the fast development of microelectronic devices. The low energy densities of even the most advanced batteries are a major hindrance to lengthy use of portable consumer electronics such as laptops and of military equipment that most soldiers carry today. Furthermore, battery disposal constitutes an environmental problem. Hydrocarbon fuels exhibit very high energy densities in comparison, and micro-generators converting the stored chemical energy into electrical power at even modest levels are therefore interesting alternatives in many applications. This project focuses on building thermophotovoltaic (TPV) micro-generators, in which photocells convert radiation from a combustion-heated emitter into electrical power. TPV is an indirect conversion scheme that goes through the thermal domain and therefore does not exhibit very high efficiencies (10-15% max). However, because of its simple structure and because the combustor and photocell fabrication processes do not need to be integrated, the system is simpler to micro-fabricate than other generator types, e.g., thermoelectric systems and fuel cells. It is also a mechanically passive device that is virtually noiseless and less subject to wear than engines and turbines. In this TPV generator, a catalytic combustor, the suspended micro-reactor (SμRE) (Figure 1), is heated by combustion of propane and air, and the radiation emitted is converted into electrical energy by low-bandgap (GaSb) photocells. Net power production of up to 1 mW has been achieved [1], constituting a promising proof of concept. A new version of the SμRE is currently under fabrication. This new design (Figure 2) aims to address several problems existing in the earlier version, including fabrication difficulties, low burst pressure of the tubes, and low emitter surface area.

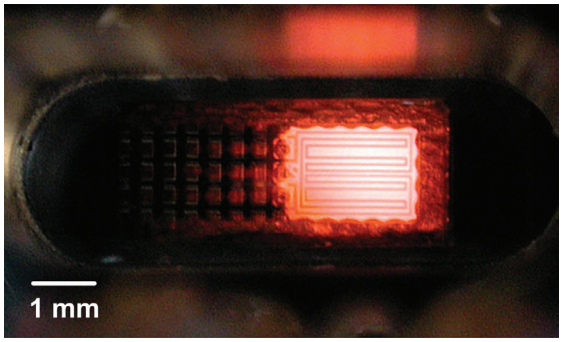

▲ Figure 1: Suspended micro-reactor (SμRE I) for fuel processing and TPV energy conversion heated to ~900°C.

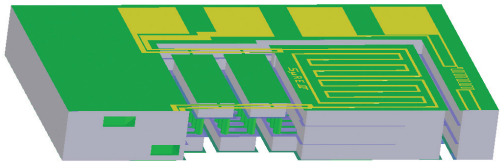

▲ Figure 2: Three-dimensional model of the new suspended micro-reactor (SμRE III).

REFERENCES

[1] O.M. Nielsen, L.R. Arana, C.D. Baertsch, K.F. Jensen, and M.A. Schmidt, "A thermophotovoltaic micro-generator for portable power applications," in *Proc. Transducers '03*, Boston, MA, June 2003, pp. 714-717.

MEMS Vacuum Pump

V. Sharma, M.A. Schmidt
Sponsorship: DARPA

There are many advantages to miniaturizing systems for chemical and biological analysis. Recent interest in this area has led to the creation of several research programs, including a micro gas analyzer (MGA) project at MIT. The goal of this project is to develop an inexpensive, portable, real-time, and low-power approach for detecting chemical and biological agents. Elements entering the MGA are first ionized, then filtered by a quadrupole array, and sensed using an electrometer. A key component enabling the entire process is a MEMS vacuum pump, responsible for routing the gas through the MGA and increasing the mean free path of the ionized particles so that they can be accurately detected.

There has been a great deal of research done over the past 30 years in the area of micro pumping devices [1, 2]. We are currently developing a displacement micro-vacuum pump that uses a piezoelectrically driven pumping chamber and a pair of piezoelectrically driven active-valves; the design is conceptually similar to the MEMS pump reported by Li *et al.* [3]. We constructed accurate computer models for all aspects of the pump's operation: a compressible mass flow model of the flow rates, the pressure, the density, and the Mach number in the different parts of the pump in both the sonic and subsonic regimes [4], and a nonlinear plate deformation model of the stresses experienced by the pistons, tethers, and walls of the pump during operation [5], for any chosen dimensions and material properties.

Using these models we have defined a process flow for our first-generation MEMS vacuum pump designed to meet our first-term goals. A schematic of this pump that we started fabricating is shown in Figure 1 below. For ease in testing we have decided to fabricate only Layers 1-3 and constructed a testing platform that will drive the pistons pneumatically. This will allow for rapid characterization of pumping performance as well as chamber and valve designs for several dies at once without having to incorporate piezos in each case. The final device will be driven using low-voltage, low-loss, piezoelectric-stacks incorporated into Layer 4 and will include Layer 5 for structural support.

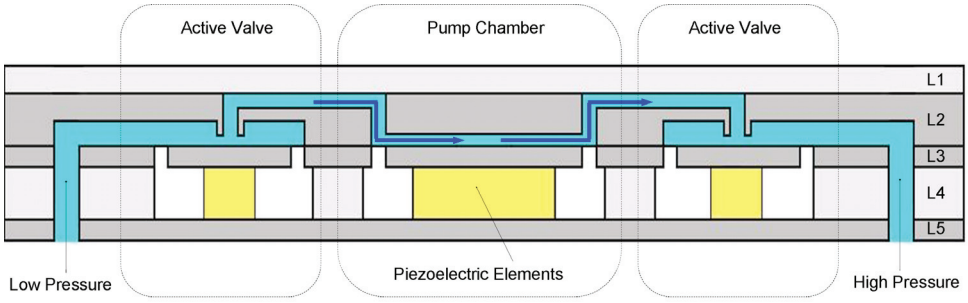

▲ Figure 1: Schematic of the MEMS vacuum pump. Layers 1 and 4 are glass, Layer 2 forms the chambers and channels using double-side polished silicon, Layer 3 forms the pistons and tethers being silicon-on-insulator, and Layer 5 is single-polished silicon. For testing and characterization, only Layers 1-3 are being fabricated.

REFERENCES

[1] D.J. Laser and J.G. Santiago, "A review of micropumps," *J. of Micromechanics and Microengineering*, vol. 14, no. 6, pp. 35-64, 2004.

[2] P. Woias, "Micropumps–past, progress and future prospects," *Sensors and Actuators B: Chemical*, vol. 105, no. 1, pp. 28-38, 2005.

[3] H.Q. Li, D.C. Roberts, J.L. Steyn, K.T. Turner, J.A. Carretero, O. Yaglioglu, Y.-H. Su, L. Saggere, N.W. Hagood, S.M. Spearing, M.A. Schmidt, R. Mlcak, and K. Breuer, "A High-frequency, high flow rate, piezoelectrically driven MEMS micropump," *IEEE Solid State Sensors and Actuators Workshop*, Hilton Head SC, June 2000.

[4] A.K. Henning, "Improved gas flow model for microvalves," Proceedings of Transducers 2003, Boston, MA, USA, pp. 1550-1553, June 2003.

[5] D.C. Roberts, O. Yaglioglu, J.Carretero, Y.-H Su, L. Saggere, and N.W. Hagood, "Modeling, design, and simulation of a piezoelectrically driven microvalve for high pressure, high frequency applications," *Proc. SPIE 2001- Smart Structures and Integrated Systems*, Newport Beach, CA, Mar. 2001, pp. 366-380.

Rapid and Shape-Controlled Growth of Aligned Carbon Nanotube Structures

A.J. Hart, L.C. van Laake, A.H. Slocum
Sponsorship: Deshpande Center, NSF, Fannie and John Hertz Foundation

We present approaches for growth of aligned carbon nanotube (CNT) structures on silicon substrates, based on atmospheric pressure chemical vapor deposition (CVD) using a Fe/Al_2O_3 catalyst film in C_2H_4/H_2. First, vertically-aligned films of small-diameter (5-10 nm) multi-walled CNTs (MWNTs) are grown to 0.9 mm thickness in 15 minutes and 1.8 mm in 60 minutes, using a conventional 1-inch-diameter tube furnace [1]. The catalyst is patterned by photolithography, and the growth rate of CNT microstructures depends on the local areal density of catalyst, which is analogous to loading effects in plasma etching process. Further, using a novel apparatus where the silicon substrate is resistively heated, we achieve CNT film thickness of 3 mm in just 20 minutes along with rapid (100°C/s) control of the substrate temperature and optically image the film during growth (Figure 1).

By placing a weight on the catalyst-coated substrate, we measure the force which can be exerted by a growing CNT film and demonstrate that the film thickness after a fixed growth time and the alignment of CNTs within the film decrease concomitantly with increasing applied force [2]. We utilize this principle to fabricate three-dimensional structures of CNTs (Figure 2) that conform to the shape of a microfabricated template. This technique is a catalytic analogue to micromolding of polymer and metal microstructures; it enables growth of nanostructures in arbitrarily-shaped forms and does not require patterning of the catalyst.

Finally, we perform combinatorial flow studies of CNT growth using an array of parallel microchannels fabricated by KOH etching of silicon [3]. We observe transitions in CNT yield and quality along the microchannels, grow CNT structures that are aligned by gas flows in the microchannels, and fabricate CNT-filled microchannels for applications such as microfluidic filters.

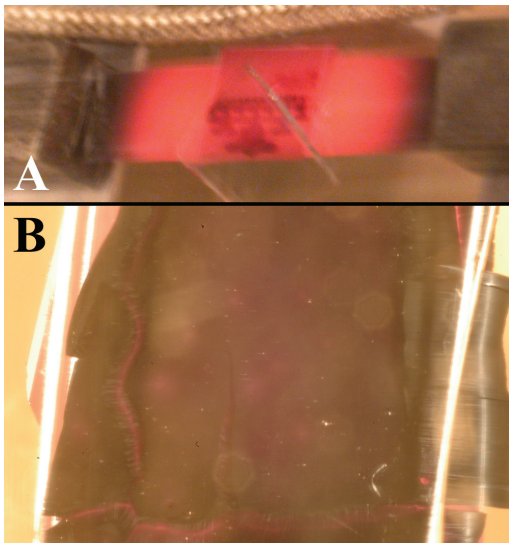

▲ Figure 1: Growth of a CNT film on a resistively heated silicon substrate: (a) suspended silicon substrate at 750°C; (b) optical top-view image of CNT film during growth.

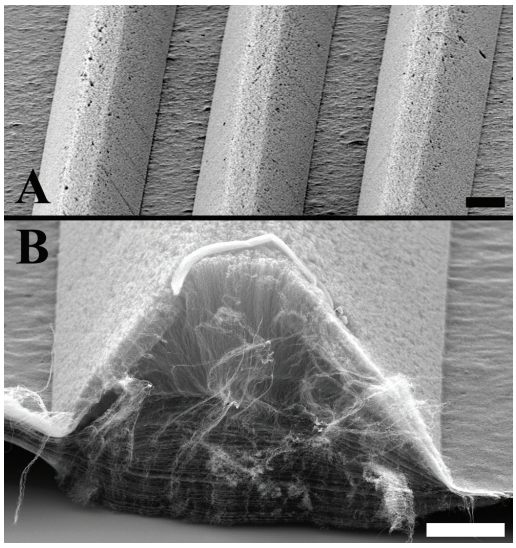

▲ Figure 2: The CNT microforms fabricated by growth under mechanical pressure: (a) Microforms fabricated using KOH-etched microchannel template. (b) Cross-section of a trapezoidal CNT microform.

REFERENCES

[1] A.J. Hart and A.H. Slocum, "Rapid growth and flow-mediated nucleation of millimeter-scale aligned carbon nanotube structures from a thin-film catalyst," *J. of Physical Chemistry B*, vol. 110, pp. 8250-8257, 2006.

[2] A.J. Hart and A.H. Slocum, "Force output and micro-scale shape replication by aligned carbon nanotube growth," *Nano Letters*, vol. 6, pp. 1254-60, 2006.

[3] A.J. Hart and A.H. Slocum, "Combinatorial glow studies of carbon nanotube growth using microchannel arrays," presented at the *Materials Research Society Fall Meeting*, 2005.

A Low Contact Resistance MEMS-Relay

A.C. Weber, J.H. Lang, A.H. Slocum
Sponsorship: ABB Corporate Research, Baden-Daettwil

A low contact resistance MEMS-relay featuring highly parallel and planar oblique contacts has been fabricated and is currently being tested. The contacts are etched in silicon using a potassium hydroxide (KOH) solution. An offset between the wafer-top and the wafer-bottom KOH masks produces the oblique contact geometry schematically shown in Figure 1A.

In contrast, many prior art MEMS devices [1-3] have rough, non complementary contacts. As these surfaces touch, they do so in a small number of high points, as shown in Figure 1B, which significantly reduces the effective contact area and leads to a high contact resistance and a low current carrying capacity. Additionally, vertical contacts are prone to poor metallization, which further affects the device's contact resistance. Our MEMS-relay, shown in Figure 2, is composed of a compliant mechanism (B), a pair each of engaging (C) and disengaging (D) rolling-point "Zipper" actuators [4-5], and a pair of planar and parallel contacts (E).The relay is fabricated by a combination of deep reactive ion etching (DRIE) and KOH etching. Nested masks are used to pattern both wafer-through etches. Low stress silicon nitride (Si_3N_4), which will later be used as a KOH mask, is patterned initially on both sides of the device wafer. A silicon oxide film is deposited on the KOH mask. The compliant mechanism and actuators are then etched through DRIE and a second Si_3N_4 film is deposited. The second Si_3N_4 film is patterned using a "shadow" (through-etched) wafer as a mask. The oxide is selectively etched to reveal the buried nitride mask. The contacts are etched in KOH solution. Both Si_3N_4 and oxide films are stripped and a thermal oxide, which insulates both the electrostatic actuators and the relay contacts from the rest of the device, is grown. Gold is evaporated over both sides of the insulated contacts and the device wafer is anodically bonded to a Pyrex handle wafer. Experimental pull-in and drop-out voltages of 70 V and 40 V, respectively, agree with the model. Contact travel of 50 μm prevents arcing as the load circuit is switched on and off. A contact resistance of 50 mΩ was demonstrated by our group using an externally actuated structure as a proof of concept for the contact design [4]. Our group continues to develop these MEMS relays for power applications.

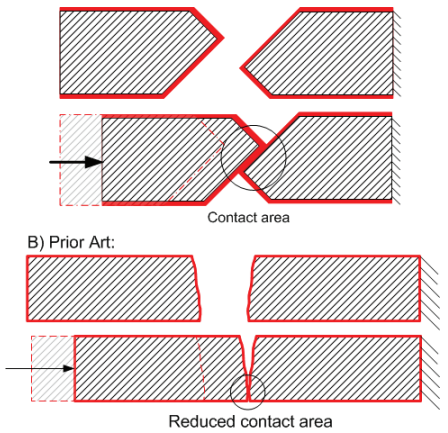

▲ Figure 1: Schematic cross section of oblique planar parallel contacts (A), schematic cross section of prior art (B).

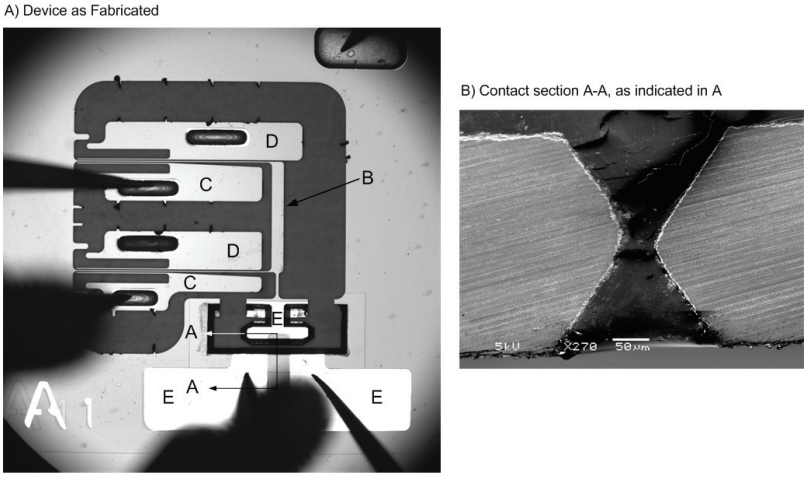

▲ Figure 2: Device as fabricated (A), SEM contact cross section A-A of oblique contacts as shown in Figure 2A (B). The die saw causes the rough edge of the static contact in (B).

REFERENCES

[1] H. Lee *et al.*, "Electrostatically actuated copper-blade microrelays," *Sensors and Actuators A*, vol. 100, pp. 105-113, 2002.
[2] J. Wong *et al.*, "An electrostatically-actuated MEMS switch for power applications," in *Proc. IEEE MEMS '00,* Miyasaki Japan, pp. 633-638.
[3] W. Taylor *et al.*, "Fully integrated magnetically actuated micromachined relays," *Journal of MEMS,* vol. 7, pp. 181-191, 1998.
[4] J. Li, "Electrostatic zipping actuators and their application to MEMS," Ph.D. thesis, MIT, Cambridge, 2004.
[5] J. Li *et al.*, "DRIE fabricated curved-electrode zipping actuator with low pull-in voltage," *12th Int. Conf. on Transducers, Solid-State Sensors, Actuators and Microsystems*, 2003, vol. 1, pp. 480-483.

Fast Three-Dimensional Electrokinetic Pumps for Microfluidics

J.P. Urbanski, J. Levitan, M. Bazant, T. Thorsen
Sponsorship: ISN

Electrokinetic pumps are attractive for portable and flexible microfluidic analysis systems, since they operate without moving parts using low (battery-powered) alternating potentials. Since the discovery of AC electro-osmosis (ACEO) in the late 1990s, there has been much work in designing planar, periodic pumps, which exploit broken symmetry in electrode spacing and width to produce a streaming flow over a surface. Although surface-height modulation has been suggested as another means of breaking symmetry[1], it has never been numerically or experimentally pursued. Recently, Bazant and Squires described more general flows due to induced charge electro-osmosis (ICEO) around three-dimensional metal structures[2], which has since been realized experimentally in microfluidic systems[3]. Motivated by ICEO around raised electrodes, we are developing a variety of new three-dimensional AC electrokinetic pumps capable of much faster directional flows than planar ACEO pumps (for the same applied voltage and minimum feature size) by an order of magnitude according to the usual low-voltage model. This phenomena and an example microfabricated device are illustrated in Figure 1. We test and improve our theoretical designs experimentally in a microfluidic loop[4], as shown in Figure 2. Our pumps involve interdigitated planar electrodes with raised metal structures from a simple electroplating step, which leads to greatly enhanced pumping.

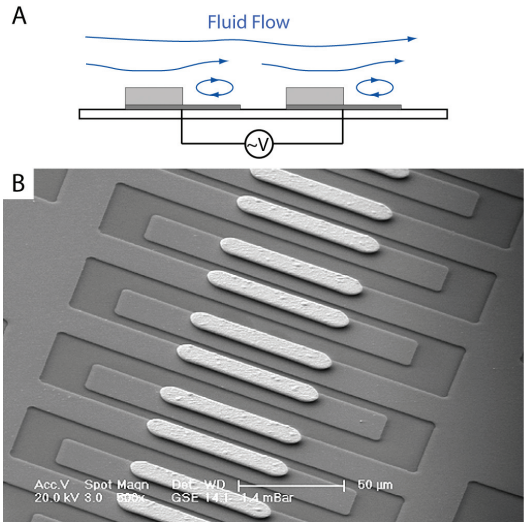

▲ Figure 1: (A) Schematic diagram of fluid flow that may be generated by an AC field between two electrodes located on a substrate. This "fluid conveyor belt," containing partially raised electrodes, exploits naturally occurring fluid rolls to pump fluid in microchannels with voltages < ~10 V. (B) Electroplating is used to create the raised geometry on repeated periods of planar patterned electrodes.

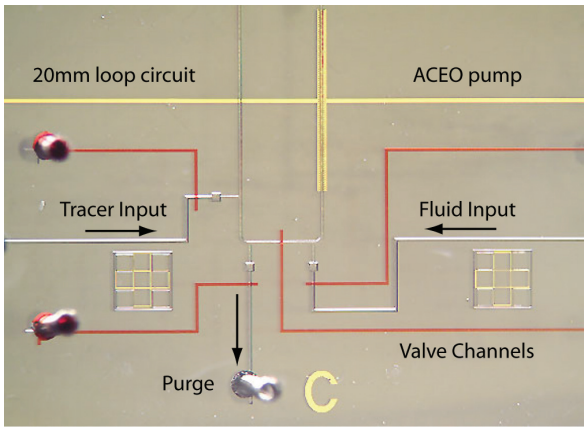

▲ Figure 2: A microfluidic device featuring a closed loop channel is used to test AC electrokinetic pump designs. The PDMS chip, which caps the electrodes, provides fluid inputs and outputs, and isolates the working pump from external pressure perturbations. This approach enables systematic characterization of pump performance as a function of input voltage and frequency. The scale bar indicates 1 mm.

REFERENCES

[1] A. Ajdari, "Pumping liquids using asymmetric electrode arrays," *Physical Review E*, vol. 61, pp. R45-R48, 2000.

[2] M.Z. Bazant and T.M. Squires, "Induced-charge electrokinetic phenomena: Theory and microfluidic applications," *Physical Review Lett.*, vol. 92, 2004.

[3] J.A. Levitan, S. Devasenathipathy, V. Studer, Y.X. Ben, T. Thorsen, T.M. Squires, and M.Z. Bazant, "Experimental observation of induced-charge electro-osmosis around a metal wire in a microchannel," *Colloids and Surfaces A: Physicochemical and Engineering Aspects*, vol. 267, pp. 122-132, 2005.

[4] V. Studer, A. Pepin, Y. Chen, and A. Ajdari, "An integrated AC electrokinetic pump in a microfluidic loop for fast and tunable flow control," *Analyst*, vol. 129, pp. 944-949, 2004.

BioMEMS for Control of the Stem-cell Microenvironment

L. Kim, A. Rosenthal, S. Sampattavanich, J. Voldman
Sponsorship: NIH

The stem-cell microenvironment is influenced by several factors including cell-media, cell-cell, and cell-matrix interactions. Although conventional cell-culture techniques have been successful, they offer poor control of the cellular microenvironment. To enhance traditional techniques, we have designed a microscale system to perform massively parallel cell culture on a chip.

To control cell-matrix and cell-cell interactions, we use dielectrophoresis (DEP), which uses non-uniform AC electric fields to position cells on or between electrodes [1]. We present a novel microfabricated DEP trap designed to pattern large arrays of single cells (Figure 1, left). We have experimentally validated the trap using polystyrene beads and cells, showing excellent agreement with our model predictions [2]. In addition, by placing interdigitated electrodes between the traps, we can prevent cells from sticking to the substrate outside the traps (Figure 1, right).

To control cell-media interactions, we have developed a microfluidic device for culturing adherent cells over a logarithmic range of flow rates (Figure 2, left) [3]. The device controls flow rates via a network of geometrically-set fluidic resistances connected to a syringe-pump drive. We use microfluidic perfusion to explore the effects of continuous flow on the soluble microenvironment. We have demonstrated logarithmically-scaled perfusion culture of mouse embryonic stem cells over 4 days, with flow rates varying > 300x across the array. Cells cultured at the slowest flow rate did not proliferate while colonies at higher flow rates demonstrated healthy round morphology (Figure 2, upper and lower right) and expressed the stem-cell marker Oct-4. These microfabricated platforms will enable precise and unique control over the cellular microenvironment, allowing novel cell biology experiments at the microscale.

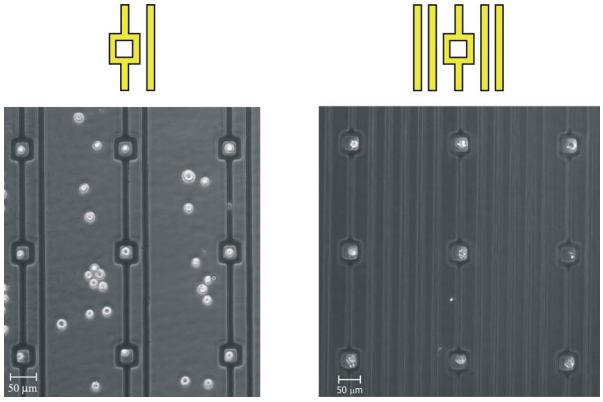

▲ Figure 1: Single DEP trap (upper left). 3 × 3 array of murine fibroblast cells loaded in the DEP traps (lower left). Single DEP trap with interdigitated electrodes (upper right). 3 × 3 array of HeLa cells loaded in the DEP traps, with interdigitated electrodes between traps to prevent cell sticking (lower right).

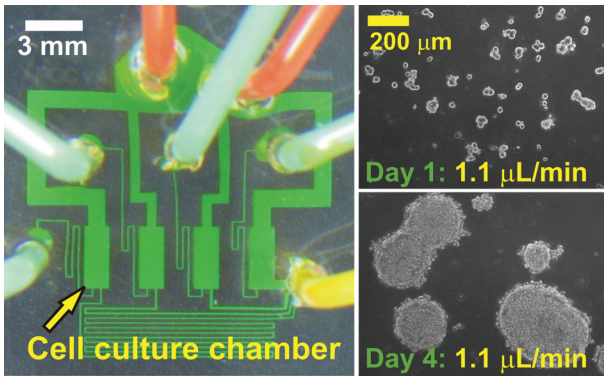

▲ Figure 2: Microfluidic 1 × 4 array of cell culture chambers for creating a logarithmic range of flow rates (left). Mouse embryonic stem cell colonies exhibit healthy morphology as they grow from Day 1 to Day 4 (right) [4].

REFERENCES

[1] H.A. Pohl, "*Dielectrophoresis: The Behavior of Neutral Matter in Nonuniform Electric Fields*," New York, NY: Cambridge University Press, 1978.

[2] A. Rosenthal and J. Voldman, "Dielectrophoretic Traps for Single-Particle Patterning," *Biophysical Journal*, vol. 88, pp. 2193-2205, 2005.

[3] L.Y. Kim, M.D. Vahey, H.Y. Lee, and J. Voldman. "Microfluidic arrays for logarithmically perfused embryonic stem cell culture," *Lab on a Chip*, vol. 6, pp. 394-406, 2006.

[4] L.Y. Kim, H.Y. Lee, and J. Voldman, "Logarithmically perfused cell culture arrays," presented at the *Biomedical Eng. Soc. Annual Meeting*, 2005.

Microfluidic/Dielectrophoretic Approaches to Selective Microorganism Concentration

H.-Y. Lee, K.A. Puchala, J. Voldman
Sponsorship: Draper Laboratories, NASA, MIT

This project focuses on the development of microfabricated microfluidic/dielectrophoretic devices capable of concentrating micron-size particles from complex liquids, for example water containing contaminants such as dust, sand, protein or soot. The concentrated particles of interest, such as pathogenic bacteria and spores, can then be delivered in small aliquots to the appropriate sensor for identification.

The micro-concentrator exploits the phenomenon of dielectrophoresis–the force on polarizable particles in spatially non-uniform electric field [1]–to trap the particles from the flow stream in order to subsequently concentrate them by release into a smaller volume of liquid. Dielectrophoresis does not negatively affect the liquid or the particles on which it operates. In our device the non-uniform electric field is created by interdigitated electrodes (IDE) at the bottom of the channel through which the contaminated solution is passed (Figure 1).

To maximize the exposure of particles to the DEP field, we mix the liquid using passive micro-fluidic mixers (Figure 1). Preliminary results with different fabricated micro-fluidic mixers exhibit up to 70% improvement in trapping efficiency as compared to devices without mixers (Figure 2). Although both the herringbone mixer (HM) and slanted groove mixer (SGM) show notable improvements over smooth channel configurations, the staggered herringbone mixer (SHM) provides the greatest enhancement in trapping efficiency. We believe that the chaotic mixing associated solely with the SHM exposes more particles to the concentrator's bank of IDEs, thus resulting in higher trapping efficiency when compared to other mixer types.

The magnitude and direction of the dielectrophoretic (DEP) force depends on the particle's dielectric properties (i.e., conductivity and permittivity); therefore, when the operating frequency of the field and the conductivity of the medium are chosen, the DEP force can be selectively applied to trap and concentrate some particles (bacterial spores of interest) and not others (dust, soot, sand or protein). In our device, initial banks of interdigitated electrodes are driven to maximize interferent trapping, while final stages capture spores from a purified solution. Using this mode of operation, we demonstrated selective trapping of *B. subtilis* spores while rejecting interferents such as pollen, chitin, sand and depleting interferents such as soot and dust. Future work will focus on improving purity and efficiency of trapping.

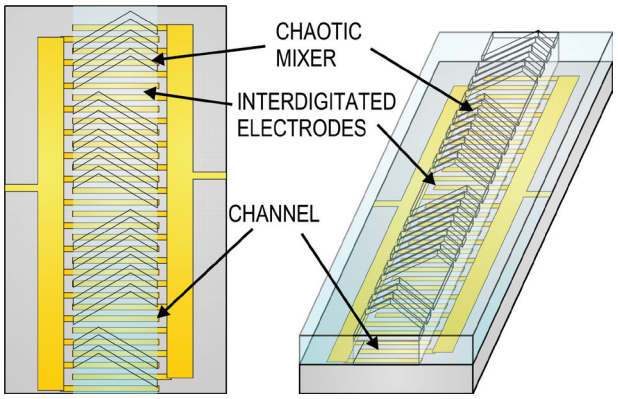

▲ Figure 1: Overhead and isometric view of the device. A channel molded in poly(dimethylsiloxane) caps a glass wafer lined with gold electrodes. Electrodes create the field that traps particles from flow when sample liquid passes through the channel.

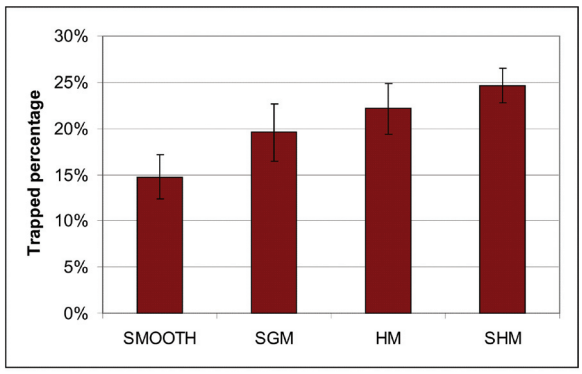

▲ Figure 2: Experimental results of the percentage of beads trapped in the channel with different types of micromixers. By using a staggered herringbone mixer (SHM), we can trap a greater percentage of particles as compared with a plain smooth channel. Other mixers, such as the herringbone mixer (HM) and slanted groove mixer (SGM), give intermediate performance.

REFERENCES

[1] H.A. Pohl, *Dielectrophoresis.* Cambridge, UK: Cambridge University Press, 1978, pp. 17-43.

Microfabricated Approaches for Sorting Cells Using Complex Phenotypes

B. Taff, S. Desai, J. Kovac, N. Mittal, J. Voldman
Sponsors: NSF Graduate Research Fellowship, NIH NCRR, Singapore-MIT Alliance

We are developing microfabricated approaches to create sorting cytometers for genetic screening of complex phenotypes in biological cells. Our goal is to create technologies that combine the ability to observe with the ability to isolate individual mutant cells from a population under study. Such cytometry merges benefits of microscopy and flow-assisted cell sorting (FACS) to offer unique capabilities on a single platform. Biologists will be able to use these technologies to isolate cells based upon dynamic and/or intracellular responses, permitting creation of new types of genetic screens.

We currently are developing optical and electrical approaches to enable image-based sorting. One of our current approaches uses an array of switchable traps (Figure 1) that rely upon the phenomena known as dielectrophoresis (DEP) [1]. The DEP-enabled traps allow for capturing and holding cells in defined spatial locations and then subsequently releasing a desired subpopulation for further study. The traps in our device are controlled using a series of row and column electrical connections. This setup avoids any need for separate connections to each of the traps in our arrays. Our chip-to-world interconnect needs thus scale only as $2\sqrt{n}$ for any $n \times n$ trap footprint. This condition enables site-specific addressing within arrays sized appropriately for bio-relevant assays (10,000 sites) using a minimal number of electrical ties (200 wires). To date, we have captured, held, and sorted small populations of individual HL60 human leukemia cells using a demonstrative 4 × 4 trap array [2]. Figure 2 shows a proof-of-concept assay where orange- and green-stained HL60 cells are first held in the 16-site array and then we sorted each of the green cells from the grid.

Developing and scaling such a platform for screening applications requires performance characteristics that are easily met only by using quantitative modeling [3]. Using such an approach, we have developed updated trap geometries and system configurations for use in larger 20 × 20 array structures. Currently we are fabricating these enhanced devices, their affiliated control and automation systems, and specific RFP-tagged cell lines for planned complex phenotype-based sorting assays. In tandem with this design cycle, we are investigating the effects of DEP trapping on cell health and the impact that it may have on our ability to assess specific phenotypic behaviors. Complementary and alternative approaches for implementing these sorting functionalities are similarly under study in an attempt to lower the threshold for acceptance and use in biological laboratories.

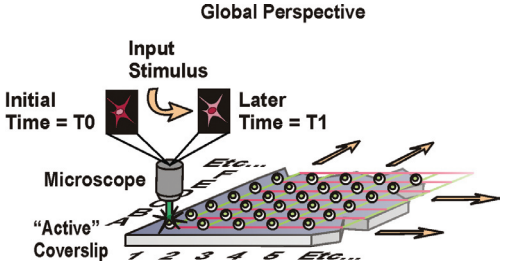

▲ Figure 1: A sorting cytometer for screening complex phenotypes. The cytometer consists of a two-dimensional array of traps, each of which holds a single cell. After loading the traps, the array is optically interrogated, and cells with phenotypes of interest are sorted.

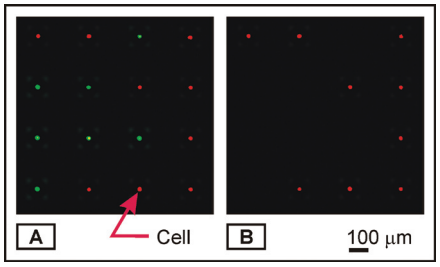

▲ Figure 2: Image-based cell sorting. (A) shows an image from an assay where mixtures of orange and green CellTracker-stained HL-60 cells are loaded into a 4 × 4 array. Though the initial placement of the green and orange cells is random in nature, the addressable traps enable selective sorting for all cells of a prescribed color in (B).

REFERENCES:

[1] R. Pethig, "Dielectrophoresis: Using inhomogeneous AC electrical fields to separate and manipulate cells," *Critical Reviews in Biotechnology*, vol. 16, no. 4, p.331-348, 1996.

[2] B. Taff, *et al.*, "A scalable addressable positive-dielectrophoretic cell-sorting array," *Analytical Chemistry*, vol. 77, no. 24, pp. 7976-7983, 2005.

[3] A. Rosenthal, *et al.*, "Quantitative modeling of dielectrophoretic traps," *Lab on a Chip*, vol. 6, pp. 508-515, 2006.

A Continuous, Conductivity-Specific Micro-organism Separator

M.D. Vahey, J. Voldman
Sponsorship: NIH NIBIB, MIT Buschbaum Fund, CSBi/Merck Graduate Fellowship

Increased throughput in the techniques used to engineer new metabolic pathways in unicellular organisms demands similarly high throughput tools for measuring the effects of these pathways on phenotype. For example, the metabolic engineer is often faced with the challenge of selecting the one genomic perturbation that produces a desired result out of tens of thousands of possibilities [1]. We propose a separation method–iso-dielectric separation, or IDS–which separates microorganisms continuously based on their dielectric properties. This technology would enable high-throughput screening of cells based upon electrically distinguishable phenotypes.

Iso-dielectric separation uses dielectrophoresis (DEP) and media with spatially-varying conductivity to separate cells by their effective conductivity. It is similar to iso-electric focusing, except that it uses DEP instead of electrophoresis, and is thus applicable to uncharged particles, such as cells [2]. We apply this method to the separation of polystyrene beads (based on surface conductance), vesicles (based on the conductivity of the internal fluid), and cells (based on viability). Current efforts are focused on the separation of *Escherichia coli* based upon the amount of the intracellular polymer poly(hydroxybutyrate) that each cell contains.

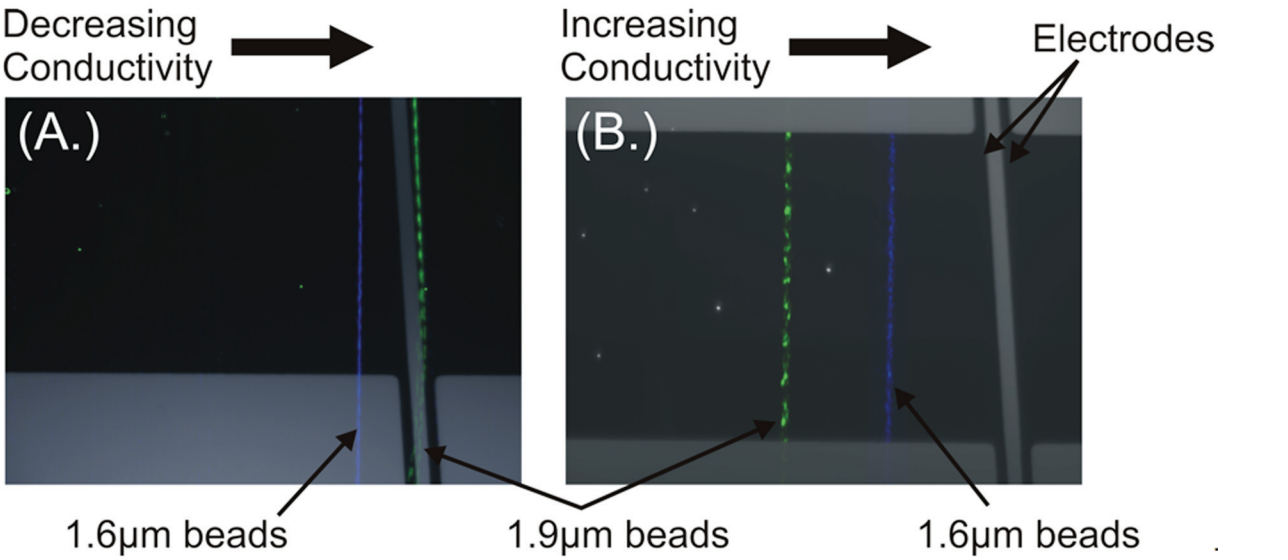

▲ Figure 1: (A) Trial separation of polystyrene beads using nDEP. The smaller, more conductive beads separate out into higher conductivity, as would be expected. The 1.9 μm particles reach their IDP in-frame, where they are seen passing over the electrodes. (B) Using pDEP, the smaller beads still separate into higher conductivity, corresponding to a further displacement (from left to right) to reach the IDP than that for the larger beads.

REFERENCES

[1] G. Stephanopoulos, "Metabolic fluxes and metabolic engineering," *Metab. Eng.*, vol. 1, no. 1, pp. 1-11, 1999.
[2] H.A. Pohl and J.S. Crane, "Dielectrophoresis of cells," *Biophysical Journal*, vol. 11, no. 3, pp. 711-727, 1971.

MEMS Vibration Harvesting for Wireless Sensors

A. Mracek, W.S. Kim, Y. Manioulloux, S. Tonn, H. Wong, B.L. Wardle (in collaboration with S.-G. Kim)
Sponsorship: Cambridge-MIT Institute, NSF

The recent development of "low power" (10's-100's of μW) sensing and data transmission devices, as well as protocols with which to connect them efficiently into large, dispersed networks of individual wireless nodes, has created a need for a new kind of power source. Embeddable, non-life-limiting power sources are being developed to harvest ambient environmental energy available as mechanical vibrations, fluid motion, radiation, or temperature gradients [1]. While potential applications range from building climate control to homeland security, the application pursued most recently has been that of structural health monitoring, particularly for aircraft.

This SHM application and the power levels required favor the piezoelectric harvesting of ambient vibration energy. Current work focuses on harvesting this energy with MEMS resonant structures of various geometries. Coupled electromechanical models for uniform beam structures have been developed to predict the electrical and mechanical performance obtainable from ambient vibration sources. The uniform models have been validated by comparison to prior published results [2] and verified by comparison to tests on a macro-scale device [5]. Models of a uniform harvester with proof mass are currently undergoing macro-scale testing and validation. A non-optimized, uni-morph beam prototype (Figure 1) has been designed and modeled to produce 30 μW/cm^3 [3]. A MEMS fabrication process for a prototype device is presented based on past work at MIT [4]. Dual optimal frequencies with equal peak powers and unequal voltages and currents are characteristic of the response of such coupled devices when operated at optimal load resistances (Figure 2). Design tools to allow device optimization for a given vibration environment have been developed for both geometries.

Future work will focus on fabrication and testing of optimized uni-morph and proof-of-concept bi-morph prototype beams. System integration and development, including modeling the power electronics, will be included.

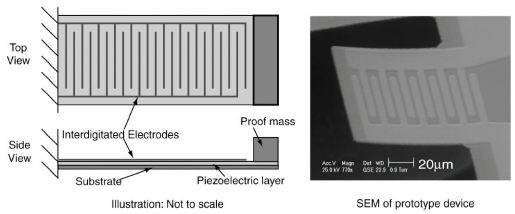

▲ Figure 1: Illustration of MPVEH unimorph configuration (left) and SEM of a prototype device (right, courtesy of S.-G. Kim).

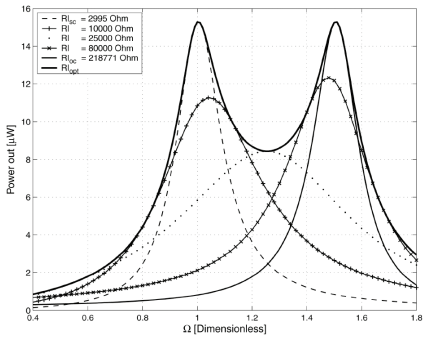

▲ Figure 2: Power vs. normalized frequency with varying electrical load resistance [3].

REFERENCES

[1] S. Roundy, P.K. Wright, and J.M. Rabaey, *Energy Scavenging for Wireless Sensor Networks with Special Focus on Vibrations,* Norwell, MA: Kluwer Academic Publishers, 2004.

[2] H.A. Sodano, G. Park, and D.J. Inman, "Estimation of electric charge output for piezoelectric energy harvesting," *Strain*, vol. 40, no. 2, pp. 49-58, May 2004.

[3] N.E. duToit, B.L. Wardle, S.-G. Kim, "Design considerations for MEMS-Scale piezoelectric mechanical vibration energy harvesters," *Integrated Ferroelectrics*, vol. 71, pp. 121-160, 2005.

[4] R. Sood, Y.B. Jeon, J.-H. Joeng, and S.-G. Kim, "Piezoelectric micro-power generator for energy harvesting," in *Proc. of Solid-State Sensor and Actuator Workshop*, Hilton Head, South Carolina, June 2004.

[5] N.E. duToit, and B.L. Wardle, "Experimental verification of models for microfabricated piezoelectric vibration energy harvesters," presented at *14th AIAA Adaptive Structures Conference*, 2006.

Fabrication and Structural Design of Ultra-thin MEMS Solid Oxide Fuel Cells

N. Yamamoto, D. Quinn, P. Capozzoli, N. Wicks, S. Wicks, S.M. Spearing, B.L. Wardle (in coll. with B.A. Wilhite, J. Hertz, J. Cui, K. Deshpande, K.F. Jensen, H. Tuller, M.A. Schmidt)
Sponsorship: ARO

Microfabricated solid oxide fuel cells are being investigated for portable power applications requiring high energy densities [1-2]. Reducing the thickness of the fuel cell stack (anode, electrolyte, and cathode) improves the electrochemical performance over that of traditional devices. This motivation for thinner structures, combined with significant temperature excursions during processing and operation (~600-1000 °C), leads to a major challenge of thermomechanical stability of such membranes. Figure 1 shows a buckled electrolyte/SiN thin film. To predict and control structural stability and failure, the structural characterization of thin films is being investigated.

Our group has characterized the residual stress and microstructure of the electrolyte layer. Complete studies were done on residual stress in sputter-deposited yttria-stabilized zirconia (YSZ) thin films (5 nm-1000 nm thickness) as a function of substrate temperature [3]. The results indicate variations in intrinsic stress from ~-0.5GPa to ~50 MPa as in Figure 2. Changes in microstructure are characterized using x-ray diffraction of as-deposited and annealed films and correlated with relevant mechanisms/ models of residual stress evolution. Based on the design frameworks using the data above, a large-area full fuel cell stack (anode, electrolyte, and cathode) has been fabricated and tested to be thermomechanically stable at high operating temperatures. Tri-layers (Pt-YSZ/YSZ/Pt-YSZ, 50-200-μm wide, each 250-nm-thick) were sputter-deposited at high temperature (500-600C). Devices are being tested for electrochemical performance and power generation. In addition, proton-conducting electrolytes, typically capable of significant power generation at temperatures lower than YSZ are also being investigated in ultra-thin film form. Crack-free barium cerium-yttrium-oxide (BaCeYO) films with uniform thickness (300-500-nm thick) have been successfully sputter-deposited. Electrochemical and residual stress characterization for this material is currently underway.

Additional ongoing work includes bulge-testing to determine the electrolyte's elastic/thermal/fracture properties in ultra-thin membrane form, investigation of the mechanical and chemical properties of anode cathode materials, and nonlinear modeling of film postbuckling and failure.

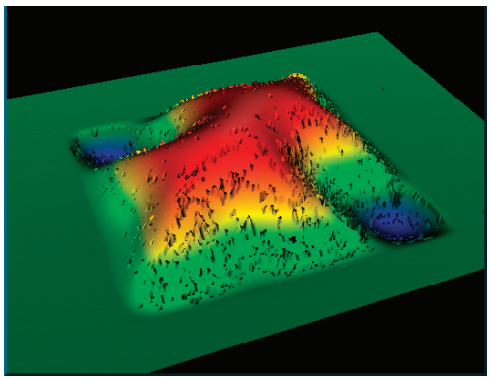

▲ Figure 1: Postbuckled YSZ/SiN membranes on Si. Displacement contour plot.

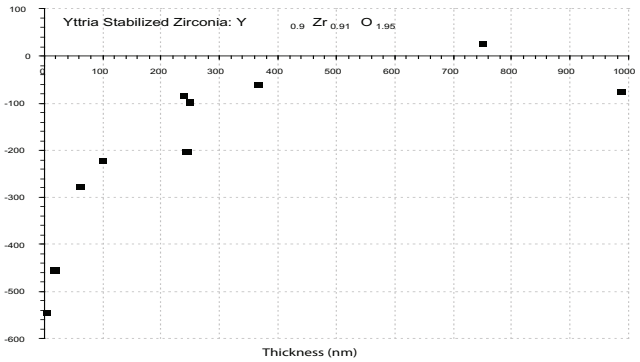

▲ Figure 2: The YSZ electrolyte film stress as a function of film thickness.

REFERENCES

[1] C.D. Baertsch, K.F. Jensen, J.L. Hertz, H.L. Tuller, V.T.S. Vengallatore, S.M. Spearing, and M.A. Schmidt, "Fabrication and structural characterization of self-supporting electrolyte membranes for a μSOFC," *J. Materials Research*, vol. 19, pp. 2604-2615, 2004.

[2] V.T. Srikar, K. Turner, T.-Z. A. Ie, and S.M. Spearing, "Structural design considerations for micromachined solid oxide fuel cells," *J. Power Sources*, vol. 125, pp. 62-69, 2004.

[3] D. Quinn, S.M. Spearing, and B.L. Wardle, "Residual stress and microstructural evolution in thin film materials for a microsolid oxide fuel cell (SOFC)," *MRS Fall Conference*, Boston, MA, December 2004.